POLITECNICO DI MILANO

School of Industrial and Information Engineering

Department of chemistry, materials and chemical engineering "G. Natta"

Master of Science in Materials Engineering and Nanotechnology

Nanomaterials for the consolidation of iron-tannate dyed textiles

Riksantikvarieämbetet

SWEDISH NATIONAL HERITAGE BOARD
RIKSANTIKVARIEÄMBETET

KTH Royal Institute of Technology

Supervisor: Prof. Daniela Comelli

Candidate: Nicoletta Palladino
Matr.: 872086

Academic Year 2018-2019

A papà

Abstract

This thesis was developed as conclusion of a double degree program between Politecnico di Milano (Materials Engineering and Nanotechnology) and KTH (Engineering Physics). The experiments were run in the labs of the Swedish national heritage board in Visby (Sweden), under the supervision of Marei Hacke, who coordinated the PhD project of Helen Wilson and proposed its follow-up.
The project investigates the use of nanocellulose- and nanosilica-based dispersions for the consolidation of iron-tannate dyed textiles, whose degradation is an internationally recognized issue whose mechanism is still not clear and well-researched.
The nanomaterials used were developed within the European project Nanorestart; isopropanol together with water was used as solvent in order to keep the advantages of the latter while minimizing its drawbacks.
The materials were applied by nebulization in order to test a suitable method for delicate fragile objects. The project also aims at using the least amount of material to achieve consolidation.
Different ageing regimes at the same relative humidity of museum environments were tested, including one at lower temperature and longer time to better resemble natural ageing.
The first set of treatments did not provide the expected results because of the acidic environment and the small amount of material deposited, conditions which hindered the effectiveness of the consolidation; afterwards a new set of experiments was planned: a deacidifier was added aiming to a larger weight uptake in order to prove the consolidating effect of the nanomaterials also upon ageing.
Deacidification and a proper weight uptake successfully slowed down the degradation and consolidated the textiles, and validated nebulization as a more controlled application method of these nanomaterials, especially on fragile delicate substrates.
The project showed the possibility for nanosilica- and nanocellulose-based materials to be used for the consolidation of iron-tannate dyed textiles; silica nanoparticles functionalized with carbomethylcellulose and cellulose nanocrystals seemed to be the most promising materials for further studies using nebulization as application method. Nanoparticles of $CaCO_3$ proved to be a successful deacidifier for the textiles, so their behavior upon different ageing conditions may be investigated in the future, as deacidification revealed to be necessary to have effective consolidation.

Acknowledgments

First of all I would like to thank Marei Hacke for involving me in this project and giving me much more than just professional support together with her family.
A big thank you to prof. Monica Ek who put me in contact with Marei kindly listening to my thesis request, and to prof. Daniela Comelli for her ready interest to this project and her support though the distance.
I would like to thank Romain Bordes for providing me the consolidating materials and for his support and trust during the project.
Thanks also to Giovanna Poggi for providing me the deacidifier and for her kind advice, and to prof. Muhammet Toprak for readily accepting to be my examiner at KTH.
I would like to thank all the people met at Riksantikvarieämbetet for their interest to my project and for making me feel at home during my staying in Visby.
Finally, thanks to my mother Carmelina and my sister Benedetta for supporting and encouraging me stronger than anyone else in these years despite distances and hard times.

Nicoletta

Contents

List of Figures

List of Tables

Chapter 1

Introduction and state of art

The cultural heritage may be defined as the entire corpus of material signs - either artistic or symbolic - handed on by the past to each culture and, therefore, to the whole of humankind. As a constituent part of the affirmation and enrichment of cultural identities, as a legacy belonging to all humankind, the cultural heritage gives each particular place its recognizable features and is the storehouse of human experience. The preservation and the presentation of the cultural heritage are therefore a corner-stone of any cultural policy.

Draft Medium Term Plan 1990-1995(UNESCO, 25 C/4, 1989, p.57)

Engineering and cultural heritage may sound like two parallel lines to most people, but technology and interdisciplinary cooperation are essential to protect and preserve the beauty and the traces created by human beings.

1.1 Purpose of the thesis

The degrading effect of iron-tannate dyes on woven textiles is a relevant but not well-investigated problem in conservation science. This work continues Helen Wilson's project about deacidification and antioxidation of iron-tannate dyed textiles [1] by adding considerations about consolidation; nanocellulose- and nanosilica-based materials will be investigated as consolidation for aged iron-tannate dyed cotton model textiles.

1.2 Nanomaterials for cultural heritage

Since the pioneering vision of the world-famous scientist Richard Feynman [2], nanotechnology has completely revolutionized many fields, from materials science to electronics, energy production, medicine, biotechnology; conservation of cultural heritage has been more and more affected by the development of nanomaterials, too.

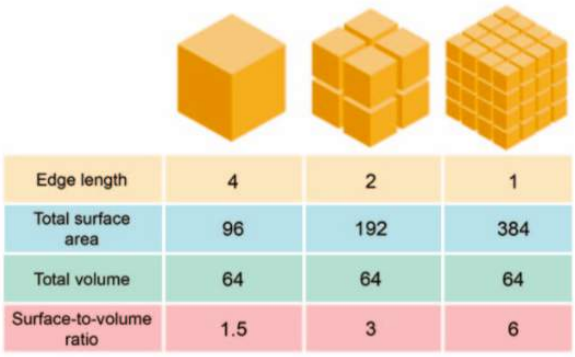

Edge length	4	2	1
Total surface area	96	192	384
Total volume	64	64	64
Surface-to-volume ratio	1.5	3	6

Figure 1.1: Surface, area, volume and their ratio variation with size. From [3], image by Baglioni, Michele.

A material can be defined as nanostructured if at least one dimension is of the order of 10^{-9} m. [3].
The red thread ensuring that there is "plenty of room at the bottom" [2] is the larger amount of surface area compared to volume as size decreases [3] (Figure 1.1). This implies higher reactivity and possibility of interaction with other materials [4], and improves the stability of particles dispersions together with the effectiveness of their application (a relevant point for this project). Size and shape of nanostructures [5] can be designed together with wettability properties. Decreasing the size also promotes the penetration of particles into more or less porous matrices (e.g. cotton), improving the effectiveness of the treatment and reducing the presence of unaesthetic or even detrimental stains caused by the concentration of material at surface.
The effectiveness of a treatment can be preserved or improved using less concentrated solutions [6], an advantage from both the economic and safety / environmental point of view. The use of water or no-toxic solvents for solutions and dispersions of nanomaterials follows the same line. All these characteristics agree with the principle of minimum intervention, a stronghold of art restoration [7].

1.3 Iron-tannate dyed textiles

Iron-tannate dyes have been used in different ages all around the world to give textiles a black-brownish color. Different substrate materials have been dyed, from cotton to wool and indigenous fiber species, but the chemistry of the dye is not so friendly to the objects themselves [8]: it is the main cause of their color fading and loss of mechanical properties. The degradation can be so fast and severe to permanently affect the possibility to handle and exhibit objects.
The relevance of the problem has been increasing more and more since the craftsmanship abilities to reproduce these dyeing techniques have been disappearing (e.g.

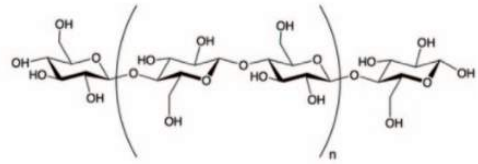

((a)) *Cellobiose unit. From [3].*

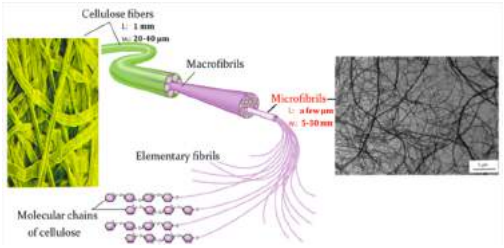

((b)) *Hierarchical structure of cellulose. From [12].*

Figure 1.2: Cellulose structure.

in some African tribes [1] or amongst Maori people [8]).
The chemistry of iron-tannate dyes is similar to iron-gall inks, cause of ink corrosion (1.3.2). More research has been performed to solve the latter problem within many European projects as InkCor [9].

1.3.1 Model textiles

Cotton (either undyed or dyed with model dyes) was the substrate used to evaluate the effectiveness of the consolidation treatments developed in this thesis [10].
Cotton is almost pure cellulose (around 90 %), a semi-crystalline polysaccharide made of β-D-glucopyranose units linked through (1→4)-glycosidic bonds [11]. The repetitive unit of this homopolymer is called cellobiose, and consists of two glucose units flipped of 180° (Figure 1.2(a)).

The nature of the bond between monomers gives cellulose a linear primary structure with a molecular weight higher than $1.5 \cdot 10^6$ g/mol [13] for the native biopolymer. The degree of polymerization (DP), which is the number of units in a polymeric chain, is usually quite high (from 9000 to 15000 according to the cellulose source). Cotton has good mechanical properties thanks to a high DP together with low polydispersity. The latter parameter is important to assess the degradation of cellulose; it is generally lowered with ageing, with consequent worsening of the mechanical properties. Degradation is quantified through the percentage of scissored glycosidic bonds (%S) to avoid dependence on the technique used to measure it [3], and is accompanied by a significant decrease of DP detrimental for the mechanical properties of the object.
The equatorial hydroxyl groups of the glycosyl units promote intra- and inter-molecular hydrogen bonds which stiffen the chain and lead to the formation of sheets stocked together into a crystalline structure (degree of crystallinity between 70-80 % [13]) through Van der Waals and hydrophobic interactions; these give rise to micro- (2-4 nm in cross-section, 100 nm in length) and macrofibrils (100-400 nm wide), as shown in Figure 1.2(b).
The internal cohesion of the crystallites can be explained by a "fringe-fibrillar"

structure where crystalline domains are interconnected through amorphous domains made of the same polymeric chains. This hierarchical structure makes cellulose stiff and dissolvable only in strong acids or strong hydrogen bonding systems, and the huge amount of hydroxyl groups makes it hydrophilic and hygroscopic, so able to absorb and release water according to temperature and relative humidity (RH). However hydrophobicity occurs in the axial direction (compared to the glycosyl ring) where there are no -OH groups [11].
Degradation starts from amorphous regions. The main reasons of cellulose degradation are [3]:

- acid hydrolysis of the (1→4)-glycosidic bonds, until reaching a leveling-off degree of polymerization (LODP);
- oxidation, often interconnected with acid hydrolysis, which weakens the glycosidic bond (e.g. due to a change in electron density upon ring opening, or the production of carboxyl groups and acids).

1.3.2 Dye chemistry

Iron-tannate dyes are metal complexes or mordant dyes produced upon different recipes and techniques depending on production area and time. They generally consist of iron ions and tannins dissolved in water, either combined and applied on the textile or applied separately on the textile [1]. Common sources of iron ions are iron sulphate, Roman vitriol, iron acetate or iron-rich mud; tannins may come from plant sources as gall nuts, bark, leaves, seeds, fruits of different species. The latter compounds are classified as either hydrolysable (glucose esters of phenolic acids) or condensed (oligomers or polymers of flavan-3-ol monomers). Their different electron-accepting properties provide different absorption spectra, which means different colors (condensed tannins are responsible for a green-black color, so they were not used in the dyes studied in this thesis) [8]. Other elements (transition metals as Cu, Ti, ...) may be present in the formulation, too. The obtained color depends on reagents concentration and on the used sources together with their freshness, purity, acidity (the higher the darker), so it is hard to reproduce a specific shade.
The iron source and the product of tannins hydrolization form an acid (e.g. sulfuric acid) and insoluble iron (III)-tannate complexes, whose structure is not completely understood.
The complexes are responsible for the blue-black color obtained through a reversible light-induced charge-transfer across an Fe-O bond of the complex; this leads to a conjugated double bond system with an absorption peak at around 620 nm at pH 4 [1]. An example is shown in Figure 1.3.
The complexes are thought to polymerize or aggregate into a compound of higher molecular weight; this might explain the insolubility of the dye and its good

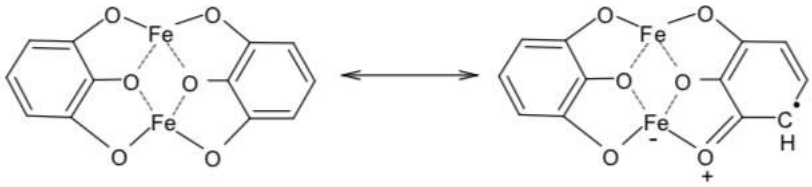

Figure 1.3: Charge transfer in an iron(III) pyrogallol complex. From [1].

permanence on the textile itself (more difficult diffusion). Iron(III) is the most stable oxidation state in equilibrium at low pH, so stable complexes decrease the concentration of unbound iron(III) increasing the oxidation rate of iron(II) [1].
This chemistry is well-studied for iron-gall inked paper degradation (also called "ink corrosion" [13]), cause of paper discoloration, embrittlement and perforation. Iron gall inks mainly consist of gall nuts (source of tannins which hydrolyze to gallic acid), iron or copper sulfate, vinegar or wine, water and arabic gum (binder) [14].
Ink corrosion, as well as degradation due to iron-tannate dyes, takes place mainly due to two reasons:

- acid-catalyzed hydrolysis, caused by the acidic environment generated by the ink/dye and leading to a decreased DP due to random chain cleavage;
- transition metal-catalyzed (auto-)oxidation of cellulose [13], caused by the presence of free metal ions as Fe^{2+} or Cu^{+} (also favored in acidic environment).

Free metal ions can change their oxidation state through redox reactions, detrimental especially when they promote the formation of radicals, hydrogen peroxide and hydroperoxide radicals (Equations 1.1 and 1.2). Further decomposition of peroxides leads to cellulose oxidation (the oxidation of iron(II) to iron(III) ions gives rise to hydroxyl ions and radicals according to the Fenton reaction mechanism shown in Equation 1.3).
The fact that iron-tannate dyed textiles are usually washed after dyeing may support the idea that the breakdown of iron-tannate complexes due to natural ageing is the main source of unbound iron ions rather than an excess due to the dye formulation itself [1].

$$Fe^{2+} + O_2 + H^{+} \longrightarrow Fe^{3+} + HOO\cdot \tag{1.1}$$

$$Fe^{2+} + HOO\cdot + H^{+} \longrightarrow Fe^{3+} + H_2O_2 \tag{1.2}$$

$$Fe^{2+} + H_2O_2 \longrightarrow Fe^{3+} + OH^{-} + HO\cdot \tag{1.3}$$

Copper ions (present in the tested model dye, too) are responsible of a similar mechanism (Fenton-related reaction, Equation 1.4) and even more active than iron

ions [3], especially at pH higher than 8.5 [1].

$$Cu^{+} + H_2O_2 \longrightarrow Cu^{2+} + OH^{-} + HO\cdot \tag{1.4}$$

Paper (in case of inks [13]) usually contains reducing components which reduce the oxidized transition metals, starting again the cycle of paper degradation. An autocatalytic process is then observed.
pH plays a fundamental role in the degradation process. Not only acidic but also strongly alkaline environments promote ink corrosion [13]; the hydroperoxide radical may decompose into a proton and a superoxide anion (O_2^{-}), reducing agent for Fe^{3+} and Cu^{2+} (Equation 1.5).

$$Fe^{3+} + O_2^{-} \longrightarrow Fe^{2+} + O_2. \tag{1.5}$$

Different factors may affect the degradation behavior of the textile with time. Endogenous parameters depend on the intrinsic characteristics of the objects and include:

- dye composition (pH, metal ions);
- organic substrate composition (content of cellulose and other compounds, diffusion properties within the fibers);
- degradation products.

Exogenous parameters depend on the environment surrounding the object and include:

- storage conditions (temperature, RH, oxygen content, light, pollution);
- object handling (transport, analysis, exhibition).

The latter factors can be controlled in order to reduce the degradation rate before applying a consolidation treatment.

1.4 Consolidation

The degradation of iron-tannate dyed textiles can be so severe to require a consolidation treatment as last chance for the object survival [8]. Consolidation is a physical remedial conservation method [1] consisting in *the application or the regeneration of binding material to improve cohesion or loose of friable media or substrate and reattach it (if necessary) to its support* [15]. It can be either a tool used during a fixing/facing treatment or a permanent measure for the long-term integrity of an object, as for iron-tannate dyed textiles.
A consolidation treatment should fulfill different requirements in order to be effective and usable:

- compatibility with the substrate material in terms of physico-chemical properties [3];
- ability to preserve or slightly improve the mechanical properties of the textile (e.g. flexibility) [4];
- no color alteration (undesired gloss, surface darkness [1]);
- no leaching or removal of original parts of the object [3];
- easy application method, which must not damage and further degrade the textile material and/or the dye [8];
- no use of toxic and/or environmentally-unfriendly solvents [3];
- reversibility [8] [1];
- low viscosity to promote deeper penetration of the treatment [8];
- minimal shrinkage and fibers swelling [8];
- low cost [3].

The consolidating agent should form a coating able not only to bind and hold together the fibers, but also to protect the textile from atmospheric variations [8]. Many requirements can be better fulfilled by nanomaterials (1.2). The use of 2-propanol has shown to be compatible with metal gall inks, so it seems promising for iron-tannate dyes (1.3.2), too. Water may swell cellulose fibers due to its polarity [1]; it would improve the penetration of the consolidating material from one side, but mechanically damage the textile on the other, changing its appearance and shape. Even the removal of hydro-soluble degradation products may be detrimental; their migration into adjacent areas may accelerate degradation and overall discoloration of the substrate. The higher temperature required for the evaporation of water compared to other solvents also implies longer drying and treatment time, not so attractive from the practical point of view. Finally, water can not be used at all if the textile contains water-sensitive materials as metals or particular kinds of dye or pigment. The use of less polar solvents (e.g. alcohols) decreases the risk of swelling of polar fibers as cellulose, as well as the extraction of polar compounds. A mixture of water with a less polar solvent may limit the drawbacks of water while ensuring good dissolution and penetration of the consolidation into the fibers, not ensured by more volatile solvents (2.1). The choice of the appropriate non-aqueous solvent should be driven by toxicity considerations and the possibility of solvation of compounds not soluble in water. Short-chain aliphatic alcohols as 2-propanol have good wettability properties on hydrophilic substrates as paper and canvas thanks

[1] Not considered in this project.

to their low surface tension [16]. 2-propanol also has a small dielectric constant (20.18 at 20°C), which hinders the solubilization of undesired ionic substances in solution, and lower viscosity compared to water (2.038 vs 0.890 cP at 25°C). Finally, its kinetic stability ensures good long-term dispersibility of nanoparticles [16].
The less invasive application of consolidating solutions by nebulization has been proved effective and potentially scalable [3].
Water soluble polymers have been used for consolidation purposes [8]: they ensure stiffness increasing the diameter of the fibre though some loss of flexibility (however talking about flexibility is not really relevant at severe degradation levels). Research on innovative consolidating agents mirrors the modern tendency towards natural renewable non toxic materials, too.

Deacidification treatment

Iron and tannin sources together with other reagents (e.g. vinegar) of the dye formulation contribute to the acidity of iron-tannate dyed textiles [1]. Free iron ions and their counterions may form acidic compounds, and ageing may increase acidity through oxidation.
Deacidification is required to slow down hydrolysis and oxidation reactions responsible of substrate degradation [14]. Hydroxides, carbonates or bicarbonates are commonly used.
The requirements of a deacidification treatment are:

- complete neutralization of the object and thermodynamically-stable side products [16] acting as alkaline reservoir (pH around 7-8.5) [14, 17];
- no toxicity and/or environmentally-unfriendliness of solvents as well as no harmfulness to the textile [14, 17];
- physico-chemical compatibility with the substrate and its components (e.g. the dye);
- no change and loss of mechanical and visual properties [17];
- permanent effect [17];
- alkaline reserve around 2 % of the earth alkaline carbonate [17];
- low cost (e.g. mass deacidification) [14].

Deacidification treatments can be classified as aqueous and non-aqueous [14].
Aqueous treatments usually consist of bicarbonates of alkaline earth metal (often calcium) hydroxides solutions [13]. The high mobility of hydroxide ions makes aqueous treatments very effective. They can also directly wash out hydro-soluble dirt (improving the aesthetics of the object) and compounds involved in paper

oxidation, but have several drawbacks, too. Free hydroxide ions may produce highly alkaline environments able to depolymerize and degrade cellulose, as well as to promote decomposition or removal of inks or dyes from the substrate. Aqueous treatments may also cause undesired leaching of ink/dye and swelling of cellulose fibers [3], and are usually applied by immersion, with poor control of the amount of applied deacidifying agent [5]. Swelling of the fibers may cause cracking and changes in size and appearance of the object, and water requires much longer drying times compared to more volatile solvents. These limitations can be overcome by non-aqueous treatments [14] and the considerations introduced above (1.4) about aqueous and non-aqueous treatments for consolidation are also valid for deacidification. Non-aqueous deacidification [13] usually employs alkaline earth hydroxides (of magnesium and calcium for example) to instantaneously neutralize free hydrogen ions through water formation. The excess material is slowly converted into carbonate by reaction with carbon dioxide (CO_2), giving rise to an alkaline buffer acting as reservoir. The main advantage compared to aqueous treatments is the reduced risk of ink solubilization, migration and bleeding. The oldest non-aqueous method is the Wei To ('70s), which first obtained alkaline material upon hydrolysis of a chemical compound (magnesium methoxymethyl-carbonate) soluble in an organic solvent (methyl alcohol and chloro-fluorocarbons, toxic and not environmentally-friendly). The same principle, but with more friendly solvents (a complex of magnesium and titanium alkoxides in hexadimethyl disiloxane (HMDO)), is employed by the Battelle or Papersave Process approved by the National German Library. Magnesium alkoxide neutralizes free acids and then reacts with moisture forming magnesium hydroxide and then carbonate (the desired alkaline reservoir.) upon reaction with CO_2. The second compound forms titanium oxide and water by hydration, and its role is to increase the solubility of MgEtOH in HMDO. An example is the Bookkeeper method, a commercial dispersion of submicron-sized particles of MgO in a blend of perfluoroalkanes, which ensure inertness towards inks and paper. It is available for small-scale as well as mass deacidification. The solvent is very polar and not compatible with oxide particles (too large to be stable in the dispersion), so a stabilizer is added; the particles react with acids and also with water (if in excess) forming magnesium hydroxide and then carbonate, ensuring an alkaline reservoir for the material [16]. Also this method has some drawbacks due to the poor penetration of particles into low-porosity materials, often cause of a surface veil, detrimental for the aesthetics of the object. Stabilizers may also increase surface hydrophobicity and generate a too alkaline environment [14].

1.4.1 Nanocellulose

Nanocellulose (NC) has been proved as a natural consolidating agent for painting canvas [6] thanks to its exceptional (usually anisotropic) mechanical properties [18]. Working at the nanoscale (at least in one dimension [18]) removes the defects

linked to the hierarchical scale of cellulose, defining a new "building block" for the development of new materials with better performance [18]. The crystalline structure provides large elastic modulus (∼110-220 GPa) and tensile strength (∼7.5-7.7 GPa) together with low density (∼1.6 g/cm^3) and high aspect ratio (thickness∼nm, length∼μm). NC has a nanolining effect which generates a continuous film on the canvas surface and hinders further penetration of the nanomaterial into the textile; the addition of another component (e.g. nanosilica or cationic polymers as polyamidamine-epichlorohydrin (PAAE) [19]) may synergistically help the consolidation of the substrate at different scales [20]. The reactive side groups (-OH) allow surface functionalization (via adsorption or chemistry modification), a fantastic tool to tailor surface properties [18], especially to improve the adhesion of nanocellulose to the fibers of the substrate [19]; these groups are also responsible of undesired water sorption.
Some composites are even transparent, a good property for conservation purposes. Nanocellulose is renewable, sustainable, readily available from natural resources [4] and has basically the same composition as the substrate studied in this project, promising in terms of compatibility and interaction [19].
NC for consolidation purposes can be classified in three main classes [20]:

- carbon nanofibrils (CNF)s: long flexible morphology [19], made of 36 cellulose chains (β crystal structure) which form a structure of squared cross-section with high aspect ratio (4-20 nm wide, 500-2000 nm long), and contains both amorphous and crystalline domains; this material is finer than microfibrillated cellulose (MFC) [18] and its dispersions have high viscosity even at low solid content [21];

- carbon nanocrystals (CNC)s: highly-crystalline (54-88%) rod-like whiskers of high aspect ratio (3-5 nm wide, 50-500 nm long) produced by hydrolysis of cellulose structures; more severe hydrolysis conditions can reduce the aspect ratio even to spherical particles [18];

- bacterial nanocellulose: microfibrils (aspect ratio $>$ 50, length∼μm) secreted by bacteria, whose family and growing conditions affect the morphology of the final product [18].

A further point is to have information about the response of nanocellulose-based treatments to environment changes, especially in terms of moisture uptake at not constant relative humidity [19]. The high water retention of nanocellulose is one of the reasons to test alternative solvents as ethanol, though at least 30-40% of water is necessary to ensure homogenous resuspension for the application of the nanomaterials [4].

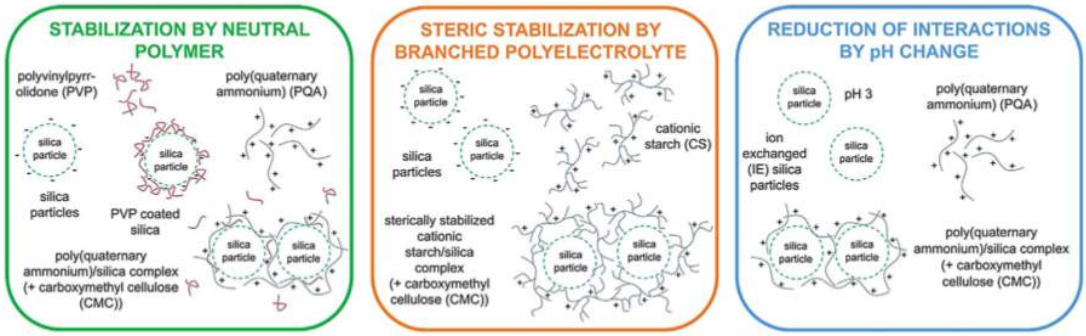

Figure 1.4: Strategies to avoid or reduce aggregation of nanoparticles of colloidal silica [7].

1.4.2 Nanosilica

Colloidal silica is non-toxic, cheap, easily as well as largely available; it has consolidating properties for paper and textiles together with an alkaline nature [6].
The main problem of colloidal dispersions is stability; the aggregation of nanoparticles is particularly detrimental for a consolidation treatment supposed to reach the whole depth of the textile and not only the surface [7]. Stability can be ensured by complexing silica nanoparticles (SNPs) with polyelectrolytes in order to avoid or reduce aggregation issues. Three main methods have been developed (Figure 1.4):

- stabilization by neutral polymer as PVP;
- steric stabilization through adsorption of branched polyelectrolytes as cationic starch;
- surface charge reduction by pH change to reduce interactions between nanoparticles.

NC has good interaction with cotton, but it mostly acts at surface (1.4.1); SNPs are perfect candidates for a synergistic action with NC.

1.4.3 Alginates

The term alginate indicates a family of polysaccharides synthesized by brown algae and bacteria. It has a structural function in seaweeds in terms of mechanical strength and flexibility, and acts as water reservoir in order to prevent dehydration upon air exposure [22]. Colorimetry measurements proved that zinc alginate can inhibit the fading of black-dyed *P. tenax* fibers; the same effect was not observed using other kinds of alginate as sodium or calcium alginate [8]. The anti-fading action must be related to certain divalent metal ions as Zn^{2+} or Ba^{2+} which stabilize the ferric-tannate complex responsible for the color of the textile. They may also displace iron ions in the tannate complex, thus avoiding the formation of crystalline

iron oxides able to accept electrons and break up the complex.
The alginate produces a chromophore similar to the one produced during ageing, but is essential for neutralization. The ion exchange between the metal ions associated to the alginate and the hydrogen ions present in the textile forms insoluble alginic acid which is then decarboxylated, so that the protons are no more available for the degradation cycle.

1.4.4 Application methods

How to apply nanomaterials to textiles is a crucial choice to ensure effectiveness and uniformity of the treatment. It affects the treatment homogeneity as well as amount, depth and characteristics of the deposited material [4].
CNFs have been applied by brushing or spray coating on paper [4]. The same methods have been used for deacidification treatments of paper [16]. Nebulization was chosen for non-aqueous treatments to avoid the mechanical action of brushing, and proved to be safe, effective and scalable on paper [3]. Treatments based on CNFs and CNCs were applied on painting canvases by air-brush spraying [6, 20, 19].
Alginates solutions have been applied by fine sable artists brush on *P. tenax* fibers. Immersion [1] and dripping are two alternative methods: the first one is quick but does not allow a good control of the amount of deposited material; the second one solves this problem but may not ensure uniform application [3]. For this reason treatments should be applied on both sides of the object [3].

1.5 Ageing

In order to evaluate the efficiency of a consolidation treatment it is necessary to see its long-term effects [23]. Obviously it is not possible to wait for years, so accelerated ageing is an essential tool in research. Its conditions should resemble mechanical properties (decreased due to the loss of DP for cellulose) and chemistry upon acid hydrolysis and oxidation of cotton due to natural ageing in certain conditions and time. It consists in exposing the sample material at higher temperatures and a certain level of RH long enough for it to degrade. Both temperature and RH can be either stable or cyclic to induce more severe degradation.
Artificial and natural ageing can be compared through Arrhenius plots which indicate the time of accelerated ageing required to simulate specific degradation conditions.
Many factors are involved, so the choice of the parameters is quite tricky. Different degradation mechanisms may occur at very high temperatures, suggesting that choosing milder temperatures (closer to the real ones) for longer times may be preferred (2.2.6); moisture content and RH affect the rate of individual specific reactions and their products suggesting the use of the same humidity conditions as

natural ageing. Even the positioning of the samples in the oven is relevant: in a stacked configuration, for example, the development of volatile compounds (VOCs) creates more severe conditions for the inner compared to the outer samples.
It is impossible to establish a systematic method of accelerated ageing, so a careful interpretation of its results is crucial [24].
Another ageing approach is given by chemical methods, where the sample is both chemically and thermally attacked (e.g. with hydrogen peroxide and sulfuric acid [25] at high temperature). The main advantage is the shorter time required for degradation (hours/days instead of weeks/months), though the degradation mechanism should be even more clear *a priori* to be able to choose the right chemicals for its simulation.

Chapter 2

Materials and methods

This chapter introduces the tested materials together with the characterization techniques used to assess the treatments during the project.

2.1 Treatments

The starting point of the thesis are the cotton model textiles dyed by Helen Wilson during her PhD [1]. The model used is Cc2, whose dye also contains Cu [10]. As will be shown in Chapter 3 the mechanical properties of the dyed textiles were already worst than the undyed, proof of the detrimental action of the dye, so the models represent a good substrate to test the consolidating materials.
Each sample consisted in a subset of 5-10 specimens (1×10 cm^2) for the tensile testing and a "free" specimen saved for further characterization. The first subset was precut in order to separate the specimens more easily after the accelerated ageing and ensure a better handling during the application of the treatments, the weighing and the ageing itself. A three-digit code was used to identify the samples:

- U for undyed, D for dyed;
- 0 for untreated, 1, 2, 3, 4, 5, 6, 7, 8, 9, 3", 7" for the treatments;
- 0 for unaged, 1, 2, 3, 4, 6 for aged, 5 for natural ageing. Undyed samples were also treated in order to evaluate color differences not dependent on the interaction of the treatment with the dye.
  Following up the suggestions of the previous work [1], and after testing an airbrush which revealed to provide a too powerful flux for the textiles, the treatments were applied by nebulization; the nebulizer (INQUA Vernebler) was fed by an air compressor (COSTECH AS18B) at a pressure of 2 bar. It did not mechanically damage the textiles (though some dripping problems) and may represent a suitable application method.
  The prepared samples were positioned in a fume hood; the ventilation was

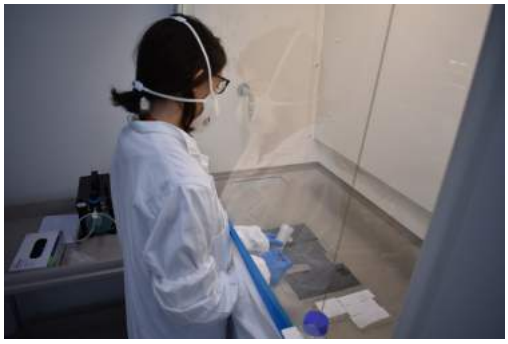

((a)) *Application of the treatments.*

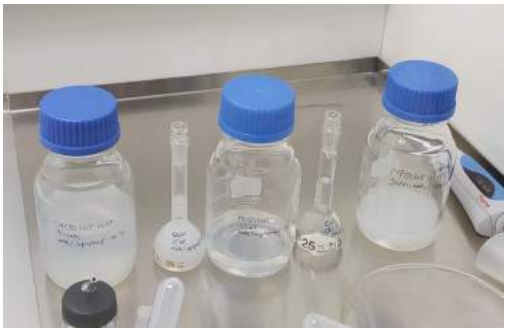

((b)) *Treatments dispersions.*

((c)) *Samples positioning.*

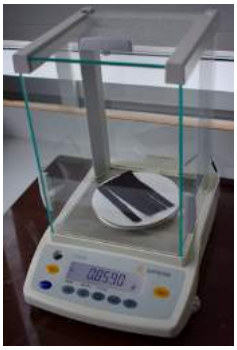

((d)) *Setup for weight measurements.*

Figure 2.1: Lab setup.

stopped just during the application of the treatments, otherwise no material at all would have been applied onto the substrate by nebulization. The amount of deposited dispersion was chosen aiming at a maximum weight uptake of 5% for the first set of treatments. The used setup is shown in Figure 2.1.

After the treatment the samples were left to dry in the fume hood and stored in controlled conditions (21 ± 1 °C and 50 ± 1% RH) before accelerated ageing. The aged samples were stored in the same conditions and without light before the characterization.
The treatments were performed using the consolidating materials developed within the NANORESTART project by Chalmers University of Technology, Department of Chemistry and Chemical Engineering; the deacidifier CSGI (-) II was provided by CSGI, University of Florence (Figure 2.1(b)). The solvents used were 2-propanol (VWR Chemicals, 98%, MW = 60.1 g/mol) and deionized water in equal parts.
The samples were weighed by a SARTORIUS ED224S scale before and after the treatment to evaluate the uptake of material, and after the ageing to evaluate the weight loss (Figure 2.1(d)). Some data are missing because a

Table 2.1: Concentration of the dispersions provided by Chalmers University of Technology.

Dispersion	Concentration [wt %]
CMC@SNP	6
PEI@SNP	5.6
PVP@SNP	9.9
CNF	2.68
CNC	2

further ageing regime was added when all the samples were already set.

2.1.1 Treatment 1: CMC@SNP:CNF

The first treatment was a mixture of CMC@SNPs and CNFs with a mass ratio around 9:1, as suggested by the results of [6]. The SNPs (AkzoNobel Pulp and Performance Chemicals, diameter∼21 nm) are functionalized by a polyelectrolyte multilayer (PEM) structure consisting of a cationic layer of polyethylenimine (PEI) (Sigma Aldrich, average MW = 25000 g/mol) and an anionic layer of carboxymethylcellulose (CMC) (Akucell AF0305, AkzoNobel Pulp and Performance Chemicals, average MW of CMC = 650000 g/mol, degree of substitution = 0.77) [6]. The multilayer structure is supposed to avoid the aggregation of the nanoparticles; the last layer is cellulosic, of similar nature as the substrate; the negative charge of CMC is required to avoid flocculation with CNFs too (also negatively charged). CNFs (Stora Enso AB, average diameter of 7 ± 3 nm and a length of $\sim$1 μm) were produced by mechanical fibrillation of softwood pulp [6].
The weight concentration of the dispersions is reported in Table 2.1. The dispersion used was 1 %wt. Each treatment step (layer) consisted in the application of 4 ml of dispersion per side per 2 g of substrate. Two layers were applied on the main samples; some extra-samples of the dyed model textiles with three treatment layers were prepared in order to evaluate the amount of material required for the consolidation. Each layer was applied after 20 min from the application of the previous one. The latter samples consisted in a subset of 3 specimens for the tensile testing and a "free" specimen for further characterization. They were treated after one month compared to the 2-layered ones, so successful results would also imply good stability of the solution.

The second and third treatment were both double-step procedures. The posi-

tive charge of PEI (from protonated amines) is supposed to provide strong interaction with cellulose (negatively-charged), so PEI@SNPs (diameter∼21 nm) were combined with CNFs, which seem to provide less stiffening compared to CNCs, which were combined with PVP@SNPs (Sigma Aldrich, average MW = 10 000 g/mol, diameter∼21 nm [7]) instead; the latter NPs are slightly positively-charged, thus provide milder interaction with cellulose [20].

2.1.2 Treatment 2: PEI@SNP+CNF

The second treatment consisted in the step-wise application of a layer of PEI@SNPs (supposed to penetrate deeper into the substrate), followed by another of CNFs on each side of the sample. The procedure was repeated twice (SNPs + CNFs → SNPs + CNFs).
The weight concentration of both the dispersions is reported in Table 2.1; both were used 1%wt.
The first layer consisted in the application of 4 ml of PEI@SNPs per side per 2 g of sample; the second layer in the application of 2 ml of CNFs per side per 2 g of sample (less amount was chosen to hinder less the penetration of the following layer of SNPs). The latter dispersion was too viscous to be nebulized, so 3 ml were diluted with 2 ml of water and 2 ml of 2-propanol directly in the nebulizer. Half of the desired material was actually deposited on the samples due to some measurement issues with the disposable pipette used (it was measuring 0.5 ml instead of 1 ml).

2.1.3 Treatment 3: PVP@SNP+CNC

The third treatment consisted in the step-wise application of one layer of PVP@SNPs followed by another of CNCs on each side of the sample. The procedure was repeated twice (SNPs + CNCs → SNPs + CNCs).
The weight concentration of both the dispersions is reported in Table 2.1. The silica-based dispersion was used 1%wt, the nanocellulose-based one 1.5% wt. The same application procedure and (correct) amount of material as in 2.1.2 were used. A power blackout occurred just after the application of the first two layers, so due to time reasons the second step was applied after 40 days. Possible good results will also show the stability of the dispersions used.
An extra sample (D3) was treated only with PVP@SNP to perform SEM on the first step.

2.1.4 Treatment 4: MgEtOH

The fourth treatment consisted in the application of MgEtOH (Acros Organics, Magnesium Ethoxide, 98%, MW = 113.43 g/mol), the most successful deacidifier of Wilson's project [1], already used on iron gall inked paper, too. As mentioned in 1.4, it reacts with water and then CO_2 to form magnesium carbonate.

$$Mg(OCH_3)_2 + 2H_2O \longrightarrow Mg(OH)_2 + 2CH_3OH \tag{2.1}$$

$$Mg(OH)_2 + CO_2 \longrightarrow MgCO_3 + H_2O. \tag{2.2}$$

It was tested in order to see any effect that can be attributed to it and not to the consolidation used in 2.1.5 (especially on the color of the samples).
Some tests were performed with ethanol, as it was already used to apply MgEtOH on gall inked paper [26]; it did not seem to provide better dissolution of the powder compared to 2-propanol (0.05 M), so the latter was chosen to keep testing the same solvent used in all the other treatments. A precipitate formed both in ethanol and in 2-propanol; only the suspended part was applied.
The same application procedure as in 2.1.1 was used, and two layers of material were deposited.

2.1.5 Treatment 5: CNC+MgEtOH

The fifth treatment consisted in the application of MgEtOH (as prepared in 2.1.4) and CNCs (as prepared in 2.1.3). CNCs show good consolidating properties but generate an undesired acidic environment [20]. The aim of the treatment is to investigate the use of CNCs when applied with a deacidifier. 4 ml of MgEtOH and 2 ml of CNCs per side per 2 g of sample were applied in a row. To be sure to have enough consolidating material another layer of CNCs was applied after one day using a freshly-made solution.
FTIR and pH measurement were performed on a treated sample. The FTIR spectrum showed no peaks from a possible carbonation, so another layer of a freshly-made solution of MgEtOH was applied, too.

The results of the first set of treatments indicated the necessity to investigate the combination of consolidating materials with a deacidifier and the necessity of larger weight uptake.
The new set of treatments aimed at a minimum 5% weight uptake taking into account yield and results of the previous set together with the amount of deacidifier required to reach at least a neutral pH. Higher concentrations

(2 %wt) were used in order to deposit more material in less time. The stepwise application method was modified applying one material per time (e.g. deacidifier → consolidant → lining) not to hinder the functions of the different materials (1.4.2).

2.1.6 Treatment 6: CSGI II

CSGI II (-) contains about 2 % of $CaCO_3$ and 0.4 % of a cellulose derivative that makes the system more stable and viscous in water and ethanol (1:1). According to the guidelines provided by CSGI, 750 μl of 1.3 %wt solution should be used per 350 mg of sample in order to achieve neutrality from a pH∼4. Five times this amount was used in order to apply enough material by nebulization (52 ml of a 2 %wt solution per 7.2 g of sample); 1.5 times the amount was used to apply the solution by brushing (3.8 ml of a 2 % wt solution per 1.8 g of sample).

2.1.7 Treatments 7/7"/3": CSGI II+PVP@SNP+CNC

The amount of consolidating material was estimated after the calculation of the uptake of deacidifier in order to ensure the same amount of both materials, a total weight uptake around ∼5% and a ratio 3:1 between SNPs and CNCs. First 15 ml of a 2 % wt solution of PVP@SNPs were applied on 1.8 g of sample treated with CSGI II, then 3 ml of a 2 % wt dispersion of CNCs. 5 ml of PVP@SNPs and 1.25 ml of CNCs were applied by brushing on 3.6 g of sample (the deacidifier was applied only on 1.8 g of sample). The treatment applied by nebulization will be indicated as 7, the one by brushing as 7"; the treatment applied by brushing without deacidifier will be indicated as 3" (Chapter 3).

2.1.8 Treatment 8: CSGI II+CNC

The amount of consolidating material was estimated after the calculation of the uptake of deacidifier in order to ensure the same amount of both materials and a total uptake of ∼5%.
15 ml of a 2 % wt dispersion of CNCs were applied on 1.8 g of deacidified sample.

2.1.9 Treatment 9: CSGI+CMC@SNP

The amount of consolidating material was estimated after the calculation of the uptake of deacidifier in order to ensure the same amount of both

components and a total uptake of ∼5 %.
16 ml of a 1 % wt dispersion of CMC@SNPs were applied on 1.8 g of treated sample [1].

2.2 Characterization techniques

Characterization aims to verify the properties of the treated samples compared to the untreated ones upon ageing. The depth of the treatments and their effects on morphology and color of the samples were investigated.

2.2.1 Tensile testing

Tensile tests provide information about the mechanical properties of the samples before and after treatment/ageing, allowing the evaluation of the rate of degradation and the effectiveness of the consolidation treatments.
The test consists in extending a specimen at constant rate until rupture according to the standards [27]. The force is measured upon elongation of the specimen and the results are expressed in terms of force-stroke curves. The first part of the curve corresponds to the response of the woven fabric to load application (Figure 2.2(a)); this behavior is characterized by the elastic modulus at low deformation. The following drastic change in slope corresponds to the response of the single fibre (Figure 2.2(a)); initially primary and secondary bonds of cellulose are stretched and shear-loaded in the amorphous regions (elastic deformation). This regime follows Hooke's law:

$$\sigma = E \cdot \epsilon, \tag{2.3}$$

where σ [N/m^2 or Pa] is the stress, ϵ [%] the strain and E [N/m^2] the Young modulus, the parameter used to estimate the stiffness of the samples when a linear relation between stress and strain holds (the higher the stiffer or less extensible). Afterwards polymer chains keep re-arranging and are able to re-acquire the initial configuration after a certain relaxation time (plastic deformation); when the breakage of secondary bonds occurs the chains are no longer able to accomodate the loading and a final break of the textile occurs [28]. The maximum loading force is the point when the first threads yield. This point is recorded together with the corresponding elongation as a measure of strength and flexibility (Figure 2.2(a)). The tests were performed by a SHIMADZU Autograph AGS-X and the data were analyzed by the software Trapezium Lite X; the change in position was recorded by optical encoders.

[1] The amount to be applied was 26 ml, but not enough material was available.

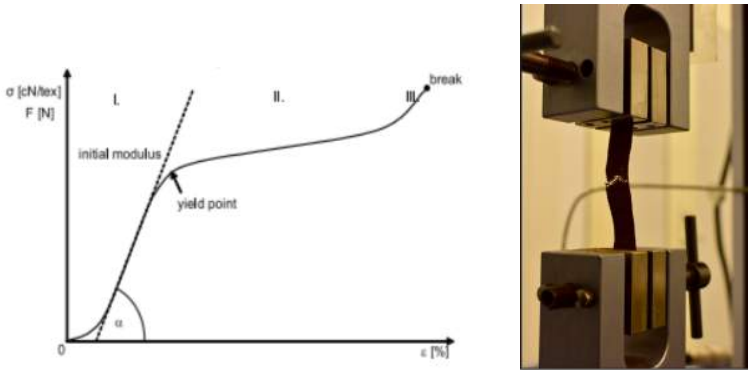

((a)) *Schematics of force-elongation curve [27].* ((b)) *Example of tensile test.*

Figure 2.2: Tensile testing.

Only the warp direction was examined not to deal with too many specimens; it is supposed to be the strongest direction of the textile, and Wilson's proved a significant clear decrease of the extensibility of cotton warp direction with ageing [1]; information about that must be sufficient to evaluate the loss of mechanical properties. The same method as Wilson's work was used [1].
The samples were conditioned at 21 ± 1 °C and 50 ± 1 % RH before performing the tests in order to have compatible results. The method used a 100 N static load cell for all the specimens apart from the undyed unaged ones, tested using a 10 kN load cell. The gauge length was fixed at 50 mm and the extension speed at 10 mm/min. The samples were positioned centrally and vertically between the gauge clamps (Figure 2.2(b)).

2.2.2 pH measurements

pH measurements were performed in order to monitor changes in the acidity of the environment upon ageing.
The pH meter used (Figure 2.3) was a glass electrode LAQUA twin, HORIBA (pH range = 2.0-12.0, resolution = 0.1). The measurements were performed on all the samples. Small squares ($\sim 0.5 \times 0.5$ mm^2) were weighed and covered with some drops of water ($\sim$ 0.33 ml per 0.003 g). After 16 h the pH of the extraction was measured.

2.2.3 Colorimetry

The purpose of colorimetry is to monitor color differences upon treatment and ageing.
The instrument used was a portable spectrophotometer KONICA MINOLTA,

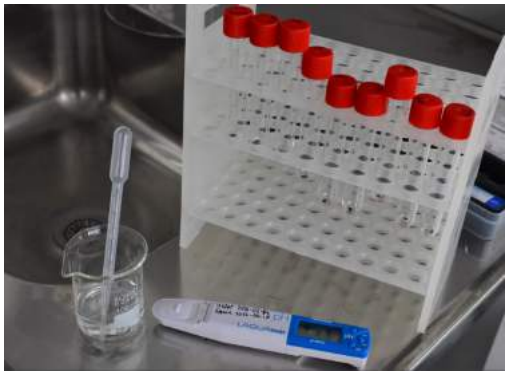

Figure 2.3: Setup used for pH measurement.

CM-2600D (Figure 2.4(a)); the software used to record and analyze the data was SpectraMagic NX. The large available aperture view (MAV, diameter = 8 mm) allowed the collection of more data decreasing possible errors. A di:8°, de:8° (diffused illumination, 8-degree viewing angle) illuminating/viewing system was used excluding the specular component (SCE mode) in order to avoid undesired reflections from the surface (Figure 2.4(b)); the detector collects only the light diffused within the integrating sphere (diameter = 52 mm).
The whole bandwidth (360-740 nm divided into 10 nm pitch components) including the UV component was investigated. The illuminant D65 and a 10° observer were used as advised by the standards [31].The light source consisted of 3 pulsed xenon lamps and the detector was a silicon photodiode array (dual 40 elements).
After zero and white calibration the measurements were performed on a black plastic substrate not to have reflections from the white paper the samples were positioned on for the ageing, thus a black background was also recorded. Five points per sample were collected, each with three averaged acquisitions. The targets were the dyed/undyed untreated unaged sheets (U00 and D00), and all the samples were analyzed. The CIE2000 formula [31] was used to calculate the L*a*b* color coordinates and the color differences dL*, da*, dB*, dE_{00} before and after treatment/ageing (Figure 2.4(c)); L* indicates the lightness (positive = white, negative = black), a* and b* respectively the green-red (positive = red, negative = green) and blue-yellow (positive = yellow, negative = blue) color component. This color space is designed to mirror the color differences perceived by human vision. A $dE \geq 1.7$ is considered just perceivable as in Wilson's work [1]. A value for the brightness [32] was also calculated in order to monitor possible undesired changes upon treatment.

((a)) *Colorimetry setup.*

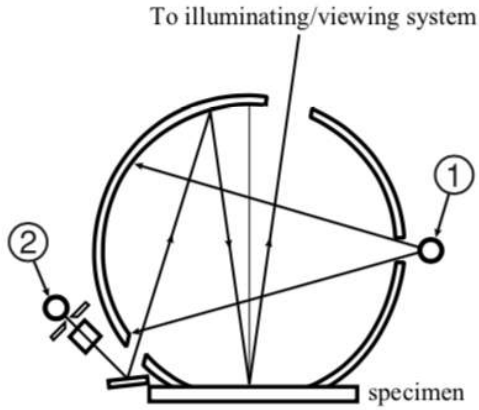

((b)) *Integrating sphere of the spectrophotometer. Only light source 1 is used in SCE mode [29].*

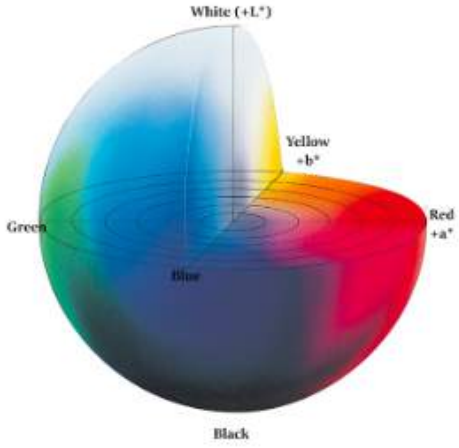

((c)) *L*a*b* color space [30].*

Figure 2.4: Spectrophotometer setup and functioning.

((a)) *Instrument.*

((b)) *Samples positioning.*

((c)) *Sputter machine for gold coating.*

Figure 2.5: SEM setup.

2.2.4 Scanning Electron Microscopy (SEM)

The main purpose of SEM analysis is to investigate the morphology of the samples at micro- or lower scale in order to observe the differences upon application of treatments and ageing.
This kind of microscopy employs an electron beam focused by magnetic lenses in order to overcome the diffraction limit of optical light. The beam is scanned over an area of the sample and its interaction with the atoms of the observed material gives information about composition and surface topography according to the kind of detected electrons (back-scattered or secondary electrons).
The used instrument was a JEOL JSM-IT500; the electron gun was a tungsten filament and the detector a Dry Silicon Drift detector (DrySD) (Figure 2.5). The data management software was SMILE VIEW Lab.
The samples ($\sim 0.5 \times 0.5$ mm^2) were positioned on carbon tape and analyzed in low vacuum (30 Pa) to avoid charging, main problem for organic materials as cotton; for the same reason the images were acquired at low voltage (5 kV) with a fast frame-accumulation system and the detected signal was from back-scattered electrons. The working distance was set at around 10 mm, the probe current at 80 pA.
A 6 nm thick gold layer was deposited on some of the samples in order to provide a ground plane, eliminate electric fields upon their surface (Quorum Q150R ES, Figure 2.5(c)) and avoid charging of the samples [33].

Preparation of the cross-sections

The cross-sections were prepared embedding the samples in a methacrylate-based light curing resin (KULZER TECHNOVIT 2000 LC). This acrylic resin

((a)) *Curing of the first layer of resin.*

((b)) *Curing of the second layer of resin.*

((c)) *Polisher.*

((d)) *Positioning of the cross-sections.*

Figure 2.6: Preparation of the cross-sections for SEM-EDX analysis.

was chosen due to its short curing times and the possibility to be used just after the hardening.
Some liquid resin was poured into polyethylene cups and cured for 5 min in a FINOLUX Light-Curing Unit 400-500 nm; the samples were positioned on the pre-cured resin and other liquid resin was poured over them and cured for 30 min (Figures 2.6(a), 2.6(b)). The sections were then cleaned with ethanol, wet-grinded and polished using silicon carbide grinding paper of increasing grit (320, 1200, 2400, 4000, 8000, 12000); the lapping was performed by a Struers Labold-5 polisher (Figure 2.6(c)). The final polishing with the 8000 and 12000 grits was performed by hand (ALCLAD 2 LACQUERS, Micromesh Polishing Cloth ALC-301 used on a foam rubber polishing grad).

Energy-Dispersive X-ray spectroscopy (EDX)

EDX performs elemental analysis through the detection of characteristic X-rays generated by the sample upon electron beam irradiation; it was used to analyze both surface and cross-sections of the samples along the warp direction in order to evaluate the penetration of the treatments into the textile (Figure 2.6(d)).
The analysis parameters were the same used for imaging apart from the higher voltage (15 kV).

2.2.5 Photoluminescence

The aim of photoluminescence is to provide further insights on the degradation mechanism of the studied textiles [34].
The setup used [35] was a time-resolved photoluminescence spectroscopy (TRPL) (Figure 2.7), where pulsed laser (CryLas FTSS 355-50, CryLas GmbH, Berlin, Germany) and a fast-gated intensified camera (C9546-03, Hamamatsu Photonics, Japan) were coupled to a spectrometer (Acton Research 2300i, focal length = 300 nm, f/4 aperture, spectral range = 380-700 nm, spectral resolution = 10 nm). The task of the laser (third harmonic of a Q-switching Nd:YAG laser, sub-ns pulses at 355 nm, repetition rate = 100 Hz, average power density on spot = 0.1 W/cm^{-2}) is to excite photoluminescence from the sample (circular spot, diameter = 1 mm). A sequence of gated spectra [2] at different delays compared to the laser pulses is collected in order to have more data. The emission process consists in the radiative decay from the excited state of a chromophore, which changes not only according to the chromophore itself, but also due to the presence of quenchers (e.g Cu^{2+}) and chemical changes (e.g. due to ageing and degradation phenomena as bond breaking and oxidation) [34].

2.2.6 Accelerated ageing

The aim of the accelerated ageing is to simulate the effects of natural ageing in order to compare long-term characteristics and properties of treated and untreated samples and judge the efficiency of the applied treatments.
Two ovens were used: WTC binder KBF240 with controlled constant RH (Figure 2.8(a)) and memmert AtmoCONTROL with dry heat (Figure 2.8(b)). Dyed and undyed samples were positioned in different stacks to avoid undesired ions transfer.

[2] In a selected temporal gate window

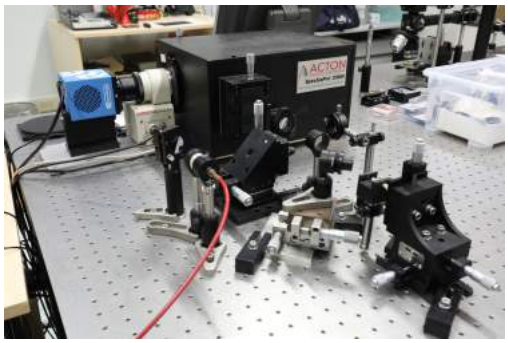

Figure 2.7: Setup used for TRPL measurements.

((a)) *Oven used for regimes 1, 2 and 3.*

((b)) *Oven used for regime 4.*

Figure 2.8: Setup for accelerated ageing.

Five ageing regimes were performed, and some samples were left to natural ageing in case of further work on these materials:

1. 70.5 ± 0.5 °C, 49 ± 2 % RH, 2 weeks;
2. 70.5 ± 0.5 °C, 49 ± 2 % RH, 4 weeks;
3. 70.5 ± 0.5 °C, 49 ± 2 % RH, 16 weeks;
4. 50 ± 0.5 °C, 5 ± 1 % RH, 16 weeks;
5. natural ageing;
6. 70.5 ± 0.5 °C, 49 ± 2 % RH, 1 week.

Regime 6 was added to test the new set of treatments; a "milder" regime (4) was performed in order to gain more realistic information about the degradation mechanism through a slower degradation rate more similar to natural conditions; the majority of strength loss should occur during the first two weeks of ageing [1], so a different starting point for the degradation may be seen and undesirable degradation reactions avoided [23, 24].
Main causes of degradation are hydrolysis of cellulose (dependent on temperature, pH, moisture), oxidation (induced by the presence of oxygen and the chemistry of the dye) and thermal degradation, which consists in the breakage of chemical bonds upon vibrations induced by higher temperatures [23]. The overall degradation rate is assumed to be proportional to temperature ($k=Ae^{-E_a/(k_b T)}$, where A is the reaction/material-dependent pre-exponential factor [24], E_a [J] the activation energy for the reaction to occur, k_b [J/K] the Boltzmann constant, T [K] the temperature), but it may vary according to the prevailing reaction.
Constant RH as in storage conditions ($\sim 50\%$) was used to simulate as much as possible a realistic deterioration mechanism, as it has been proven to be more dependent on moisture content rather than temperature [23].

Chapter 3

Results and discussion

3.1 Weight uptake and loss after ageing

Table 3.1 reports the average weight uptake upon the first set of treatments of both undyed and dyed samples.
The uptake was lower than expected, indicating that most of the nebulized material was not deposited on the samples. A yield of around 20% has been estimated for the nebulizer.
Undyed samples generally showed a slightly larger uptake than the dyed. No material at all was likely deposited by the fourth treatment, as confirmed by the invariance of pH (3.2.2).
Treatment 3 had the highest uptake but less material was accidentally deposited during treatment 2 (2.1.2), so it was not possible to compare the data of the latter treatment.

Figure 3.2 shows the average weight uptake of deacidifier and consolidation for the new set of treatments.

As expected the application by brushing resulted in larger weight uptake (Figure 3.3).

Untreated samples tended to absorb more material than the treated ones (see the uptake of PVP@SNPs of treatment 7" and 3", Figure 3.2), as confirmed by the lower yield of nebulization (∼50% less than untreated samples) of PVP-SNPs and CNCs treatments on treated samples (Figure 3.4). An exception to this trend was treatment 9, whose yield was even higher then the deacidifier. The cellulosic material covering SNPs may have favored the interaction with the substrate, hindered by the surface network formed by CNCs instead.

The weight uptake was generally around the desired minimum value of 5% (Figure 3.3).

Table 3.1: Average weight uptake.

Sample	Average weight uptake [%]	Standard deviation [%]
U10, U11, U12, U13	2.32	0.37
D10, D11, D12, D13	1.99	0.28
D10", D11", D12", D13"	1.32	0.28
U20, U21, U22, U23	1.96	0.37
D20, D21, D22, D23	1.49	0.21
U30, U31, U32, U33	3.05	0.29
D30, D31, D32, D33, D34	2.55	0.34
U40, U41, U42, U43	-0.08	0.13
D40, D41, D42, D43	-0.10	0.07
U50, U51, U52, U53	1.30	0.12
D50, D51, D52, D53	1.18	0.76

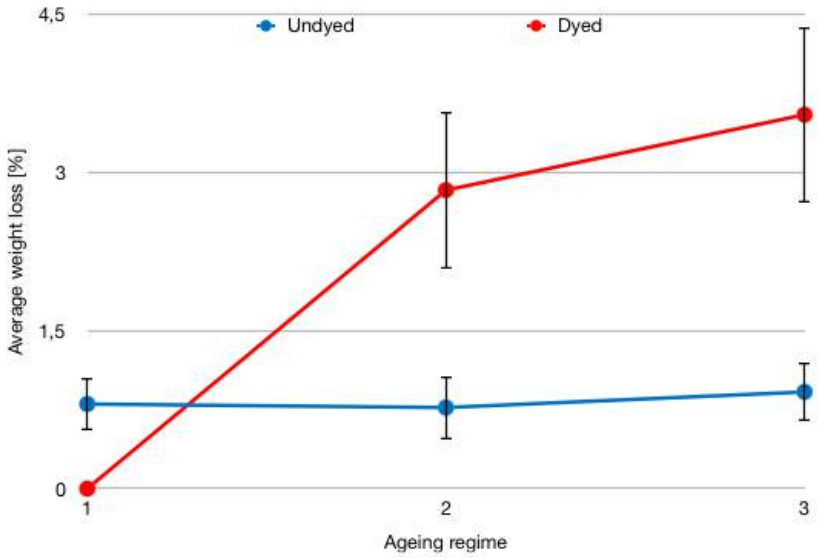

Figure 3.1: Average weight loss upon ageing for the first set of treatments. The values for the dyed samples with treatment 1 were not available.

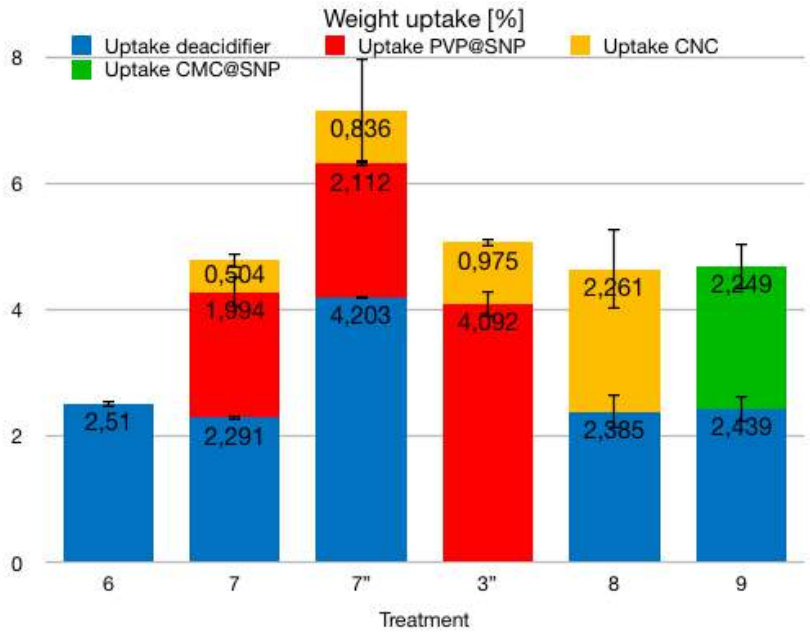

Figure 3.2: Average weight uptake for each treatment step.

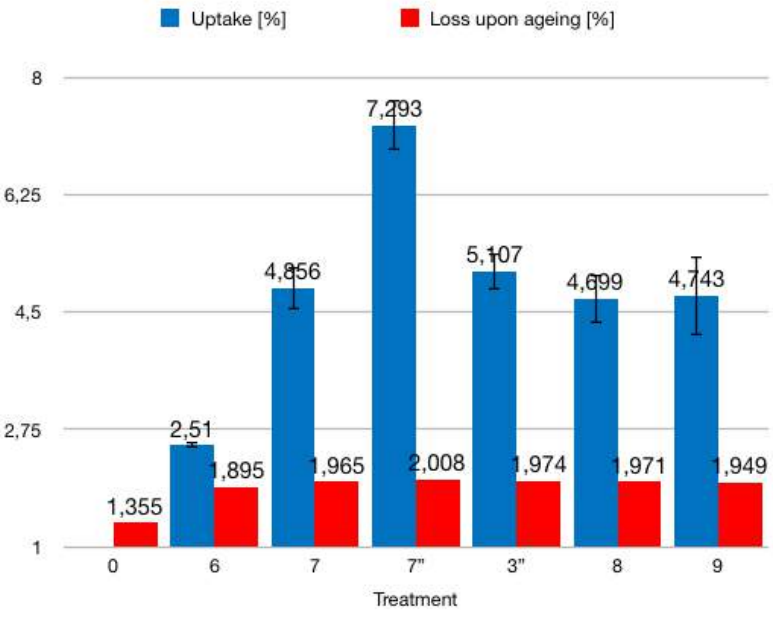

Figure 3.3: Average weight uptake and loss upon ageing for each treatment.

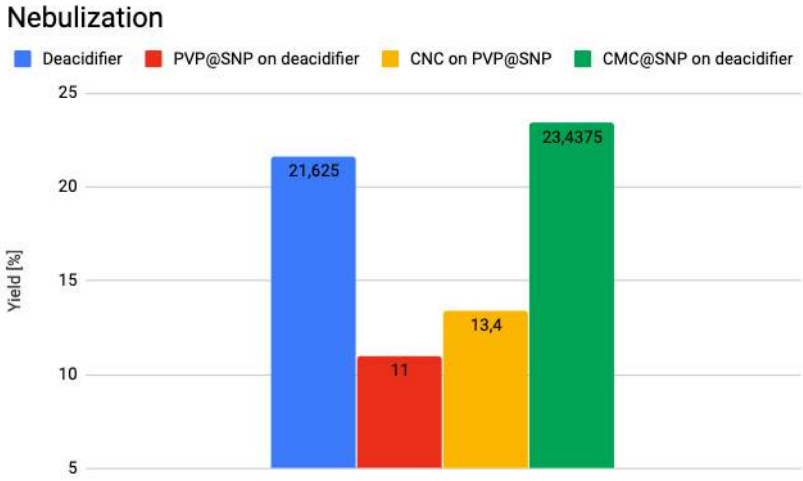

Figure 3.4: Yield values of the nebulization.

As expected the weight loss increased for more severe ageing regimes, and was much faster for the dyed compared to the undyed samples, confirming the detrimental action of the dye (Figure 3.1). It was slightly larger for the new treatments compared to the untreated sample; part of the treatment may have been lost with degradation but the uniformity of the values confirms the dependance of degradation on the dye (Figure 3.3).

3.2 Characterization

3.2.1 Tensile testing

The starting point of the thesis is the comparison of the mechanical properties between freshly-dyed [1] and naturally aged models used in this project. As shown in Figure 3.5 [1], the properties of the dyed textiles have drastically decreased compared to the undyed, confirming the detrimental action of the dye and the necessity to apply a consolidation to the textiles.

The measurements are reported in Appendix A.
Maximum force, correspondent elongation and elastic modulus of the unaged samples are reported respectively in Figures 3.6, 3.7, 3.8, 3.9. The treatments seem to improve the flexibility of the textiles and decrease their stiffness, apart from treatment 5, which stiffens the samples, expected effect of CNCs. This behavior is also confirmed by the values of the slope of the stress-strain curve at low deformation, which is the strain level real objects may be subjected

[1] Wilson's values come from the raw data of her PhD project.

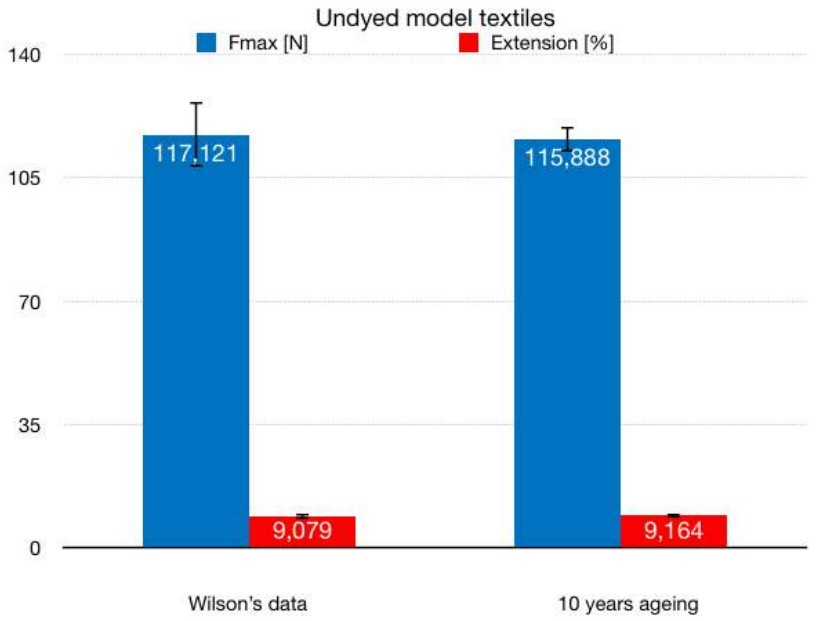

((a)) *Undyed model textiles*

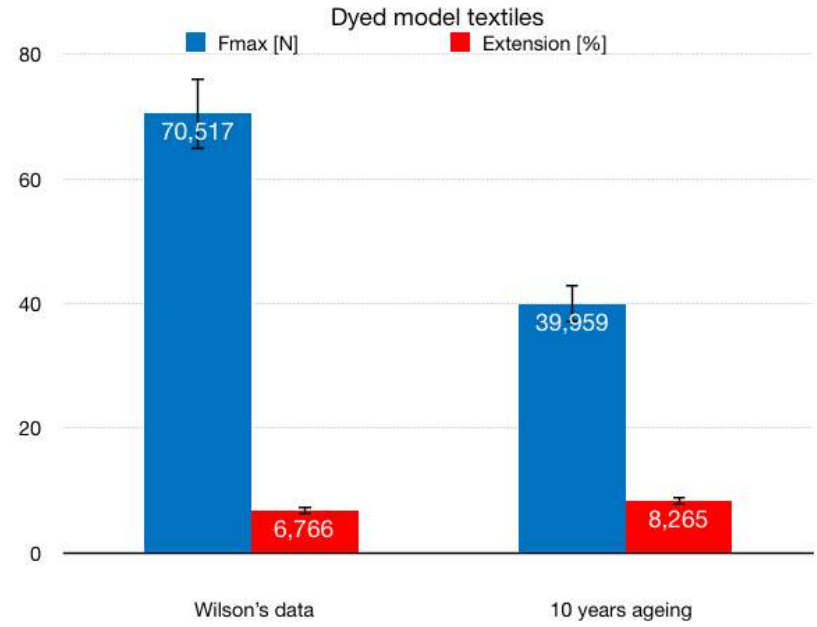

((b)) *Dyed model textiles*

Figure 3.5: Comparison of the mechanical properties of the model textiles after 10 years of natural ageing.

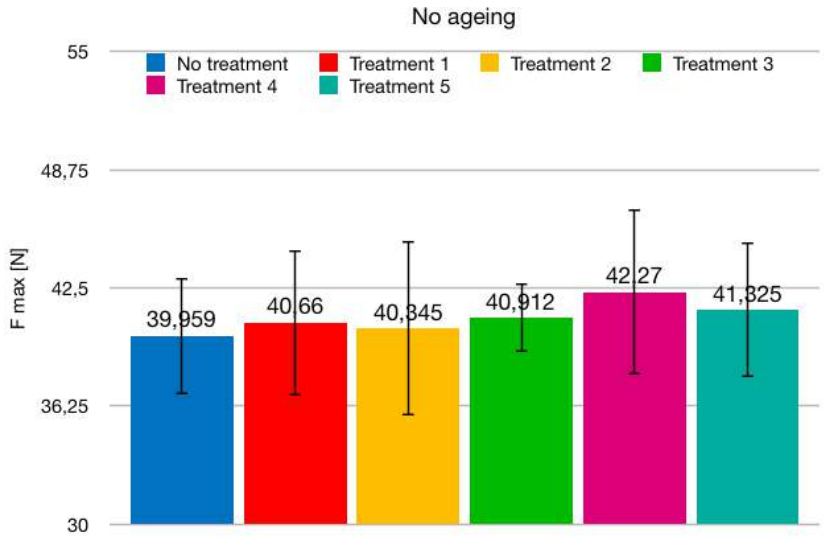

Figure 3.6: Maximum loading force of the unaged samples. The first set of treatments was applied.

to. The decreased stiffness upon treatment 3 is coherent with the enhanced flexibility (Figure 3.7) but further investigation is required to understand the causes of this behavior (Chapter 4).

The slight improvement of the mechanical properties was not preserved upon ageing (Figures 3.10, 3.11, 3.12, 3.13). The properties of the samples with treatment 1 showed a slightly more sudden decrease compared to the others, but no relevant difference compared to the untreated samples was observed. Only the stiffening at low deformation seems to be preserved, which is still a positive result considering the fact that this is the most common stress regime; the nanocellulose layer at surface may have broken down only at larger deformation, when the stiffness of the samples decreases.
The mechanical properties drastically decreased after only two weeks of ageing, confirming Wilson's observations [1] despite the lower temperature used in this project. After the first two weeks the properties kept decreasing but at a slower rate.
Ageing was much less severe; a different degradation mechanism may have been involved as some improvement of stroke at maximum was observed for treatment 5, for example.

An additional layer of treatment 1 did not cause any relevant improvement (Figures 3.14, 3.15, 3.16, 3.17). Only a slight stiffening was observed upon application of a third layer (Figures 3.16, 3.17). The amount of material deposited was not enough to achieve better consolidation as confirmed by the low weight increase (Table 3.1).

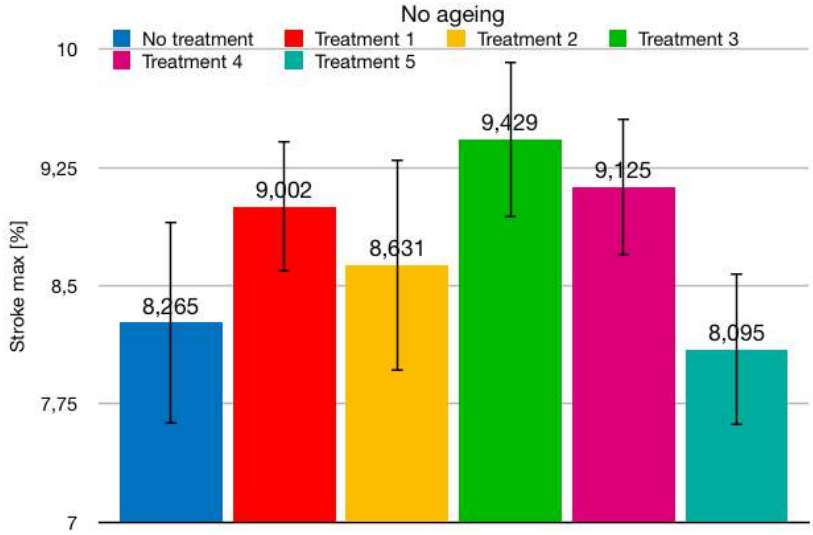

Figure 3.7: Stroke at maximum force of the unaged samples. The first set of treatments was applied.

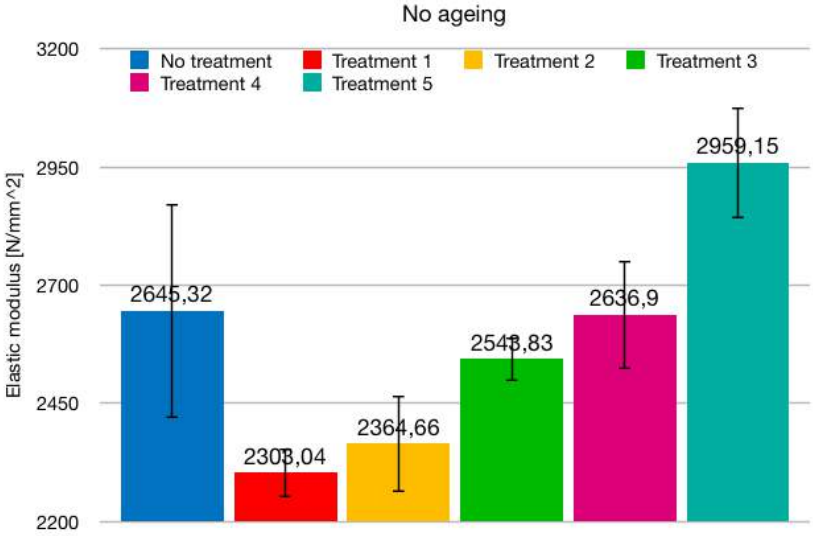

Figure 3.8: Elastic modulus of the unaged samples. The first set of treatments was applied.

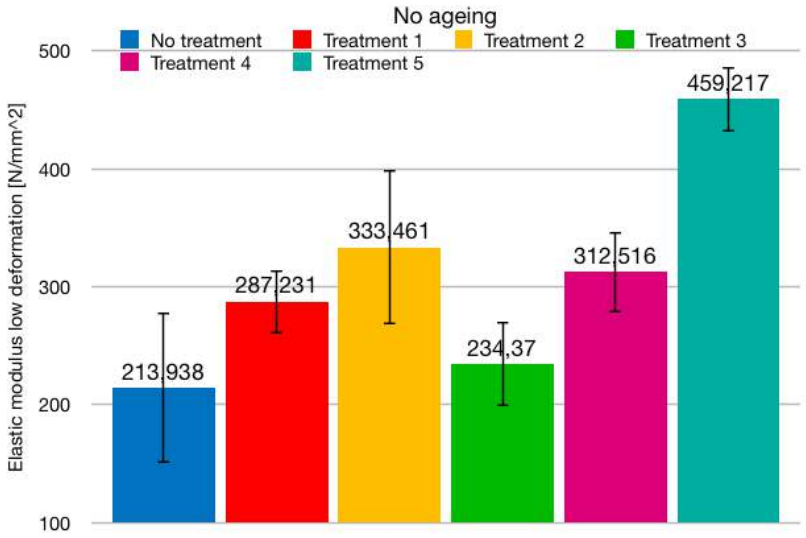

Figure 3.9: Elastic modulus at low deformation of the unaged samples. The first set of treatments was applied.

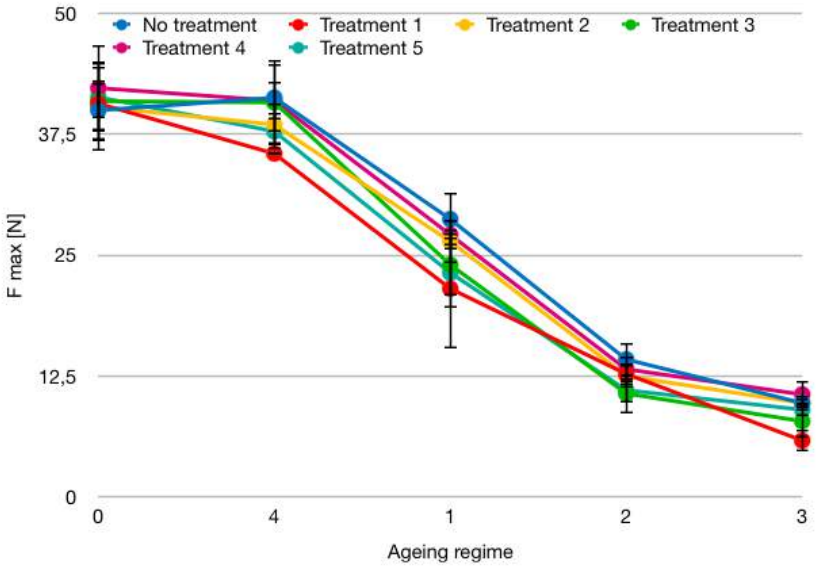

Figure 3.10: Maximum force upon ageing. The first set of treatments was applied.

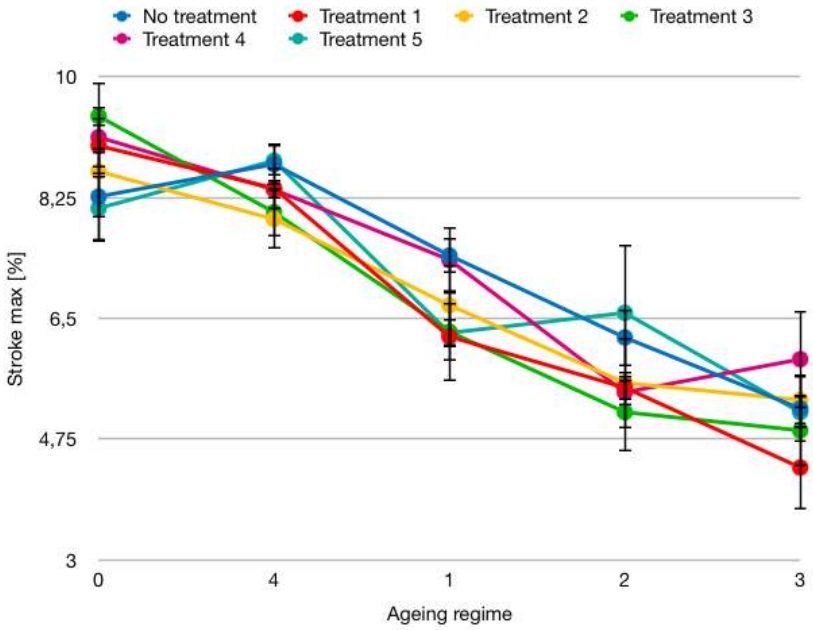

Figure 3.11: Stroke at maximum force upon ageing. The first set of treatments was applied.

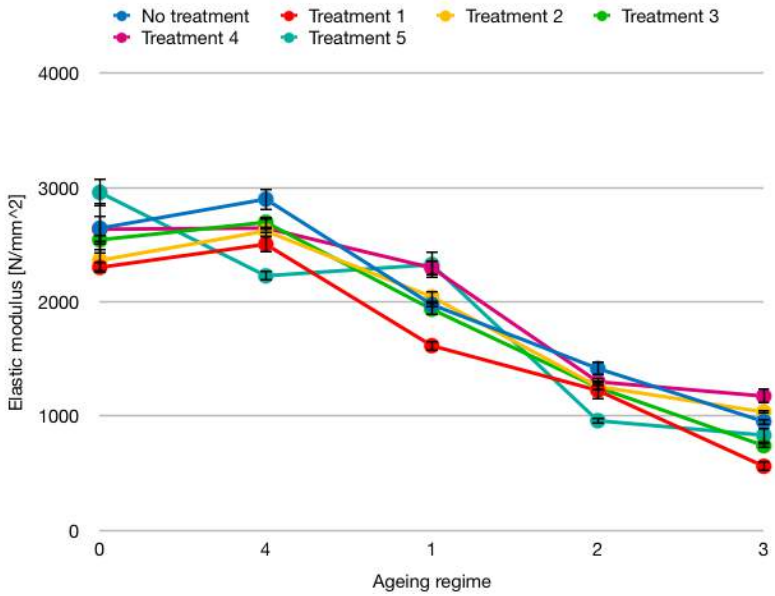

Figure 3.12: Elastic modulus upon ageing. The first set of treatments was applied.

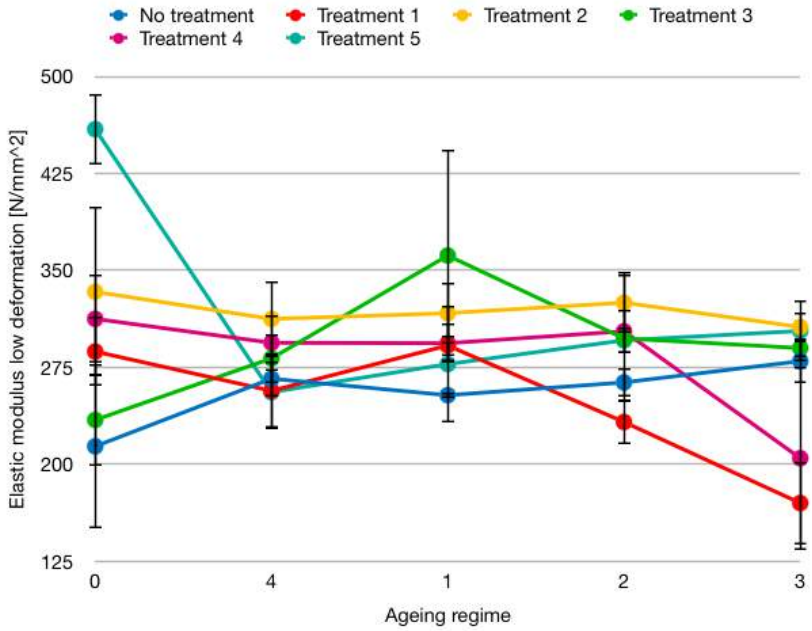

Figure 3.13: Elastic modulus at low deformation upon ageing. The first set of treatments was applied.

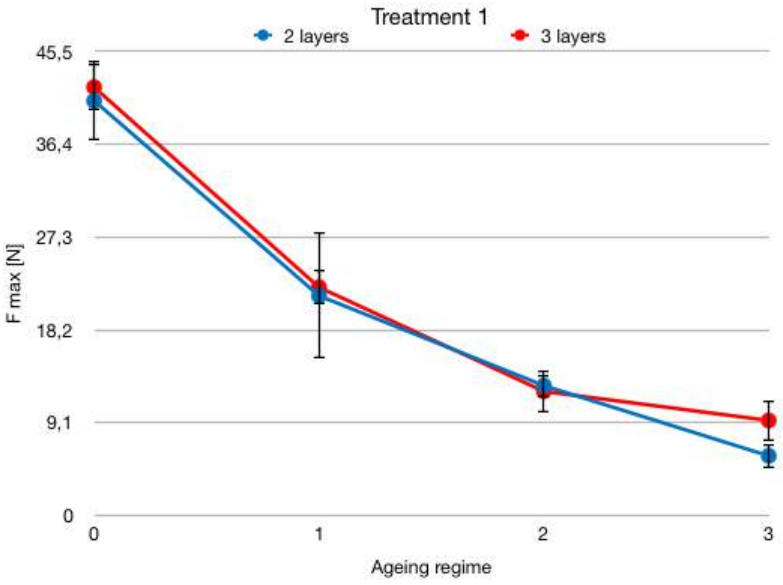

Figure 3.14: Maximum force upon ageing for samples with 2 or 3 layers of treatment 1.

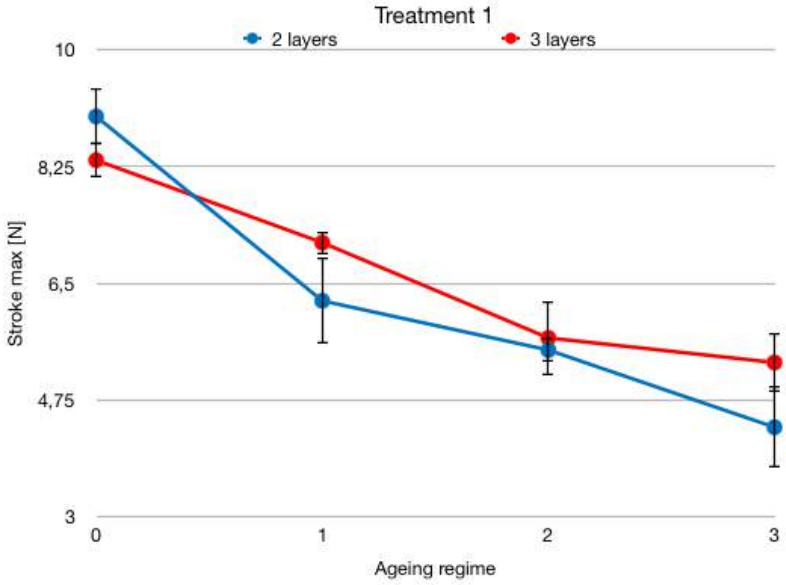

Figure 3.15: Stroke at maximum force upon ageing for samples with 2 or 3 layers of treatment 1.

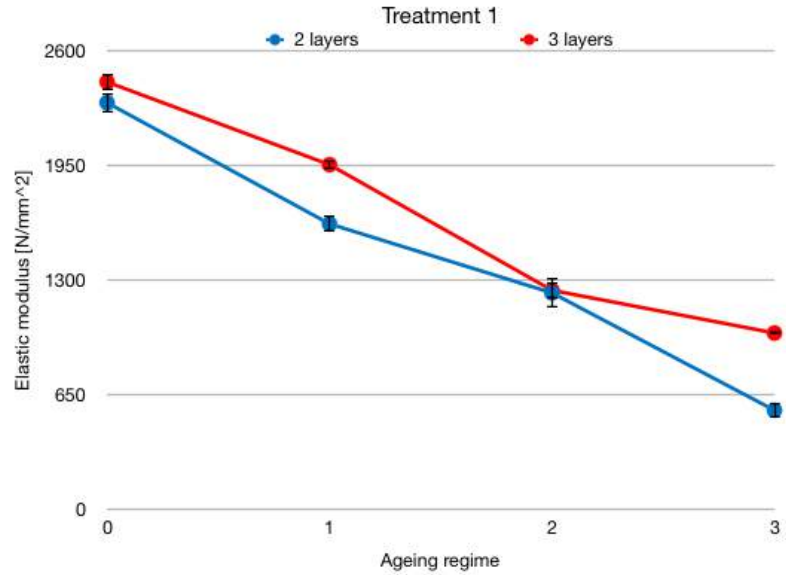

Figure 3.16: Elastic modulus upon ageing for samples with 2 or 3 layers of treatment 1.

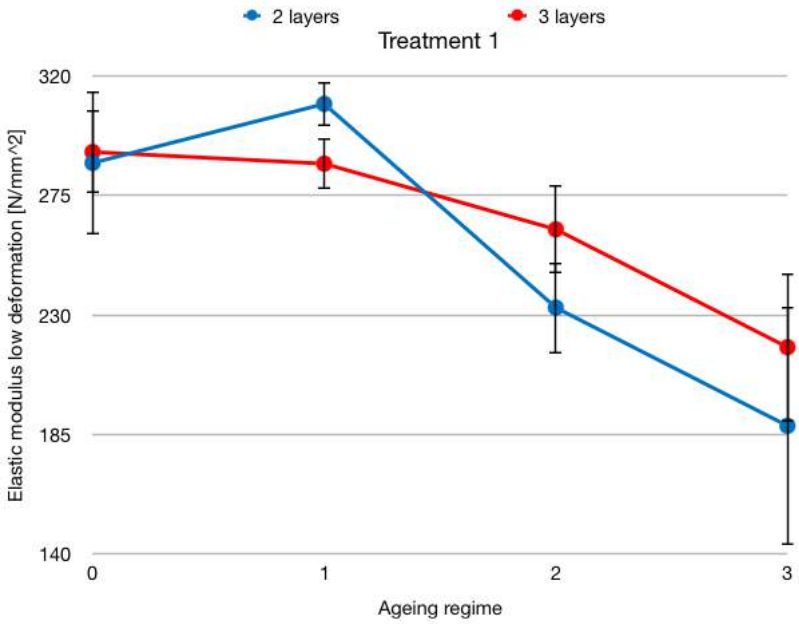

Figure 3.17: Elastic modulus at low deformation upon ageing for samples with 2 or 3 layers of treatment 1.

As discussed in 3.2.2, considering both the decrease of mechanical properties and of pH, two are the possible main reasons for the lack of effective consolidation:

- lack of deacidifier (consolidation alone was not able to withstand the degradation continuously occurring during accelerated ageing);
- low yield of nebulization, (much less material than expected was actually deposited, not enough to see the effects of consolidation).

New set of treatments

The measurements are reported in Figure A.6.
Treated samples performed better not only before but also after ageing (Figures 3.18, 3.19, 3.20, 3.21). Treatment 6 did not provide any consolidation but was essential to stop or slow down degradation, as shown by the pH measurements (3.2.2). This explains why treatment 3" behaved worst (weaker, less extensible, stiffer samples) than 7" though the same amount of consolidation (Figure 3.2), and confirms the results of the previous treatments, thus the necessity of a deacidifier. The application by brushing considerably increased strength and stiffness at low deformation, but had not a significant effect on extensibility

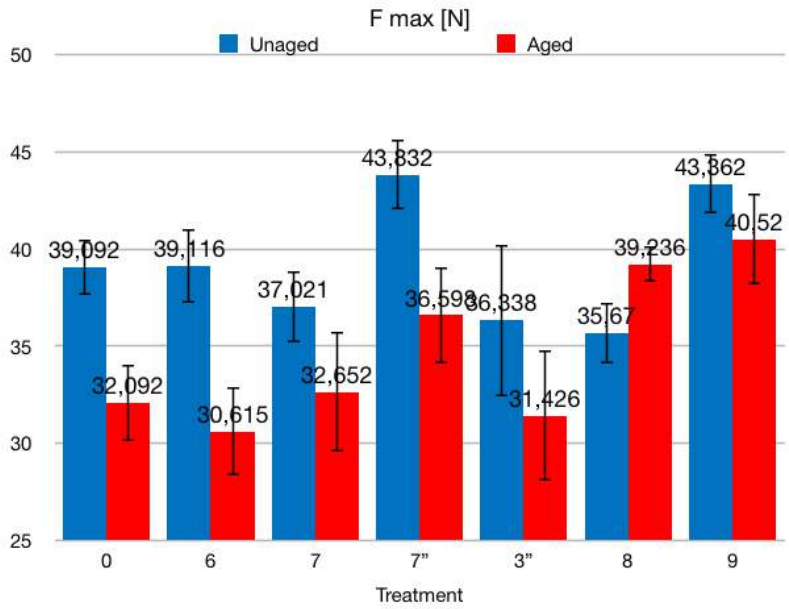

Figure 3.18: Maximum loading force of unaged and aged samples with the new set of treatments.

and overall stiffness; deacidification rather than weight uptake seems to have a crucial role for an effective consolidation. CNCs confirmed their beneficial effect on stiffness and strength as shown by the results of treatment 8; the presence of cellulosic material in the shell covering SNPs in treatment 9 may have had the same effect. It seems to perform better thanks to a right balance of deacidifier, silica and cellulose.

3.2.2 pH measurements

pH measurements confirmed the ongoing degradation of dyed samples. The already acidic pH (due to carboxyl and hydroxyl groups of tannic acid) lowered more and more upon ageing while it was almost unvaried for the undyed samples (Figure 3.22).
The alkalinity of silica was not enough to withstand the acidic environment induced by degradation either due to too few amount of material deposited or intrinsic not effectiveness compared to the sites where acid hydrolysis and oxidation occur. Deacidification seems to be necessary to evaluate the effectiveness of the consolidating material. A slightly alkaline pH may be required to neutralize acidic compounds as proved for paper [17] in order to guarantee minimal catalytic activity of Fe and Cu ions (Figure 3.23(a)), and avoid the formation of radicals as well as the acid hydrolysis of cellulose.

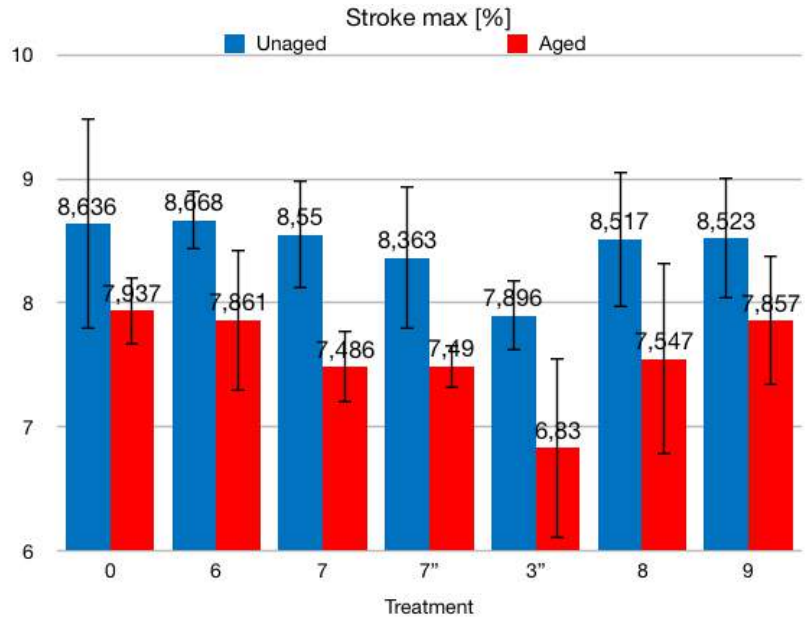

Figure 3.19: Stroke at maximum force of unaged and aged samples with the new set of treatments.

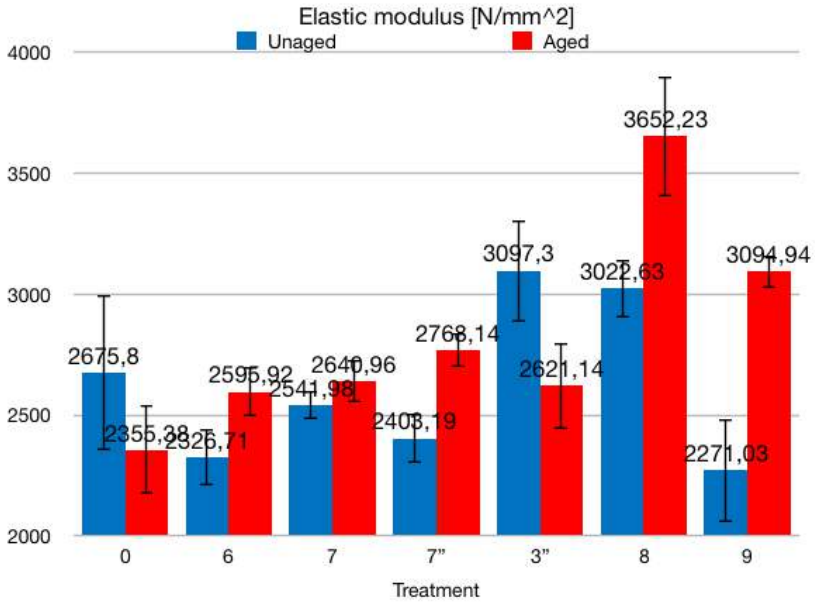

Figure 3.20: Elastic modulus of unaged and aged samples with the new set of treatments.

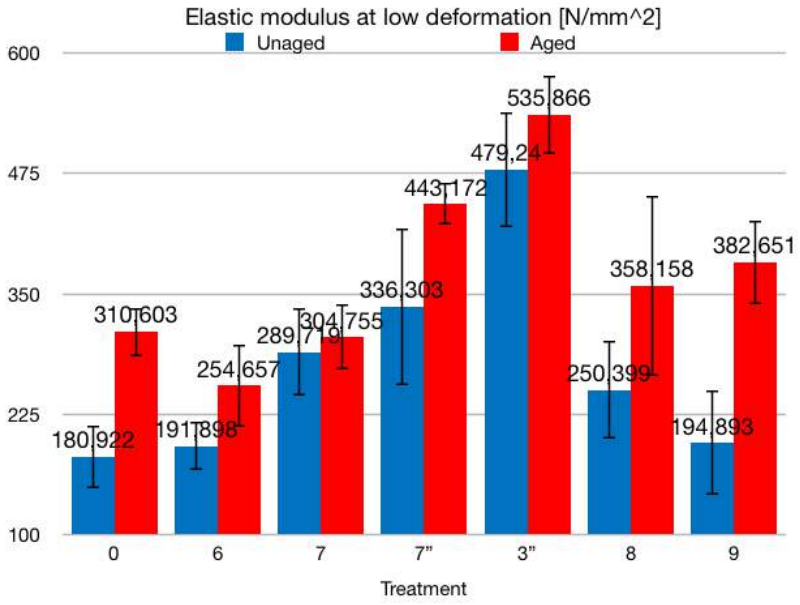

Figure 3.21: Elastic modulus at low deformation of unaged and aged samples with the new set of treatments.

Calcium compounds are preferred over magnesium ones on paper because the higher water solubility of the latter may lead to higher pH (> 9) [13].

New set of treatments

The deacidifier successfully increased the pH around neutrality even upon ageing (Figure 3.23(b)), as confirmed by good surface coverage and penetration of $CaCO_3$ NPs (3.2.4).

3.2.3 Colorimetry

Figure 3.25 shows the effect of the treatments on the color of the textiles.
The color of the undyed samples was almost unaffected apart from the increase in brightness.
The treatment which caused the largest color change on the dyed samples was the third one, maybe due to the polymeric component of PVP. All of the treatments also darkened the sample (negative L* component), an acceptable and even desirable effect to enhance the blackness provided by the dye [1]. Treatment 1 did not cause a perceivable change in color, even less than treatment 4, which most likely resulted just in the application of water and 2-propanol. Though the presence of PEI [6] treatment 2 caused no yellowing of

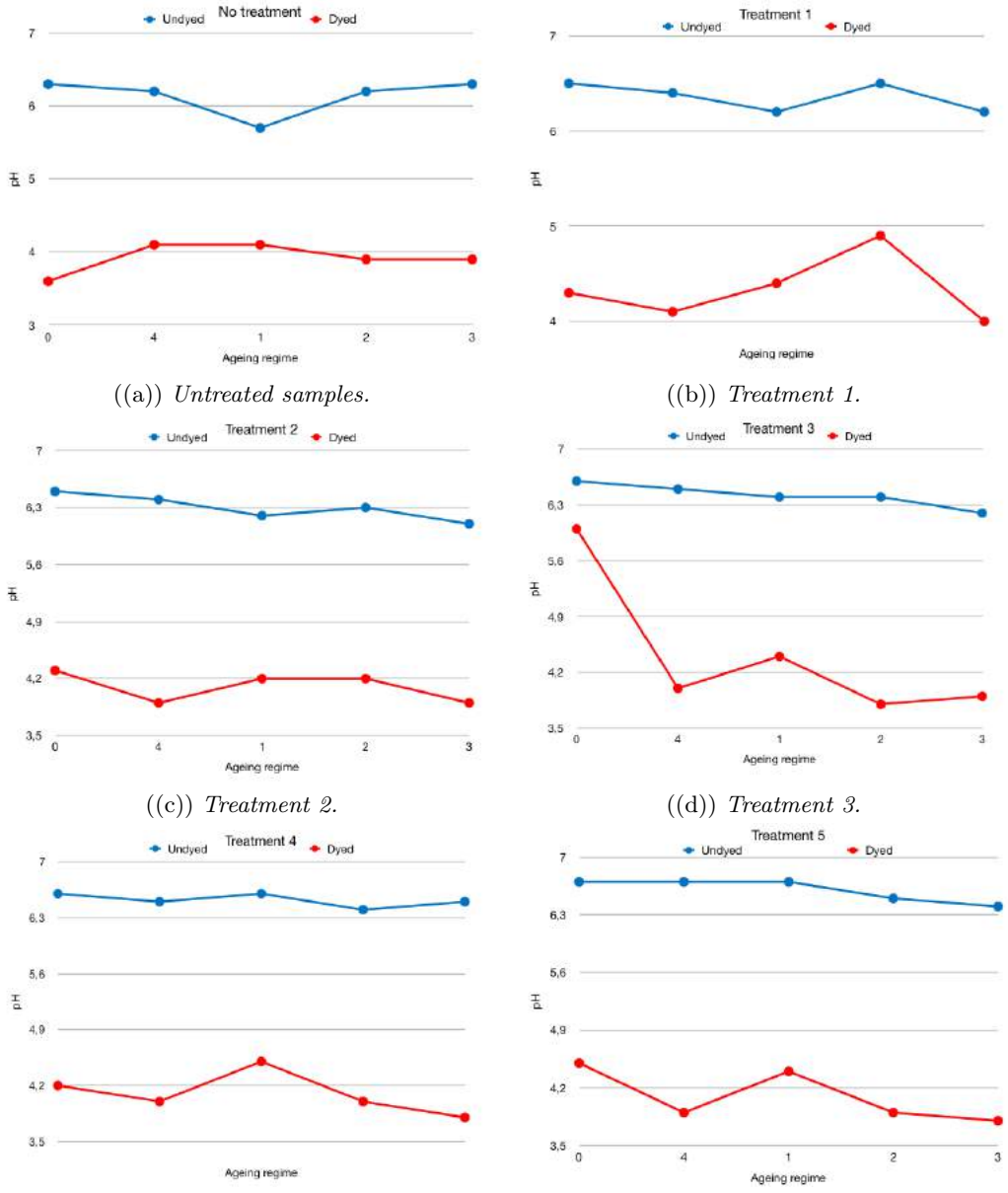

((a)) *Untreated samples.*

((b)) *Treatment 1.*

((c)) *Treatment 2.*

((d)) *Treatment 3.*

((e)) *Treatment 4.*

((f)) *Treatment 5.*

Figure 3.22: Effects of the ageing on the pH.

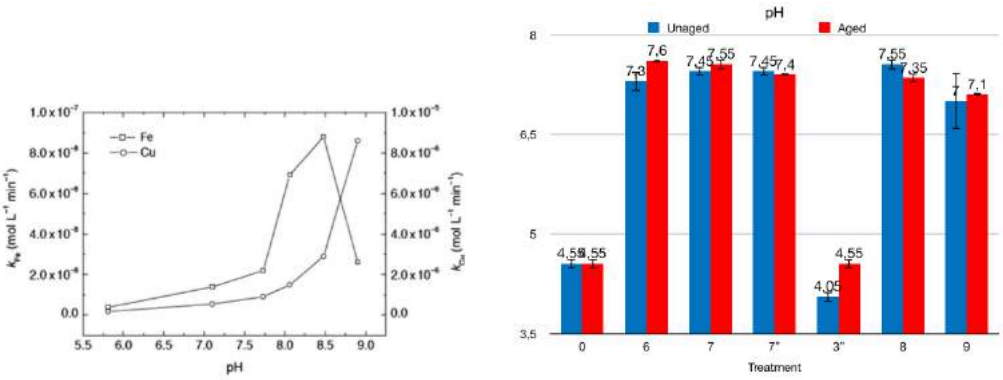

((a)) *Reaction rate constants for systems containing iron or copper ions at 25°C [36].*

((b)) *pH of unaged and aged samples.*

Figure 3.23: Alkalinity and pH of new set of treatments

the dyed textile, which occurred in very small amount only upon application of treatments 1 and 5. The increase in redness was also low for all of the treatments.

Figures 3.27, 3.28, 3.29, 3.30, 3.31 show the behavior of each color component, the overall dE and the brightness upon ageing of each treatment on both dyed and undyed textiles. Hardly any change was observed on the undyed samples, and only due to the yellow component, especially for treatment 2 at more severe ageing (maybe enhanced by the presence of PEI [6]). The dyed textiles showed larger changes in color and brightness, following the same trend observed upon tensile testing (3.2.1), which clearly relates the degradation to the presence of the dye. All the treatments darkened upon ageing; the increase in redness (positive da* component) and yellowness (positive db* component) followed the same trend for both treated and untreated samples, while the brightness decreased a bit more on treated samples. Darkness seems to be dependent on the applied treatments, the color change mostly on degradation, so the browner color is caused by the break-down of the iron-tannate complexes. This behavior is coherent with the almost null change of color of the undyed samples. An initial yellowing is observed only upon treatment 5, maybe due to the thicker layer of cellulose nanocrystals at surface. As shown in Figure 3.24, treatment 3 initially increases the blue component instead, maybe desirable on naturally aged objects yellowed with time. The largest yellowing upon ageing is observed on untreated samples indicating that the application of the treatments generally does not affect the color, or even helps to partially recover the original black color.

No relevant color/brightness changes were observed upon application of 2 or 3 layers of treatment 1, confirming the results of the tensile tests (Figures 3.32,

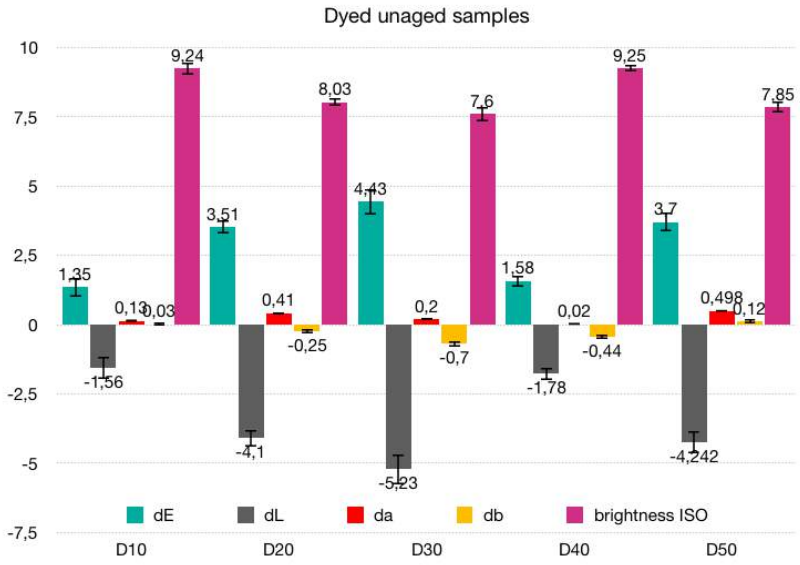

Figure 3.24: Effect of the treatments on the color of the dyed samples.

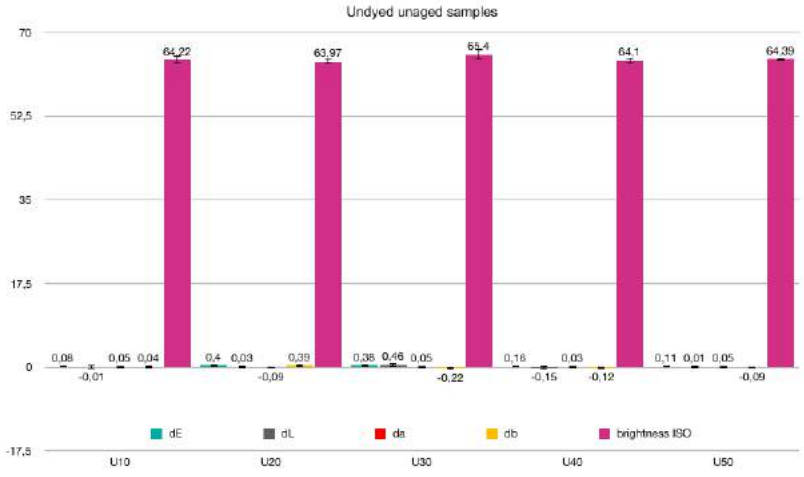

Figure 3.25: Effect of the treatments on the color of the undyed samples.

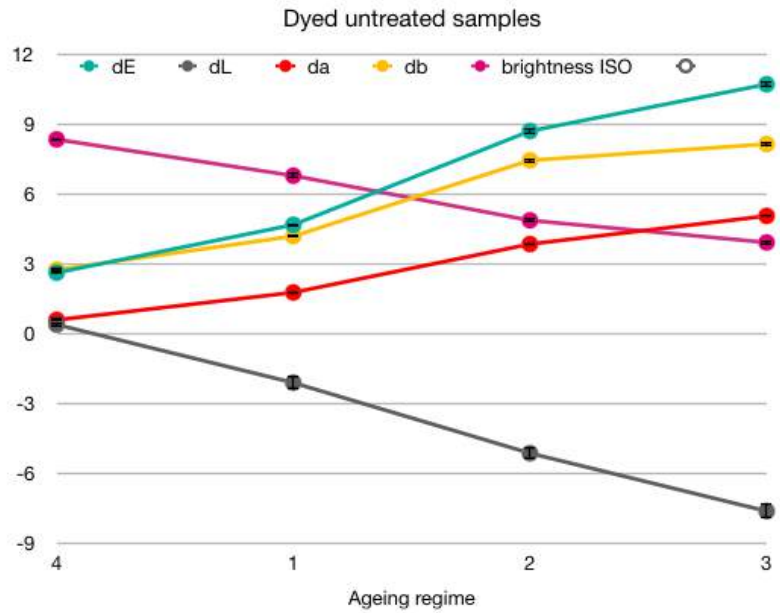

((a)) *Dyed samples.*

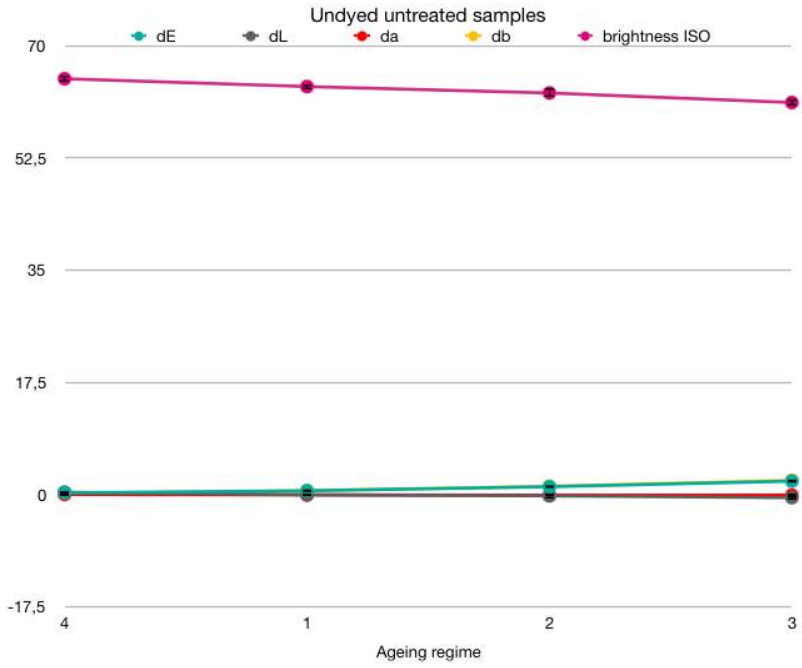

((b)) *Undyed samples.*

Figure 3.26: Effect of the ageing on the color of the untreated samples.

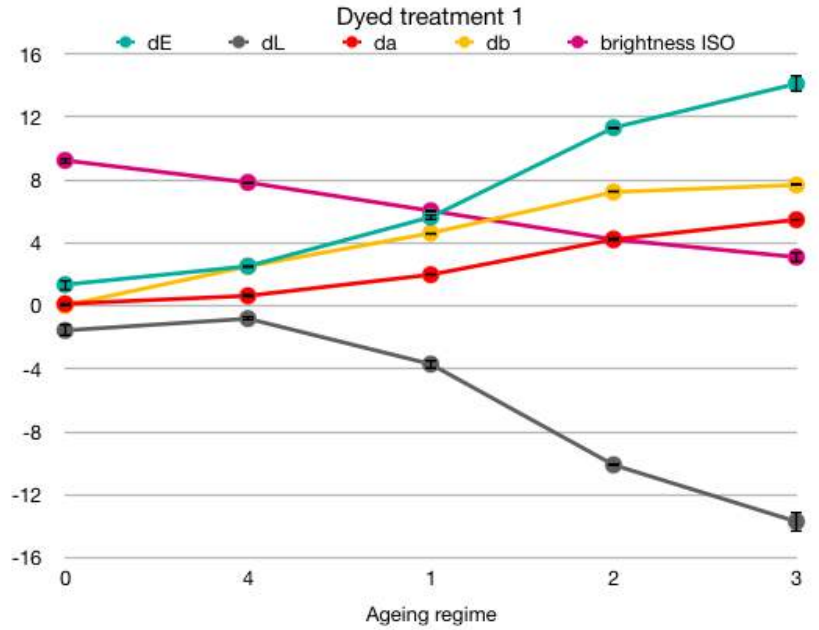

((a)) *Dyed samples.*

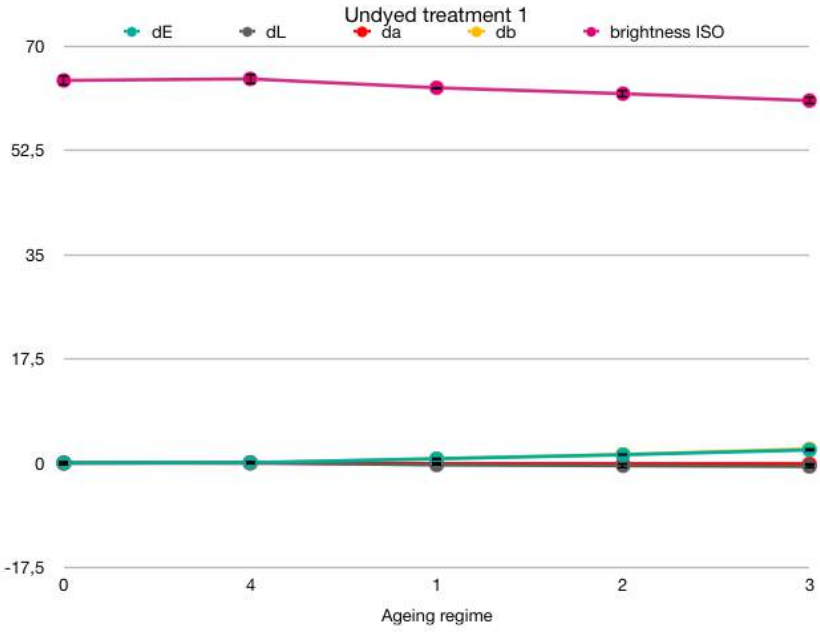

((b)) *Undyed samples.*

Figure 3.27: Effect of the ageing on the color of the samples with treatment 1.

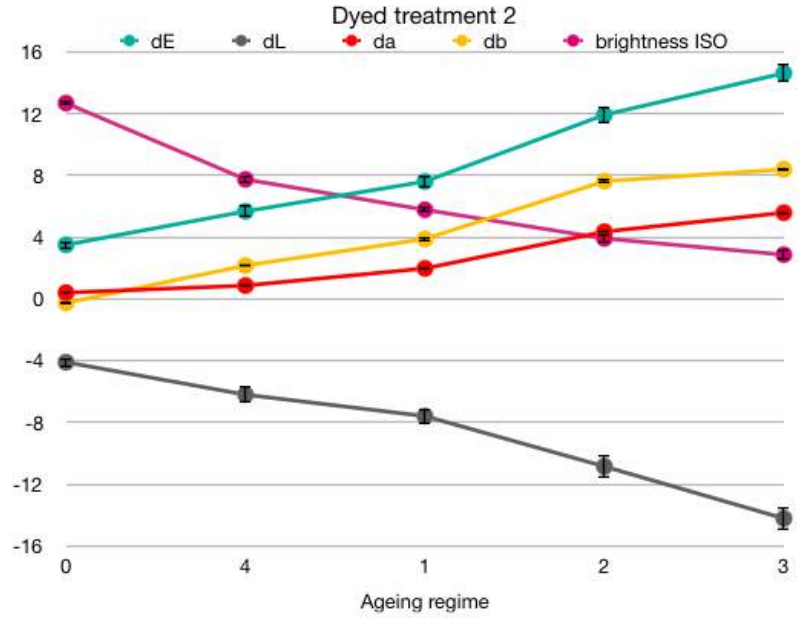

((a)) *Dyed samples.*

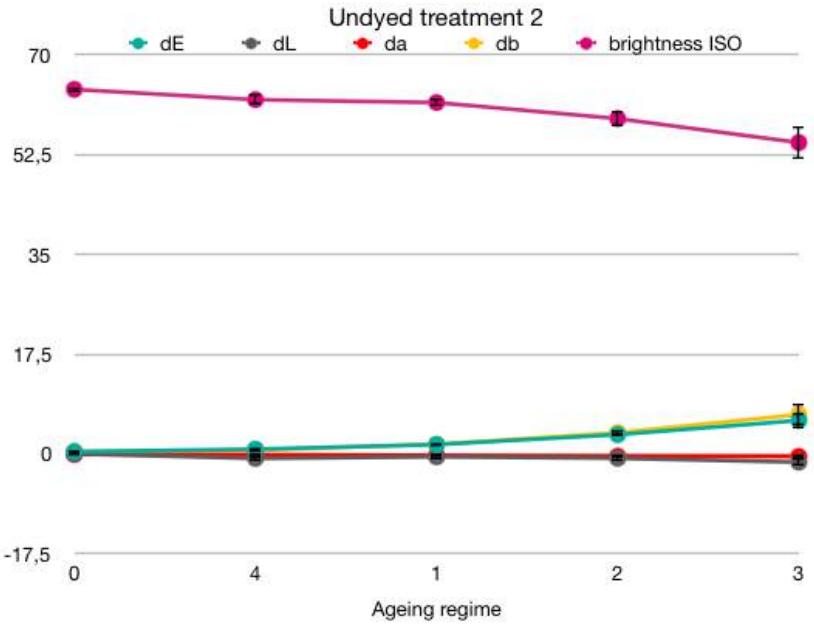

((b)) *Undyed samples.*

Figure 3.28: Effect of the ageing on the color of the samples with treatment 2.

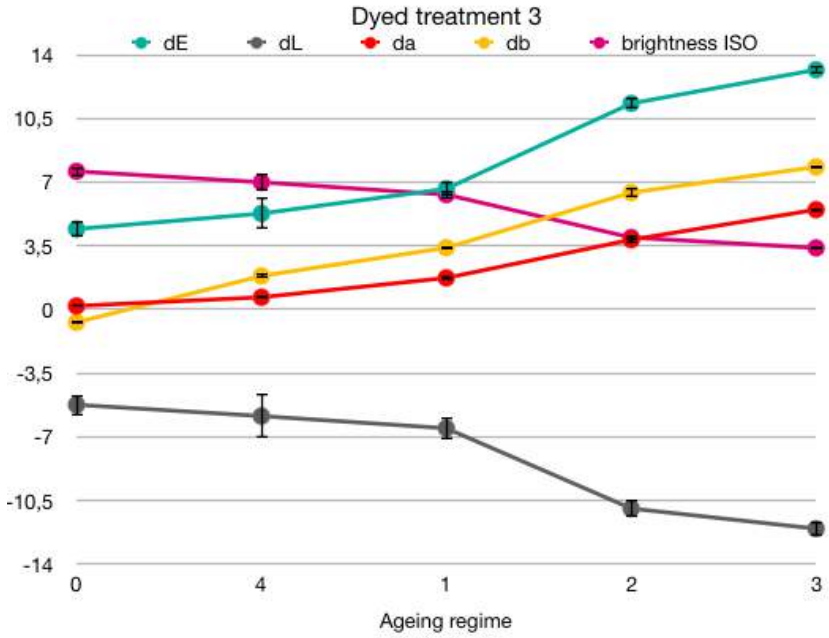

((a)) *Dyed samples.*

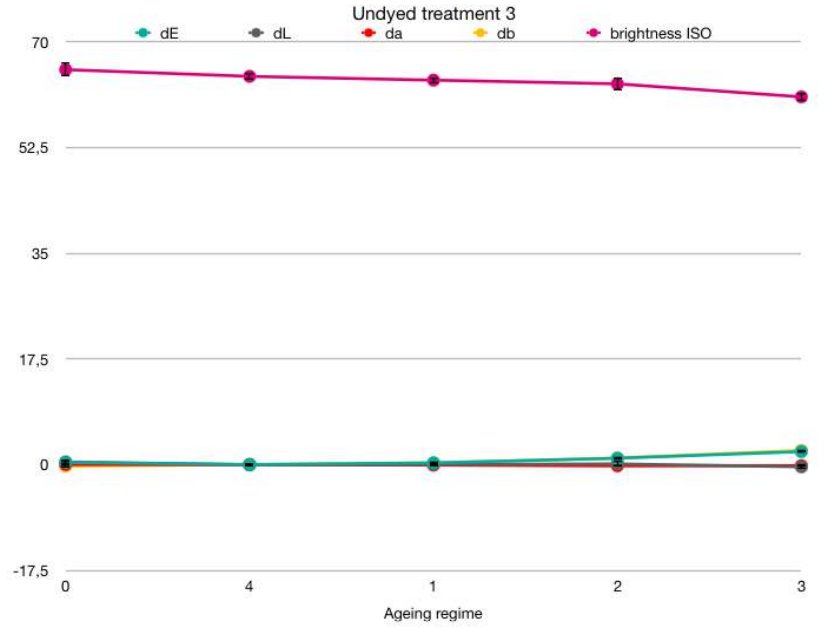

((b)) *Undyed samples.*

Figure 3.29: Effect of the ageing on the color of the samples with treatment 3.

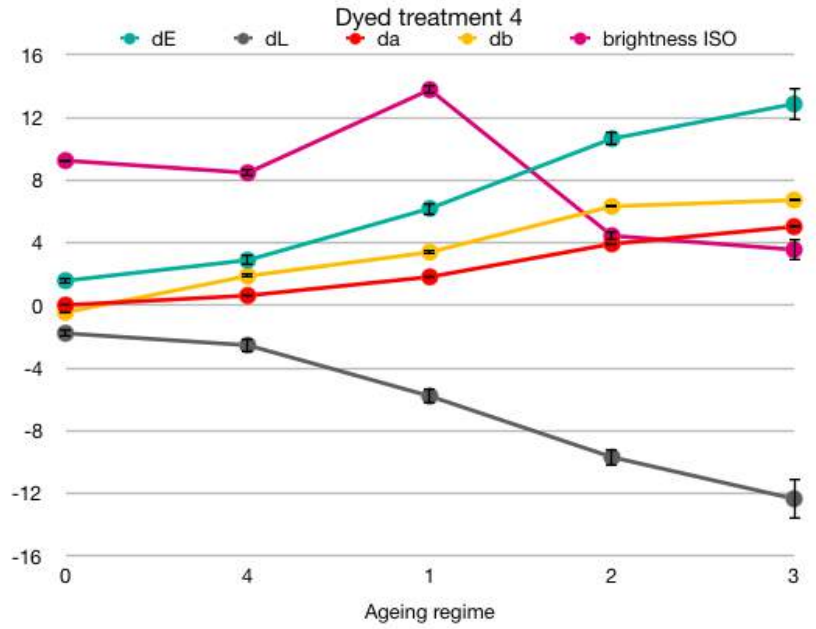

((a)) *Dyed samples.*

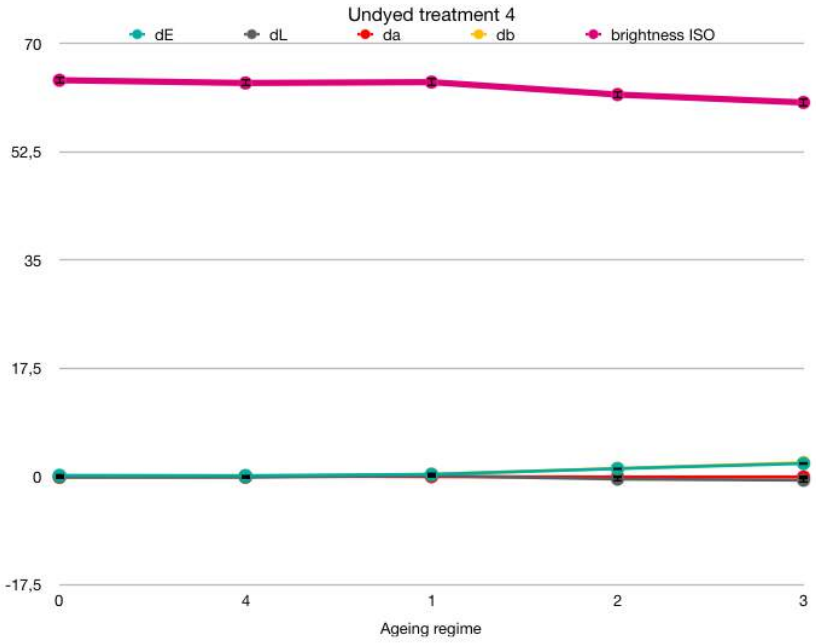

((b)) *Undyed samples.*

Figure 3.30: Effect of the ageing on the color of the samples with treatment 4.

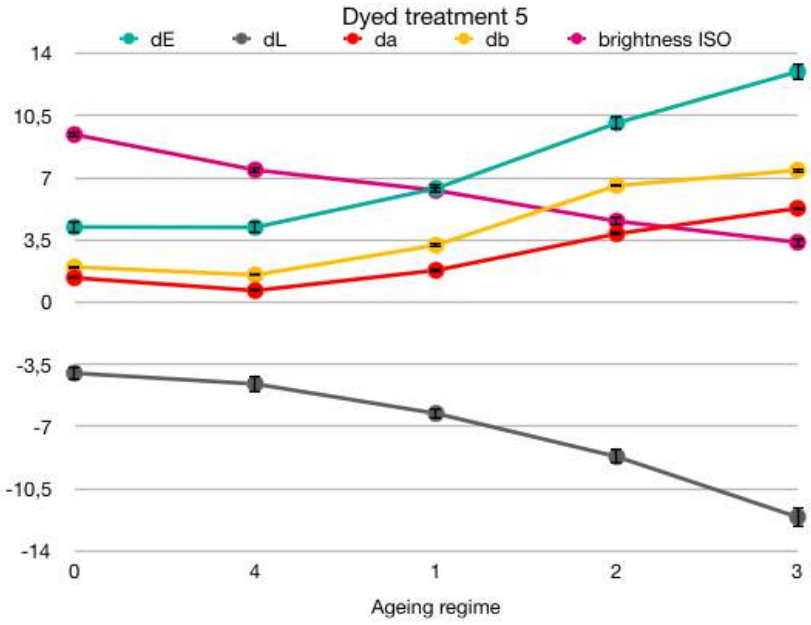

((a)) *Dyed samples.*

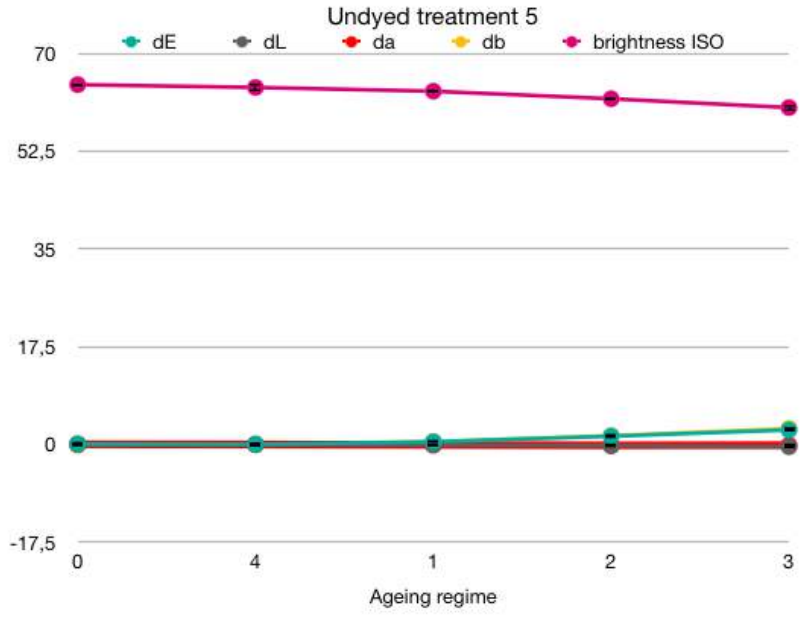

((b)) *Undyed samples.*

Figure 3.31: Effect of the ageing on the color of the samples with treatment 5.

3.33). The differences tended to decrease upon ageing, so the color should not be much affected by the application of more consolidating material.

New set of treatments

Apart from treatment 3" color differences decreased upon ageing for all the samples (Figure 3.34(a)); the comparison between treatments 3" and 7" shows that larger color differences can be attributed to the deacidifier, but also that these tend to decrease upon ageing, confirming the beneficial action of deacidification against degradation of the substrate. All the color components except db* follow this behavior; ageing causes yellowing of all the samples, especially 7" and 3" which had a larger weight uptake (Figure 3.35(c)). The deacidifier increases the redness proportionally to its amount; degradation enhances even more this component as for treatments 6 and 3" (Figure 3.35(b)). All the treatments, and especially treatment 9 (Figure 3.35(a)) darkened the samples; CMC@SNPs seem to enhance this behavior as proved by the larger dL*, whose value further proves the ongoing degradation of samples 6 and 3". Both deacidifier and CMC@SNPs mitigate the increase in brightness, whose change seems to depend more on treatments than on degradation (Figure 3.34(b)).

The application of NC reduces the color change on samples treated with SNPs by decreasing the darkening (Figures 3.37, 3.40, 3.41); it has the opposite effect on the samples treated with only the deacidifier, where it increases red and blue components (Figure 3.38).
The larger amount of SNPs applied by brushing mostly affected red and yellow components (Figures 3.37, 3.40).

3.2.4 SEM

SEM images of unaged samples show different surface morphology for some of the treated samples (Figure 3.42). Treatments 1, 2 and 3 seem to have successfully deposited SNPs which appear especially agglomerated in form of spots (Figures 3.42(b), 3.42(c), 2.1.3)), as proved by EDX (3.2.4). The sample with treatment 4 (Figure 3.42(d)) has the same morphology of the untreated one, and no magnesium was detected (3.2.4), as expected after measuring weight and pH before and after ageing.
It is difficult to evaluate the presence of a nanocellulose layer at surface as the composition is the same of the substrate and no particular feature is distinguishable.

The aged samples are clearly degraded: most fibers are broken and the silicon spots are more rare (Figure 3.43). Silicon agglomerates may have spread out

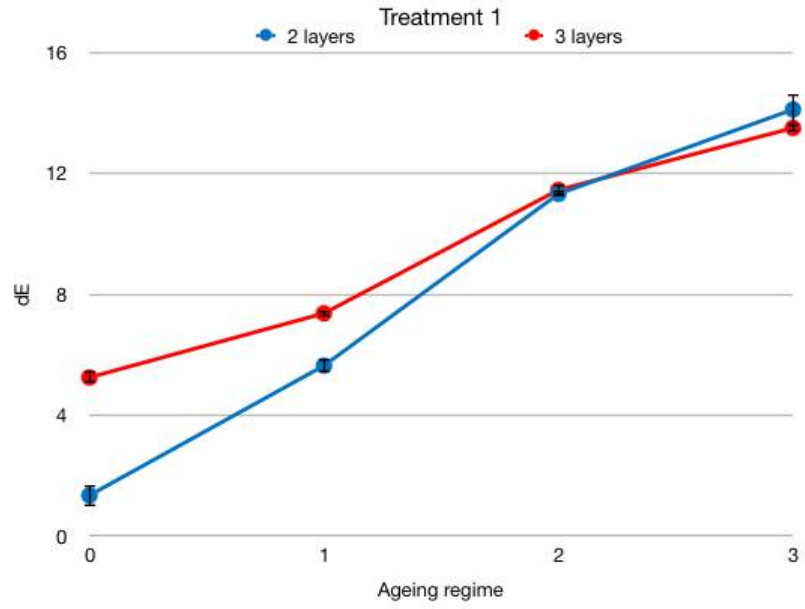

((a)) *dE*

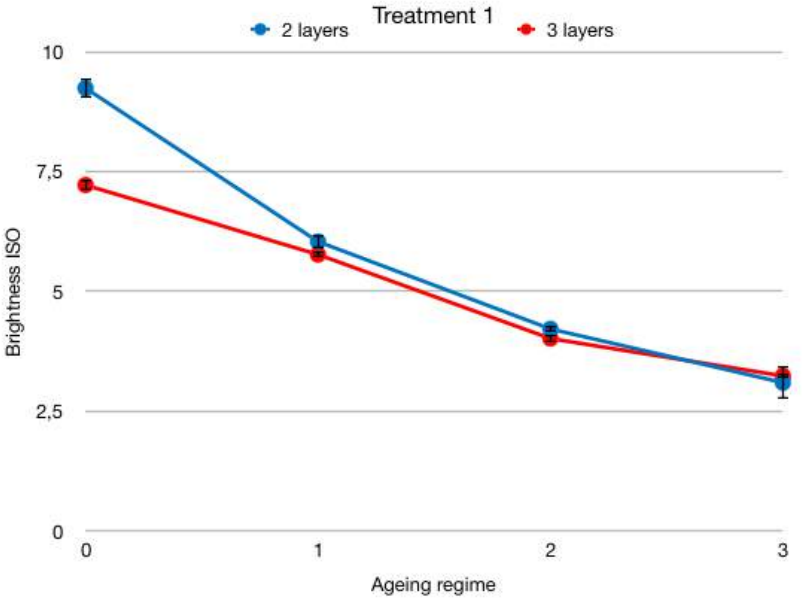

((b)) *Brightness ISO*

Figure 3.32: Effect of the ageing on the color of the samples with 2 or 3 layers of treatment 1.

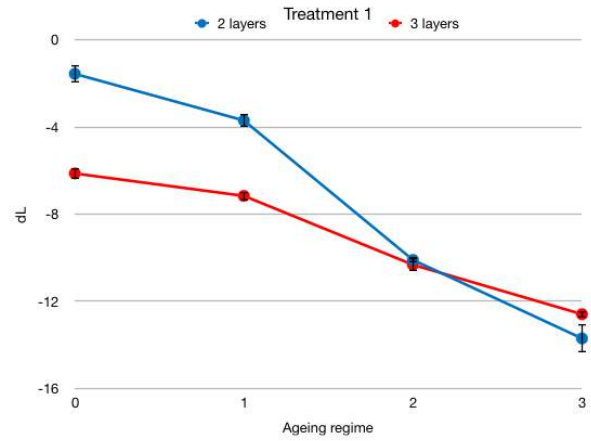

((a)) $dL*$

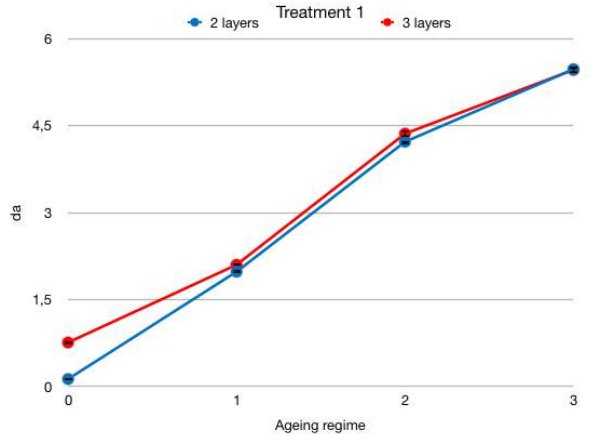

((b)) $da*$

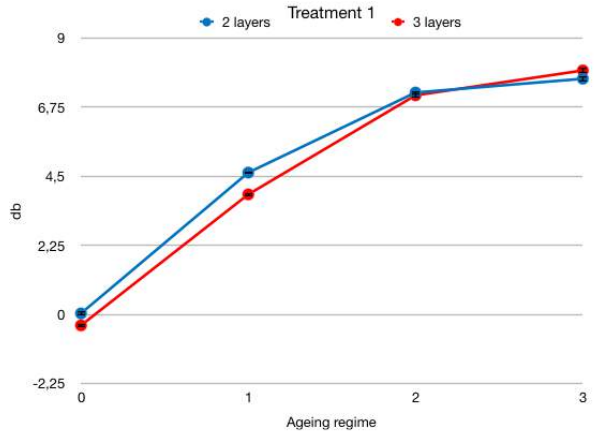

((c)) $db*$

Figure 3.33: Effect of the ageing on the color components of the samples with 2 or layers of treatment 1.

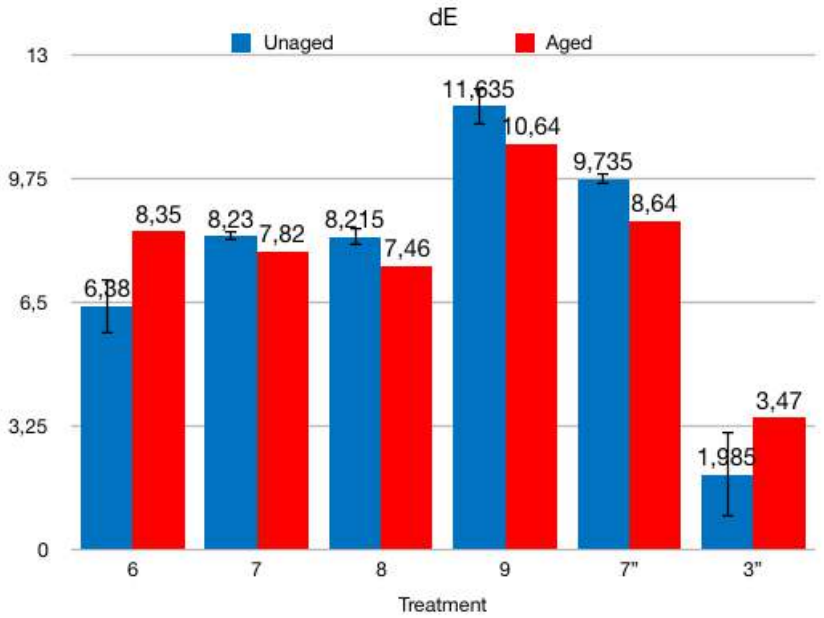

((a)) *dE*

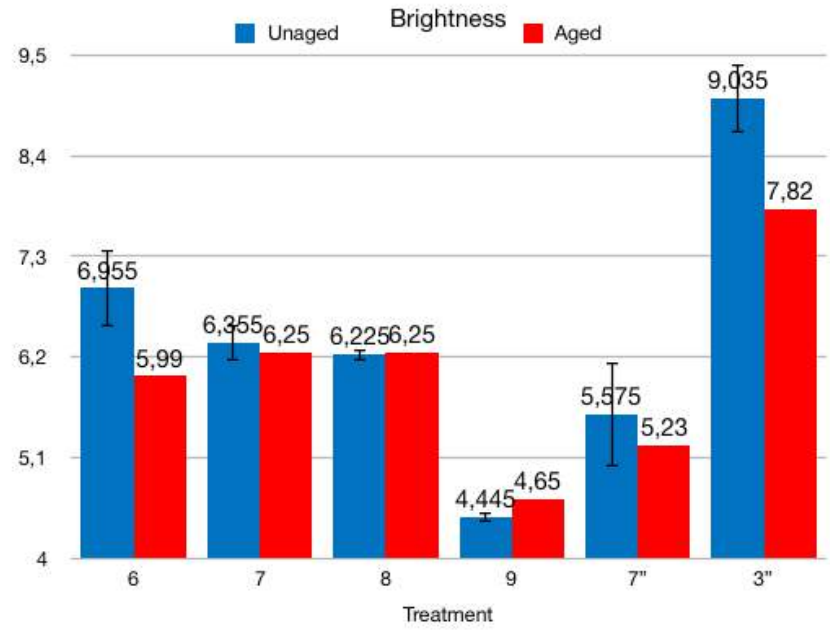

((b)) *Brightness*

Figure 3.34: Color differences between unaged and aged samples.

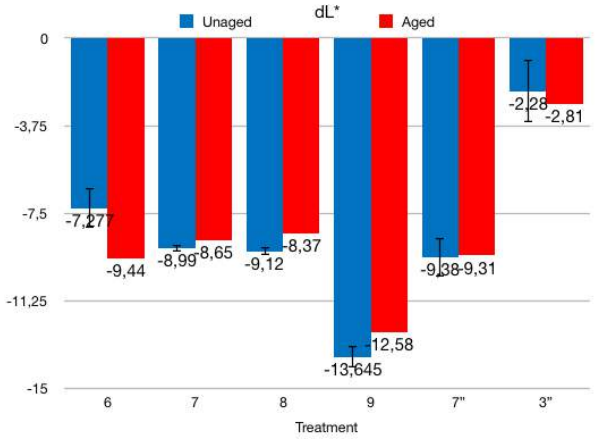

((a)) $dL*$

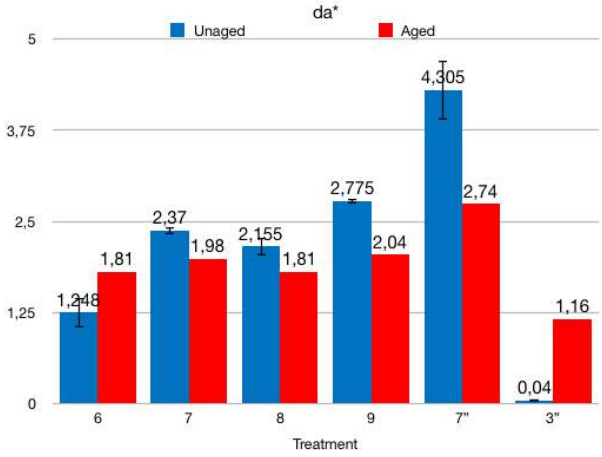

((b)) $da*$

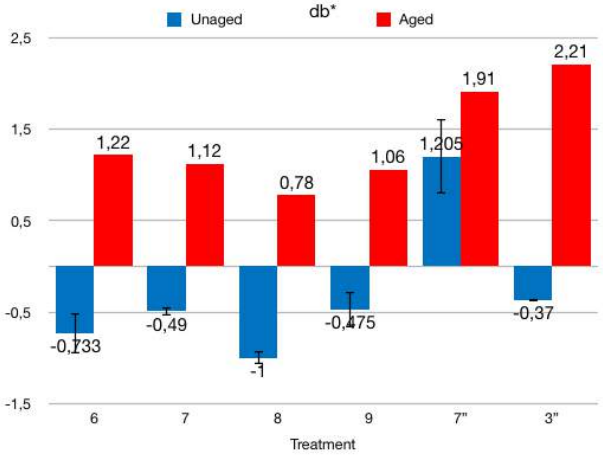

((c)) $db*$

Figure 3.35: Color space differences between unaged and aged samples.

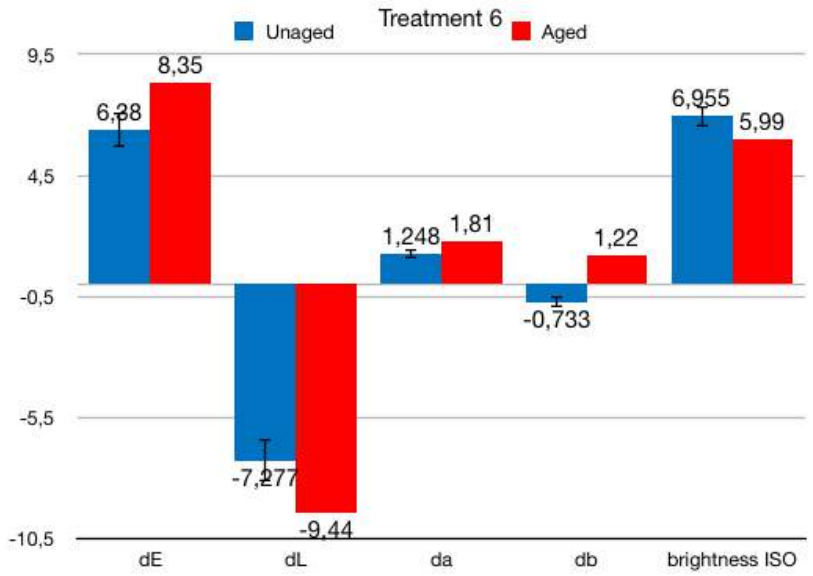

Figure 3.36: Colorimetric analysis of samples with treatment 6.

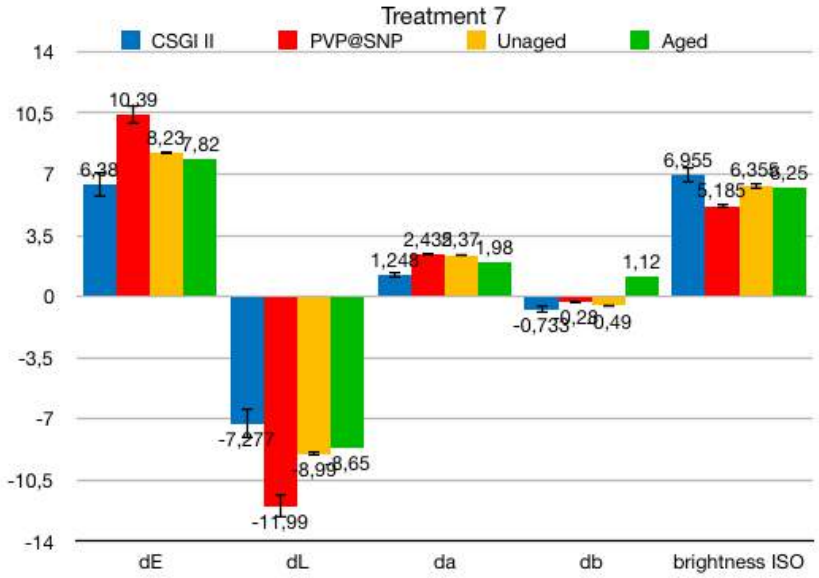

Figure 3.37: Colorimetric analysis of samples with treatment 7.

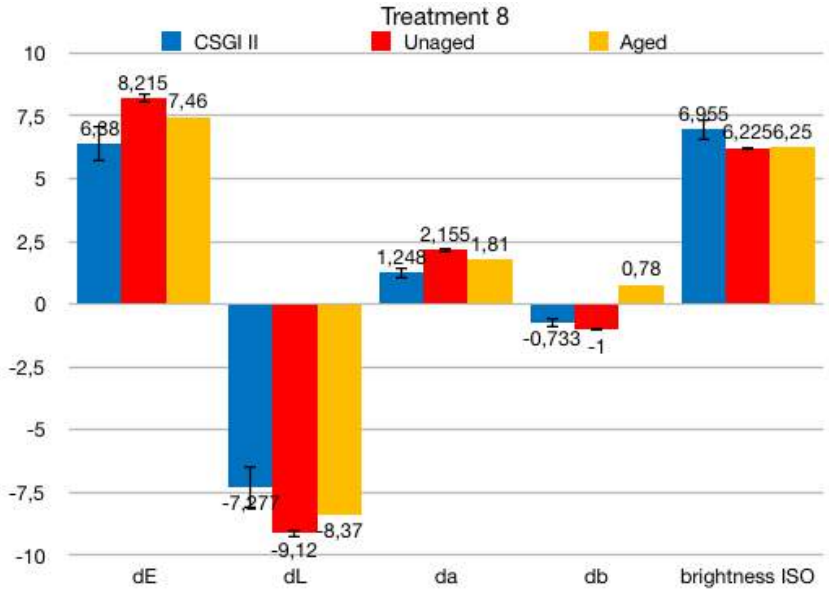

Figure 3.38: Colorimetric analysis of samples with treatment 8.

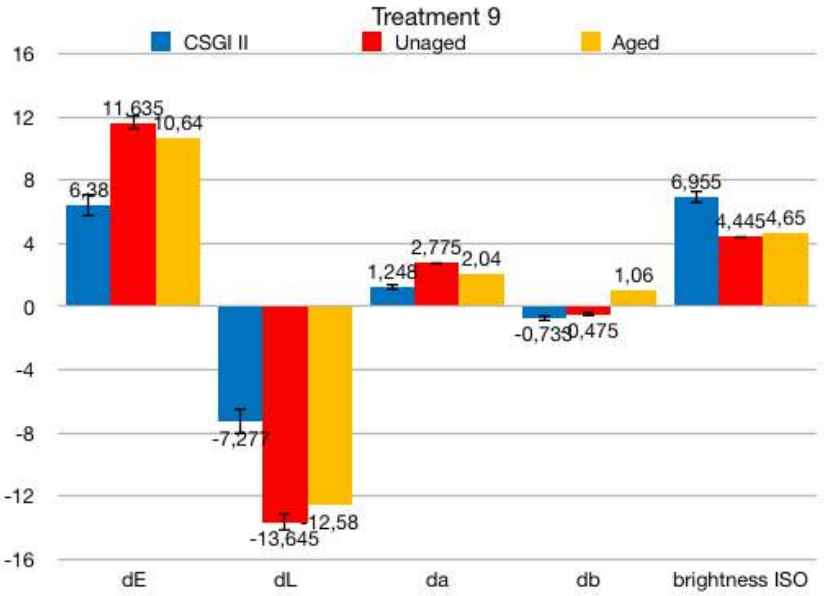

Figure 3.39: Colorimetric analysis of samples with treatment 9.

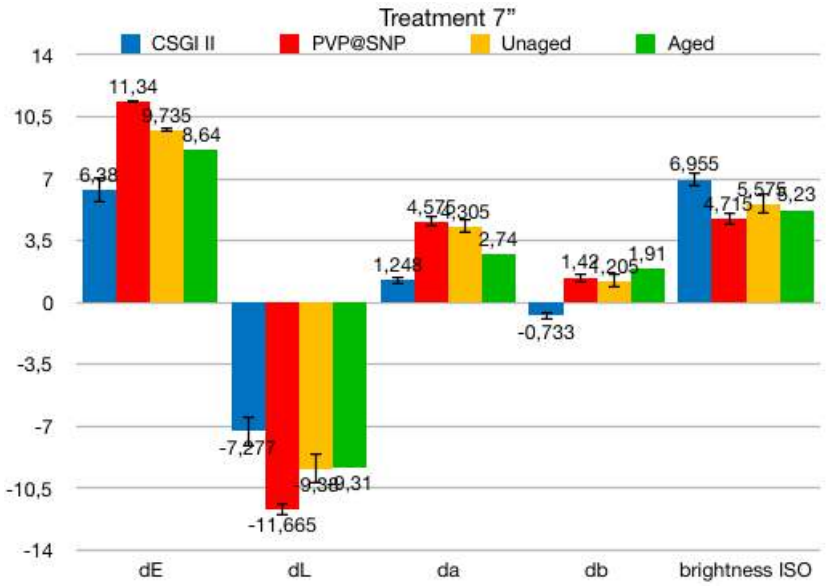

Figure 3.40: Colorimetric analysis of samples with treatment 7".

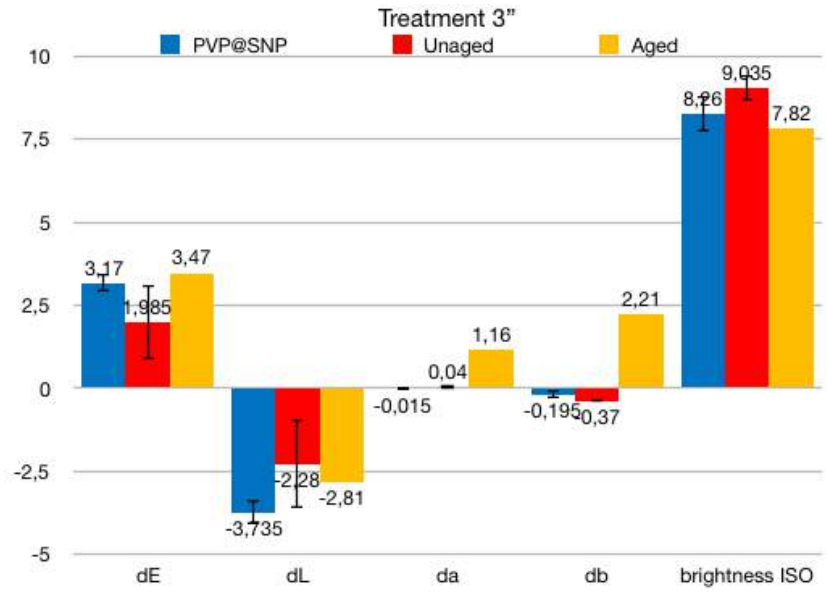

Figure 3.41: Colorimetric analysis of samples with treatment 3".

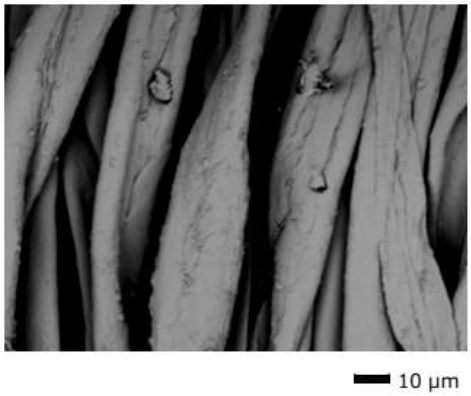

((a)) *D00, 1000 X, gold coating, WD = 10.5 mm.*

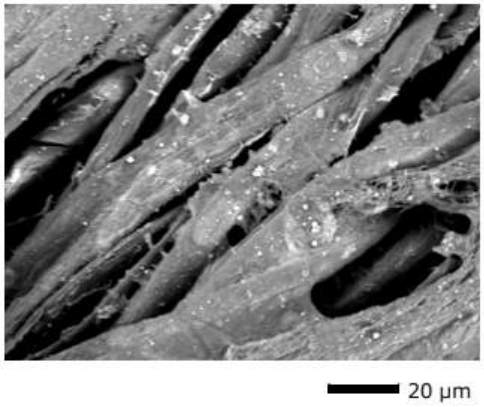

((b)) *D10″, 950 X, WD = 5.3 mm*

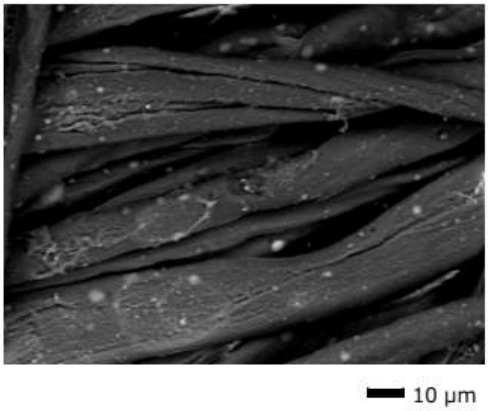

((c)) *D30, 1000 X, WD = 9.3 mm.*

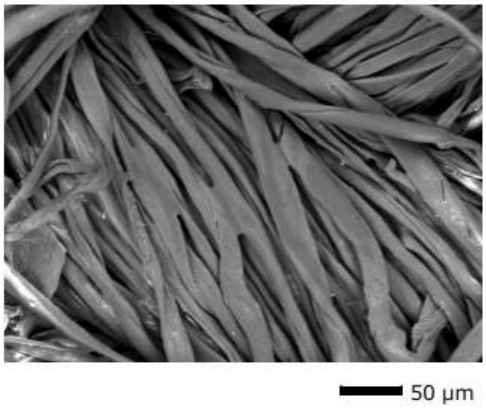

((d)) *D40, 330 X, WD = 9.4 mm.*

Figure 3.42: SEM images of dyed unaged samples. Back-scattered electrons signal, 5 kV, 30 Pa, 80 pA.

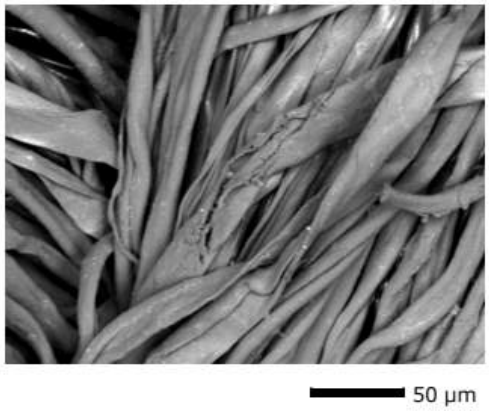

((a)) *D03, 500 X, WD = 10.2 mm.*

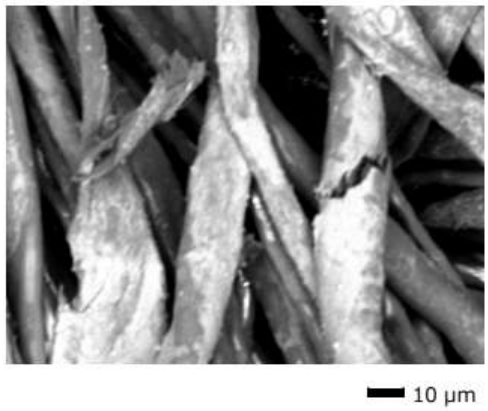

((b)) *D13", 1000 X, WD = 10.3 mm. Charging of the sample is visible.*

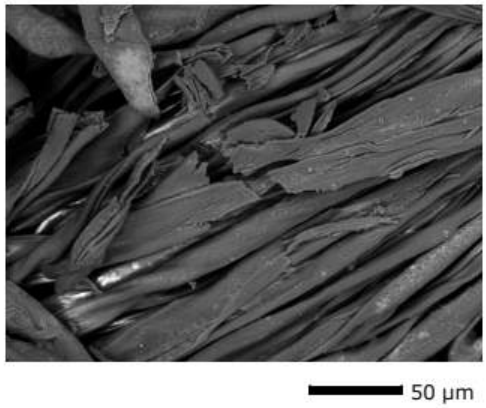

((c)) *D33, 500 X, WD = 9.3 mm.*

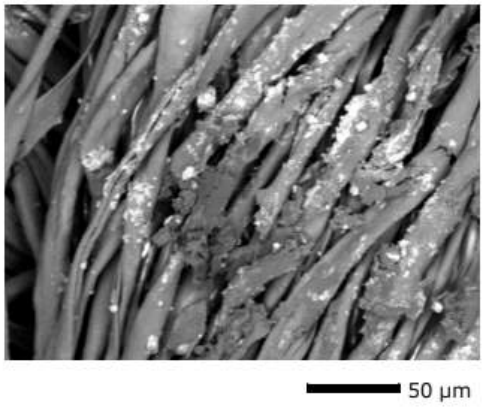

((d)) *D53, 500 X, WD = 10.1 mm.*

Figure 3.43: SEM images of dyed aged samples. Back-scattered electrons signal, 5 kV, 30 Pa, 80 pA.

upon fibers breakage due to the poor adhesion of SNPs to cellulose fibers, but this should be proved by further analysis as discussed later (Chapter 4).

New set of treatments The new treatments also showed the presence of some spots on cellulose fibers (Figures 3.44(a), 3.44(b), 3.44(e)) due to silica and $CaCO_3$ NPs (3.2.4); treatments 7" and 3" seem to have a more uniform coverage, maybe due to the presence of more material (Figures 3.44(f), 3.44(g)). Treatment 8 led to a veil-like surface morphology due to CNCs (Figures 3.44(c), 3.44(d)); their presence was not so evident with treatment 7, 7" and 3" due to the less amount of CNCs deposited (Figures 3.44(b), 3.44(f), 3.44(g)).

Some of the aged samples (Figures 3.45(a), 3.45(b)) had clear marks of degradation coherently with the results of the tensile tests (3.2.1). The spot-

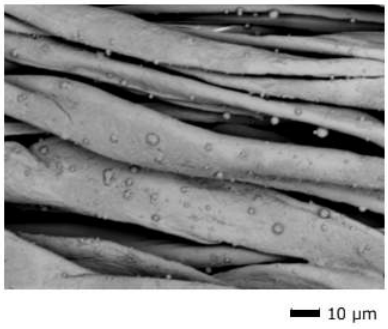

((a)) *D60, 1000 X, WD = 10.4 mm.*

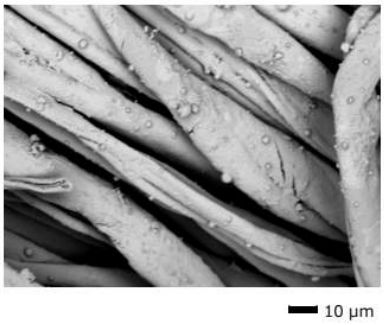

((b)) *D70, 1000 X, WD = 10.2 mm.*

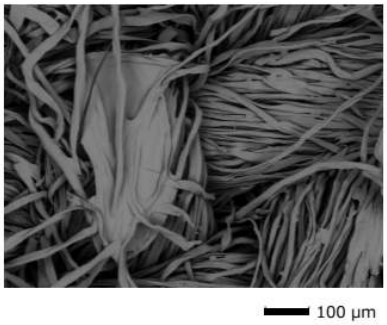

((c)) *D80, 150 X, WD = 10.2 mm.*

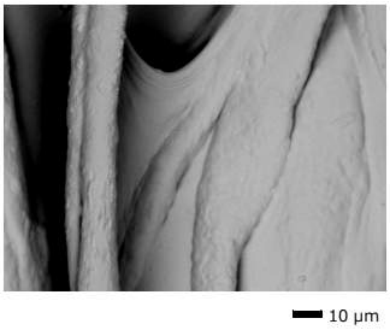

((d)) *D80, 1000 X, WD = 10.1 mm. Particular of the veil-like morphology.*

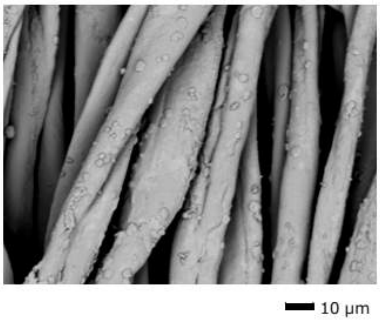

((e)) *D90, 1000 X, WD = 10.2 mm.*

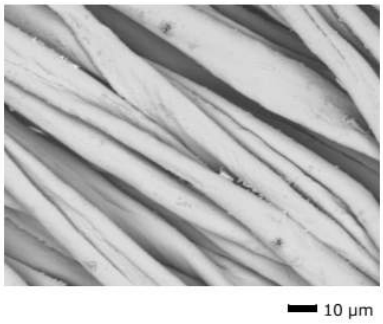

((f)) *D70", 1000 X, WD = 10.3 mm.*

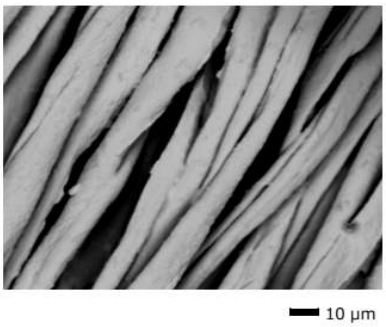

((g)) *D30", 1000 X, WD = 10.2 mm.*

Figure 3.44: SEM images of dyed unaged samples with new treatments. Back-scattered electrons signal, gold coating, 5 kV, 30 Pa, 80 pA.

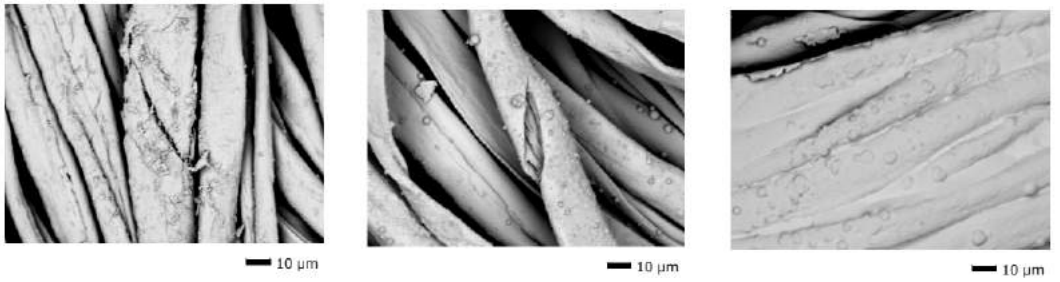

((a)) *D06, 1000 X, WD = 9.9 mm.* ((b)) *D66, 1000 X, WD = 10.2 mm.* ((c)) *D86, 1000 X, WD = 10.2 mm.*

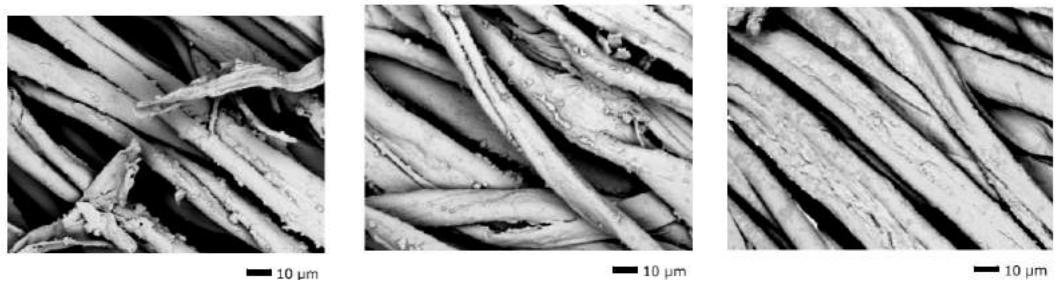

((d)) *D96, 1000 X, WD = 10.3 mm.* ((e)) *D76", 1000 X, WD = 10.3 mm.* ((f)) *D36", 1000 X, WD = 10.3 mm.*

Figure 3.45: SEM images of dyed aged samples with new treatments. Back-scattered electrons signal, gold coating, 5 kV, 30 Pa, 80 pA.

like appearance was preserved in treatments 6, 8 and 9 (Figures 3.45(b), 3.45(c), 3.45(d), 3.45(e)); the NC veil was still present in treatment 8 (Figure 3.45(c)). Treatment 3" did not show any particular feature upon ageing (Figure 3.45(f)).

EDX

Surface Silicon was detected on all of the treated samples (e.g. Figures B.1, B.2, B.3), and mostly in the previously mentioned spots (3.2.4), visible in figure B.2 [2]. SNPs were successfully deposited, but further investigation is required to understand the right amount to be aimed for these textiles.
Magnesium was detected very rarely in treatments 4 and 5, so very few material was actually present in the supernatant of the prepared solution, not enough for a low-yield method of application as nebulization.
Silicon was still detected in the aged samples, though more spread out around the fibers as shown in the spectra and maps reported in Figures B.4, B.5, B.6.

[2]The peaks corresponding to aluminum and other metals may be due to dust contamination.

[3]

New set of treatments EDX analysis confirmed the presence of Ca and Si in all of the treated samples. Some map analysis also proved that both Ca and Si uniformly covered the samples at surface both before (Figures 3.44(b), 3.44(e)) and after ageing (e.g. Figures B.14, B.15, B.16), coherently with pH measurements (3.2.2) and tensile tests (3.2.1); the areas both covered and not with the NC veil by treatment 8 were successfully covered with Ca (Figure B.14) and some Si spots appeared in treatment 7" (Figure 3.45(e)).

Cross-sections EDX showed almost no difference between the cross-sections of treated and untreated samples (Figures B.18, B.19, B.20). No Si was detected in the first layer of treatment 3 (Figure B.19), and in general Si was rarely detected compared to the surface, proving that NPs penetration was very poor. This may be one of the reasons for the lack of consolidation upon ageing. The amount of deposited material was likely not enough to promote a deeper penetration of SNPs, and the step-wise deposition of SNPs and NC may have hindered further penetration of the first material due to the formation of a surface film of NC and the presence of a drier substrate [6]. The synergistic combination of SNPs and NC may have not have been fully exploited through this application method.

New set of treatments Si and Ca were detected in the cross-sections with treatments 9 (Si mostly at surface, Ca deeper in the textile, Figure B.21), 7" (only Ca at surface, Figure B.22) and 3" (Si, even deeper in the textile, Figure B.23), both before and after ageing. Better maps with longer acquisition times (1 h-1 h 30 min) were acquired for treatments 7" (Figure 3.46, 3.47) and 9 (Figures 3.48, 3.49) after covering the cross-sections with 38.5 and 43 nm of carbon (pulsed evaporation, 54 A, pulse length = 1 s, same machine used for gold sputtering) in order to perform the analysis in high vacuum and increase the voltage to 20 kV. The treatments seem to have penetrated slightly better into the textile by brushing, and a weak iron signal appears.
These results also prove good adhesion of both $CaCO_3$ and SNPs to cellulose fibers.

[3] The detection of iron would have required longer acquisition times but as the untreated textiles were already fully characterized, only the signals of Si, Mg and Ca were considered important to be detected besides the ones of C and O related to cellulose [1]. One spectrum or map per sample is reported as example in Appendix B.

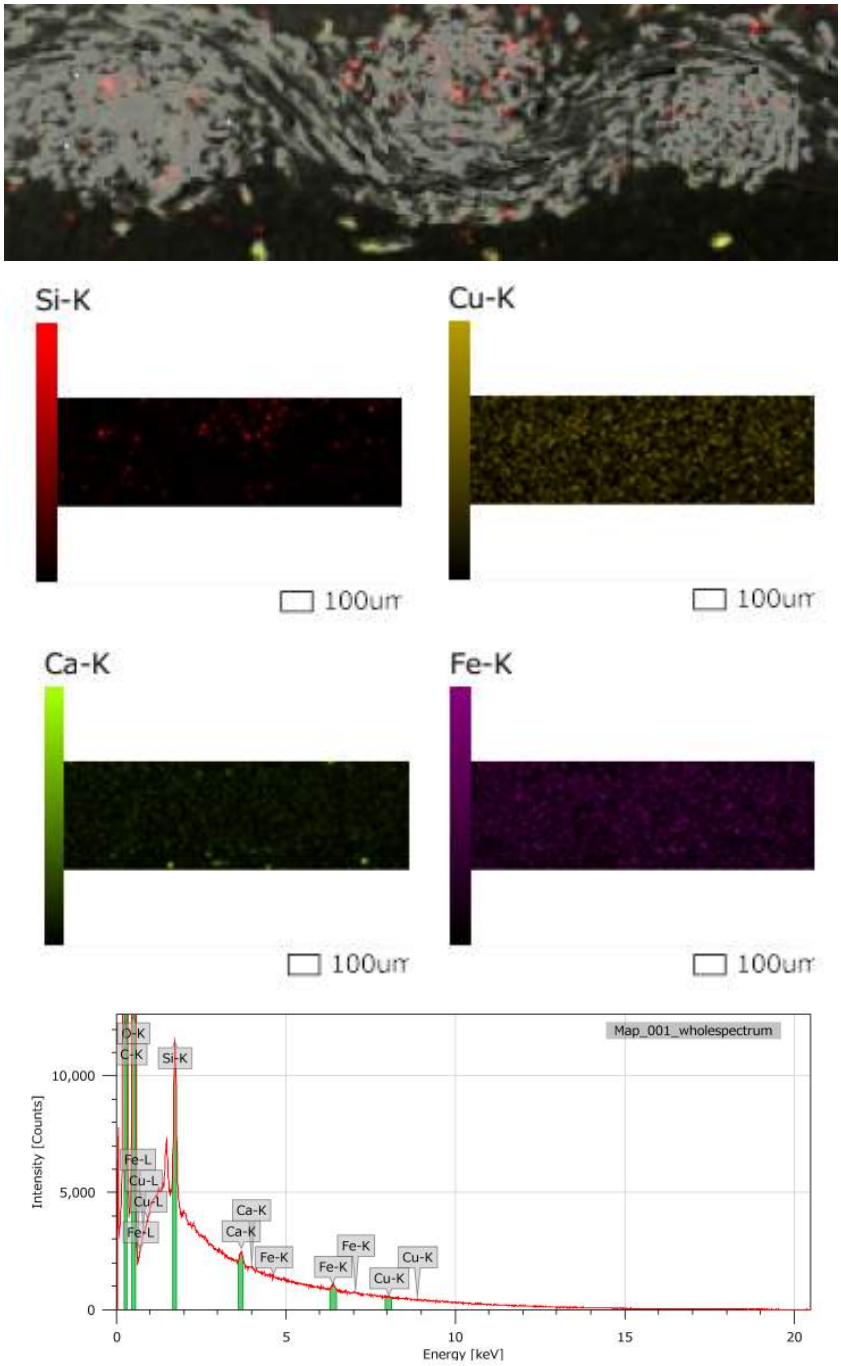

Figure 3.46: EDX map analysis of a cross-section with treatment 7".

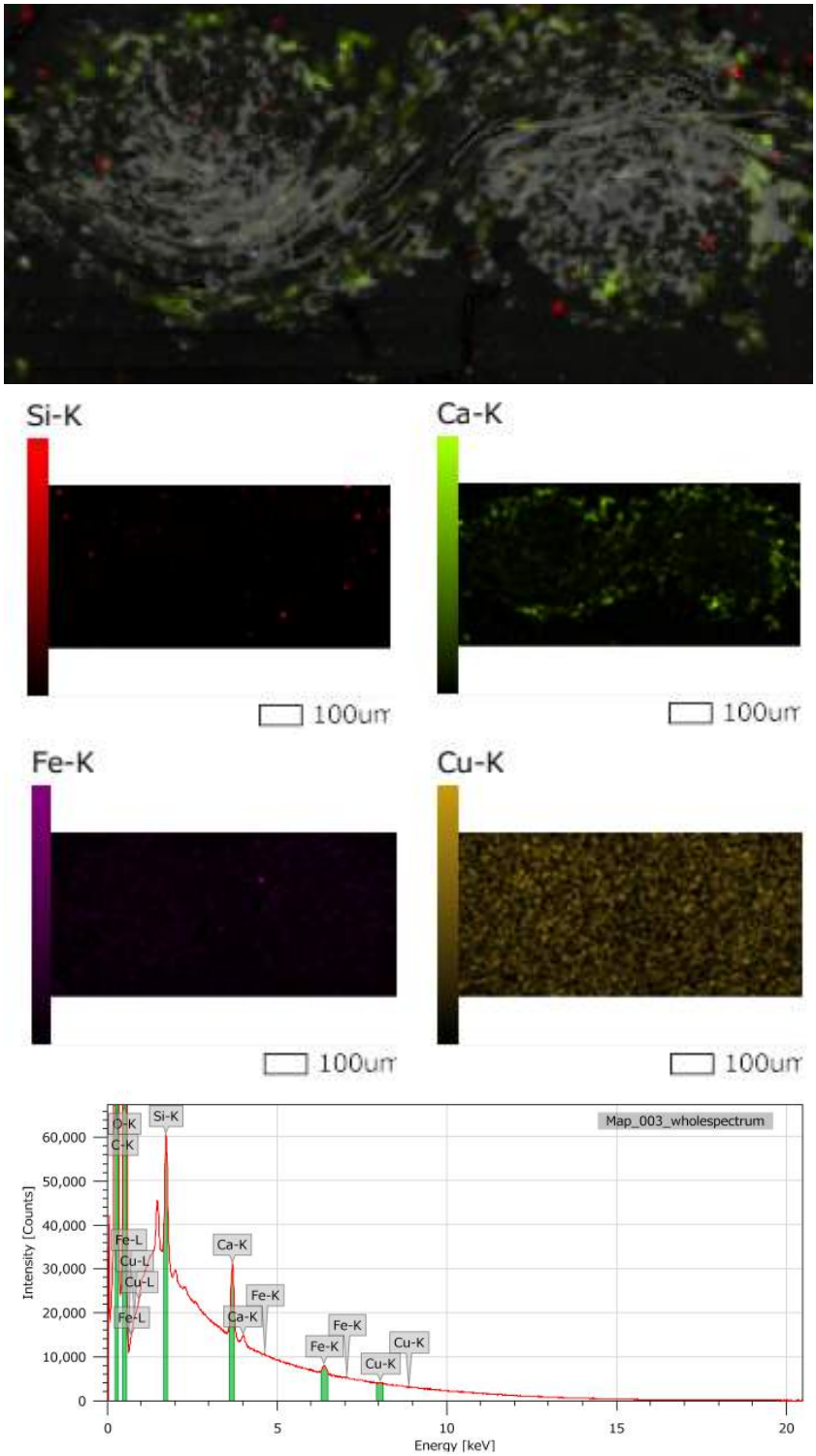

Figure 3.47: EDX map analysis of an aged cross-section with treatment 7".

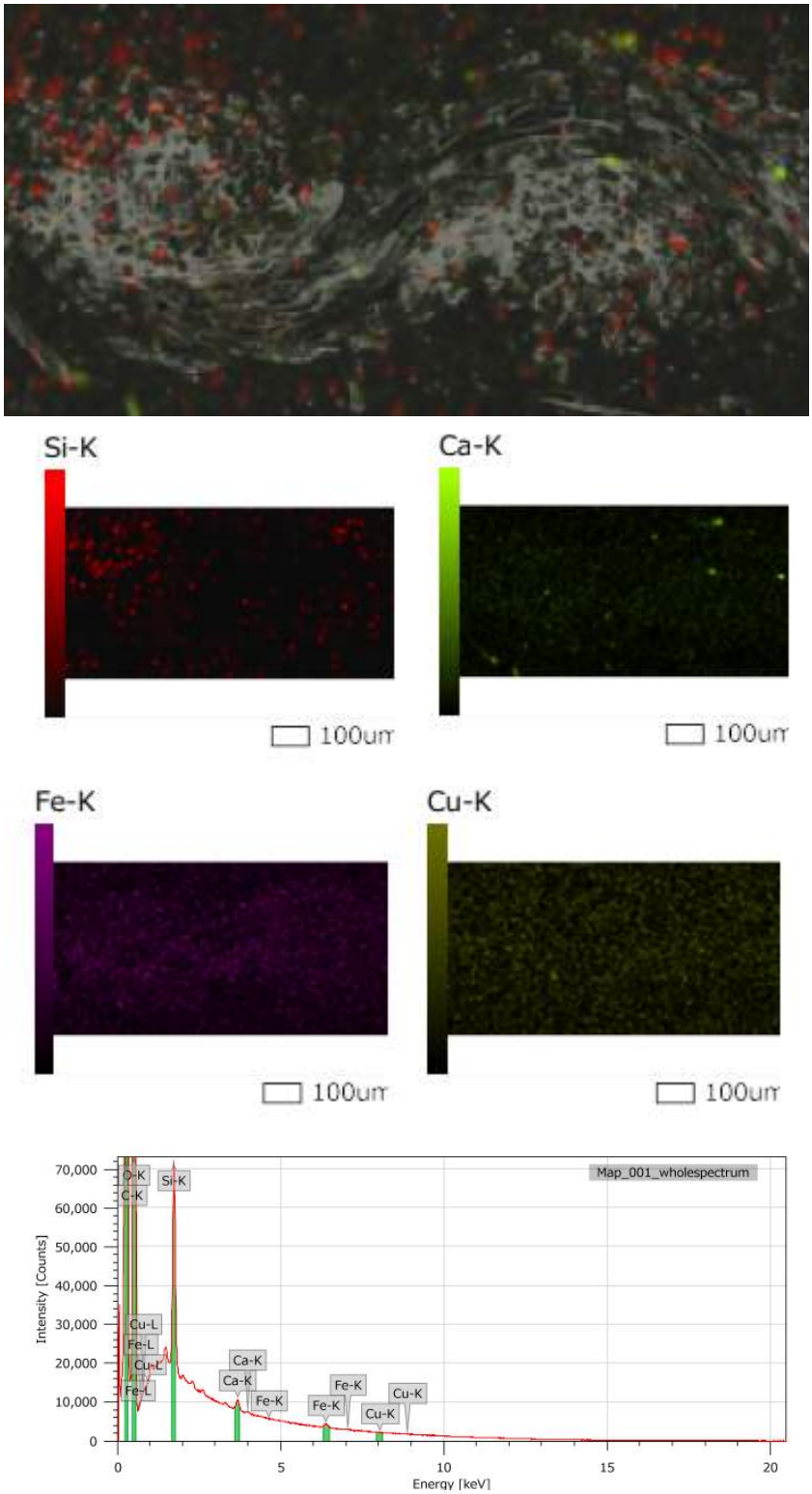

Figure 3.48: EDX map analysis of a cross-section with treatment 9.

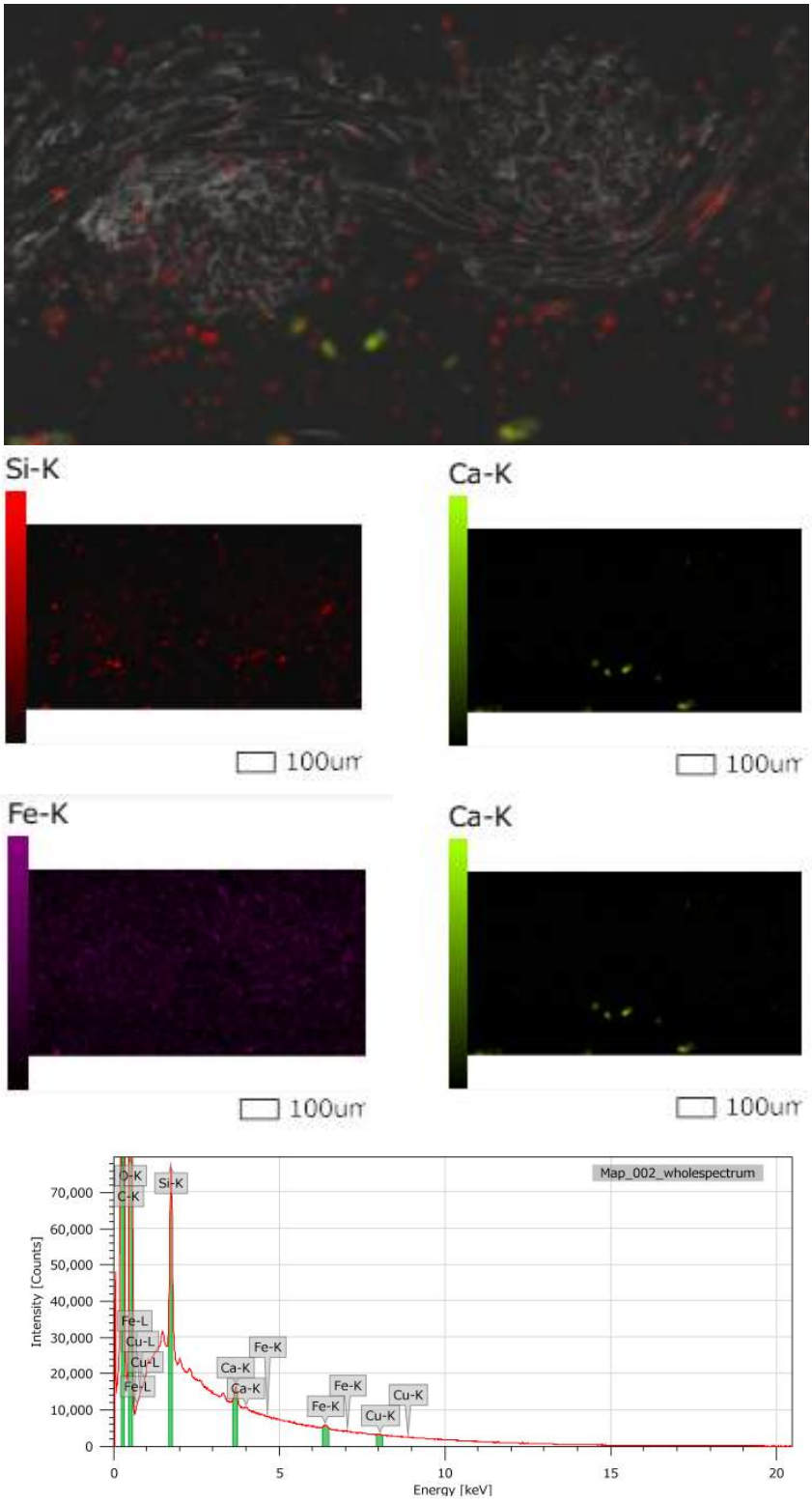

Figure 3.49: EDX map analysis of an aged cross-section with treatment 9.

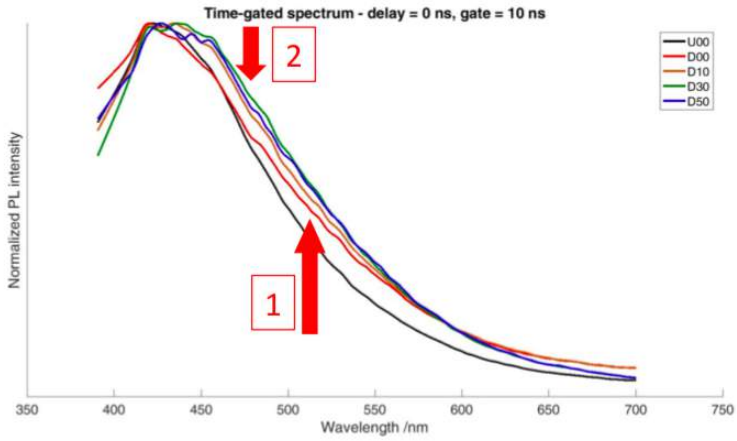

((a)) *Time-gated photoluminescence spectra of unaged undyed and dyed samples.*

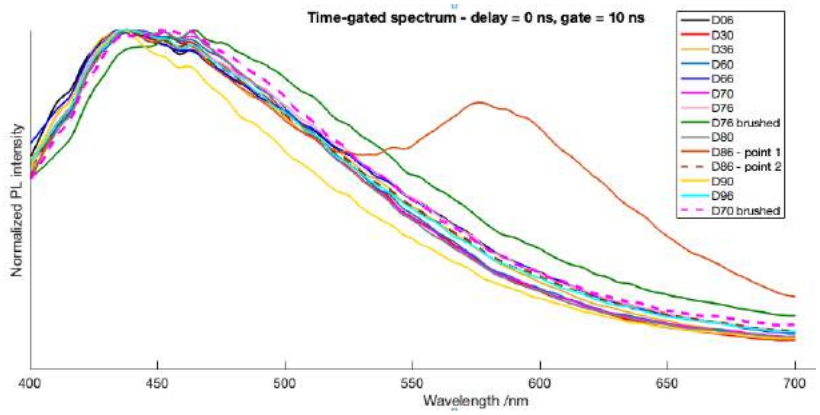

((b)) *Time-gated photoluminescence spectra of the samples with the second set of treatments.*

Figure 3.50: Results of photoluminescence analysis of the samples.

3.2.5 Photoluminescence

The undyed unaged sample shows an emission peak at around 420 nm shifted at longer wavelengths upon treatment (Figure 3.50(a)). Further analysis may study the relation between the amount of treatment and the wavelength shift. The dyed unaged sample shows another peak at around 520 nm, likely associated with the fluorophores of the dye (Figure 3.50(a)).

The samples with the new set of treatments were also analyzed (Figure 3.50(b)). Treatment 7 seems to cause a shift in emission towards longer wavelengths upon ageing only when applied by brushing (Figure 3.51(a)); the signal also seems to be more intense, coherently with the presence of more material. Treatment 8 shows a red emission peak (600 nm) upon ageing,

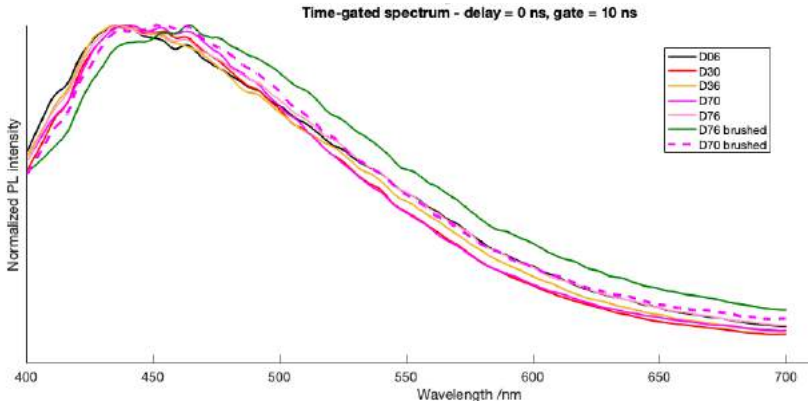

((a)) *Time-gated photoluminescence spectra of samples with treatments 3/7.*

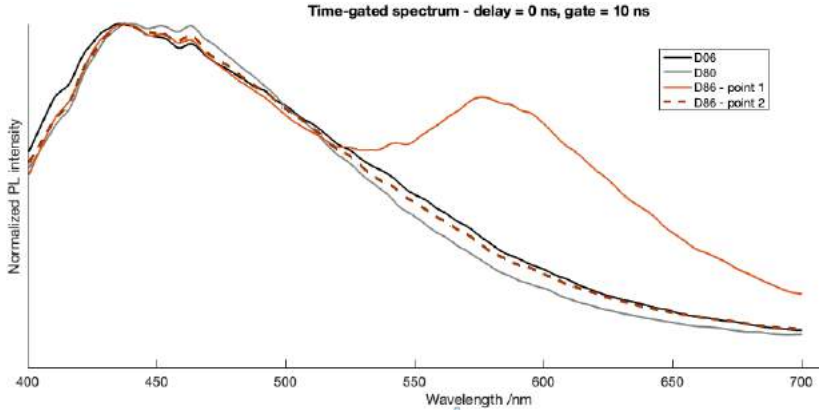

((b)) *Time-gated photoluminescence spectra of the samples with treatment 8.*

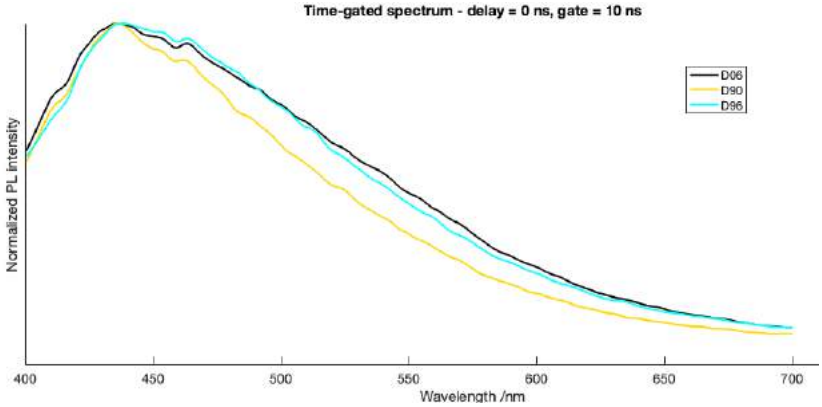

((c)) *Time-gated photoluminescence spectra of samples with treatment 9.*

Figure 3.51: Results of photoluminescence analysis of the samples with treatments 3/7, 8 and 9.

not uniformly present on the sample (Figure 3.51(b)); this may be related to compounds or impurities brought by the treatment itself upon ageing, as it is not present in any of the other samples. Treatment 9 gives rise to an emission curve similar to the undyed unaged sample, likely due to the chemical similarities of cellulose and CMC (Figure 3.51(c)).
Further more systematic analysis on samples with different amount of treatments and upon different ageing regimes should be performed in order to really evaluate photoluminescence as characterization tool for the effects of treatments and degradation of iron-tannate dyed textiles.

3.2.6 Accelerated ageing

The tested regimes effectively degraded the samples (3.2.1, 3.2.3).
Though longer, the regime at lower temperature was much less severe than all the others at higher temperature. The lower RH rather than the lower temperature may have caused this large difference; the moisture content may not have been enough to activate acid hydrolysis and the expected catalytic degradation mechanism. Moisture content rather than temperature seems to affect most the degradation of paper [24], and it may be true for cotton as well due to the chemical similarities of the two substrates.

3.2.7 Application methods

Nebulization is not an efficient application method as it requires less concentrated solutions, long application times and has a very low yield; however it allows uniform product applications which can not be achieved by other methods as brushing. Considering that only small areas of real objects may be treated with these nanomaterials, it can still be considered a suitable application method.
No differences in terms of penetration of SNPs were observed between mixture or step-wise application (3.2.4). Further investigation is required to understand the reasons: the deposited amount of silica may have not been enough to evaluate a quantitative difference. Though the low amount of material the treated samples already looked stickier and stiffer than the untreated, especially the ones with treatments 3 and 5, both containing CNCs, thus confirming their larger stiffening effect (3.2.1).
As the weight increase upon treatment was usually larger for untreated than already treated samples (3.1), SNPs should be applied as fast as possible to make sure to impregnate the textiles and achieve higher yield of deposition.

3.3 Discussion

As shown in Figure 3.52, the ageing considerably changed mechanical and color properties of the samples, which became less stiff, strong and extensible, and removed every difference between treated and untreated samples in terms of mechanical behavior. The largest color change was given at first place by treatments 3 and 5, but treatment 2 behaved worst upon ageing, maybe due to the presence of PEI (3.2.3).
It is also interesting to note that the freshly-treated samples look more extensible with treatment 3, stiffer (especially at low deformation) and slightly stronger with treatment 5. SNPs may have positively mitigated the stiffening action of CNCs confirming the expected synergistic effect of the two materials (1.4.2). However the severe ageing (and degradation) removes every difference between the two treatments; SNPs may not have been anymore able to exploit their consolidating function, consistent with the different morphology observed through SEM (3.2.4). These results also prove the stability of the CNCs dispersion (2.1.3).
A slight decrease of mechanical properties is already present upon ageing 4 though not really consistent with the changes observed upon ageing 3, reinforcing the idea that other degradation mechanisms may be involved with different ageing conditions (3.2.6).
About half of the strength, stiffness and extensibility loss occurred within the first two weeks of ageing as expected [1], while the color changed proportionally to ageing time; stiffness at low deformation was almost entirely preserved by treatment 2 (Figures 3.53, 3.54).

New set of treatments

The comparison of D00 and D06 shows that ageing caused a general stiffening (lower elastic modulus and extensibility) and weakening of the textiles; treatments 6 and 3" behaved worst both before and after ageing (Figure 3.55), though the latter gives the least color change. Neither deacidifier and use of consolidating material without deacidifier provide consolidation because the degradation is too severe at low pH. Treatment 7 does not provide much improvement compared to the untreated samples; the same treatment (7") is more effective if applied by brushing, indicating that more consolidating material is required (Figure 3.57).
Though applied by nebulization, treatments 8 and 9 provide enough strength and stiffness without reducing the extensibility of the textile; the color change may be not completely detrimental as discussed previously (3.2.3). Treatment 8 makes the textile a bit stiffer due to the presence of CNCs; the stiffness

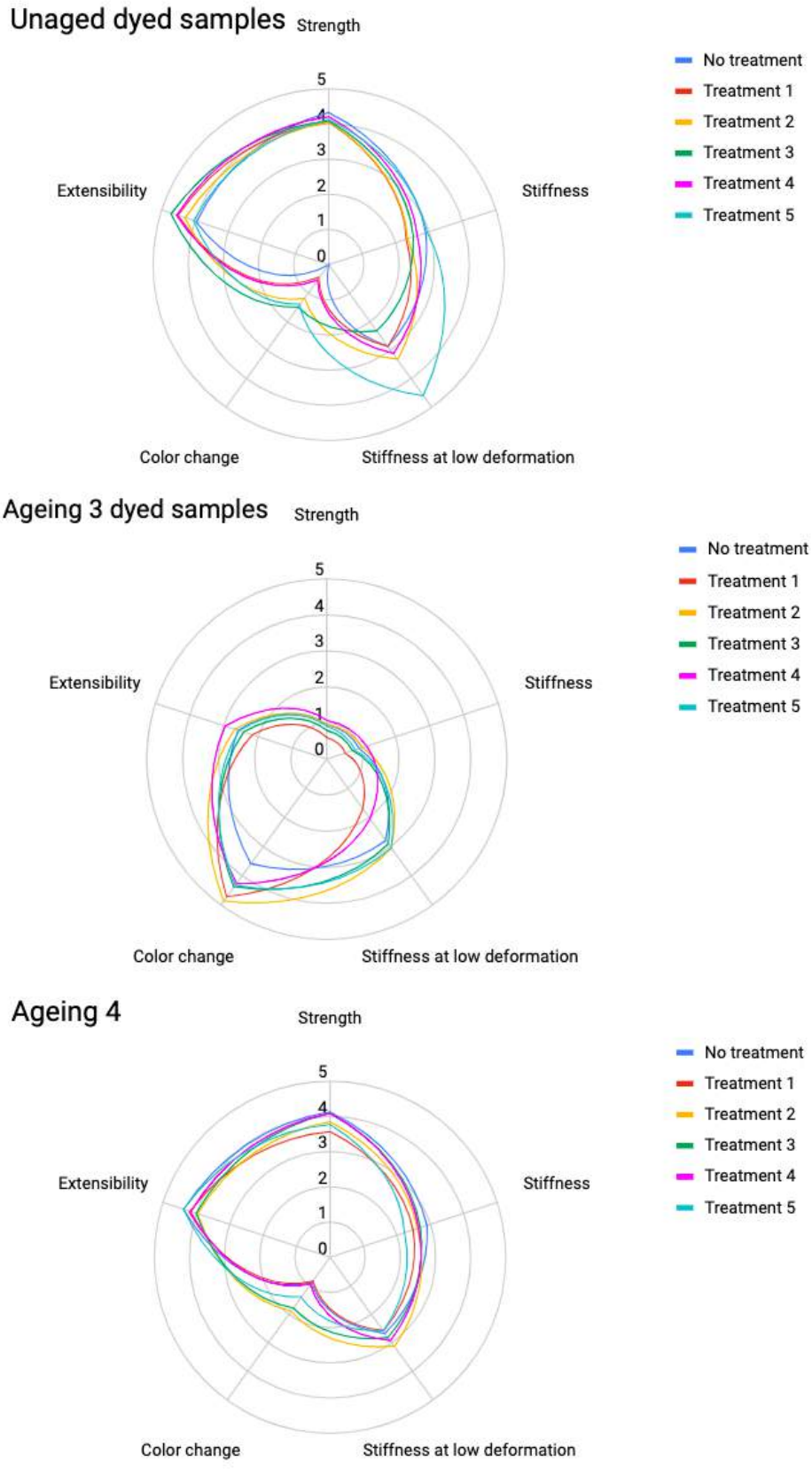

Figure 3.52: Comparison of mechanical properties and color change upon treatment at different ageing regimes.

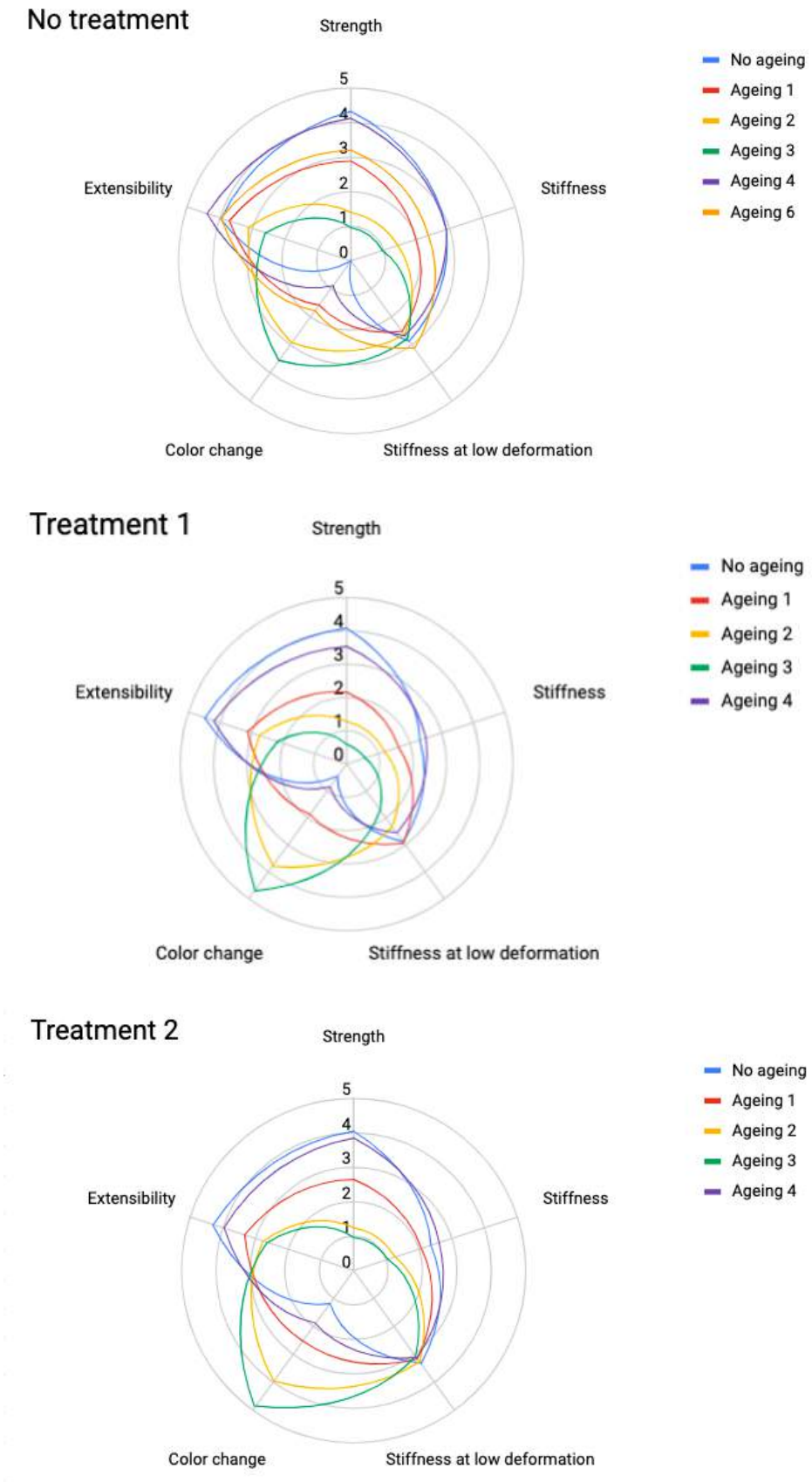

Figure 3.53: Comparison of mechanical properties and color change upon ageing.

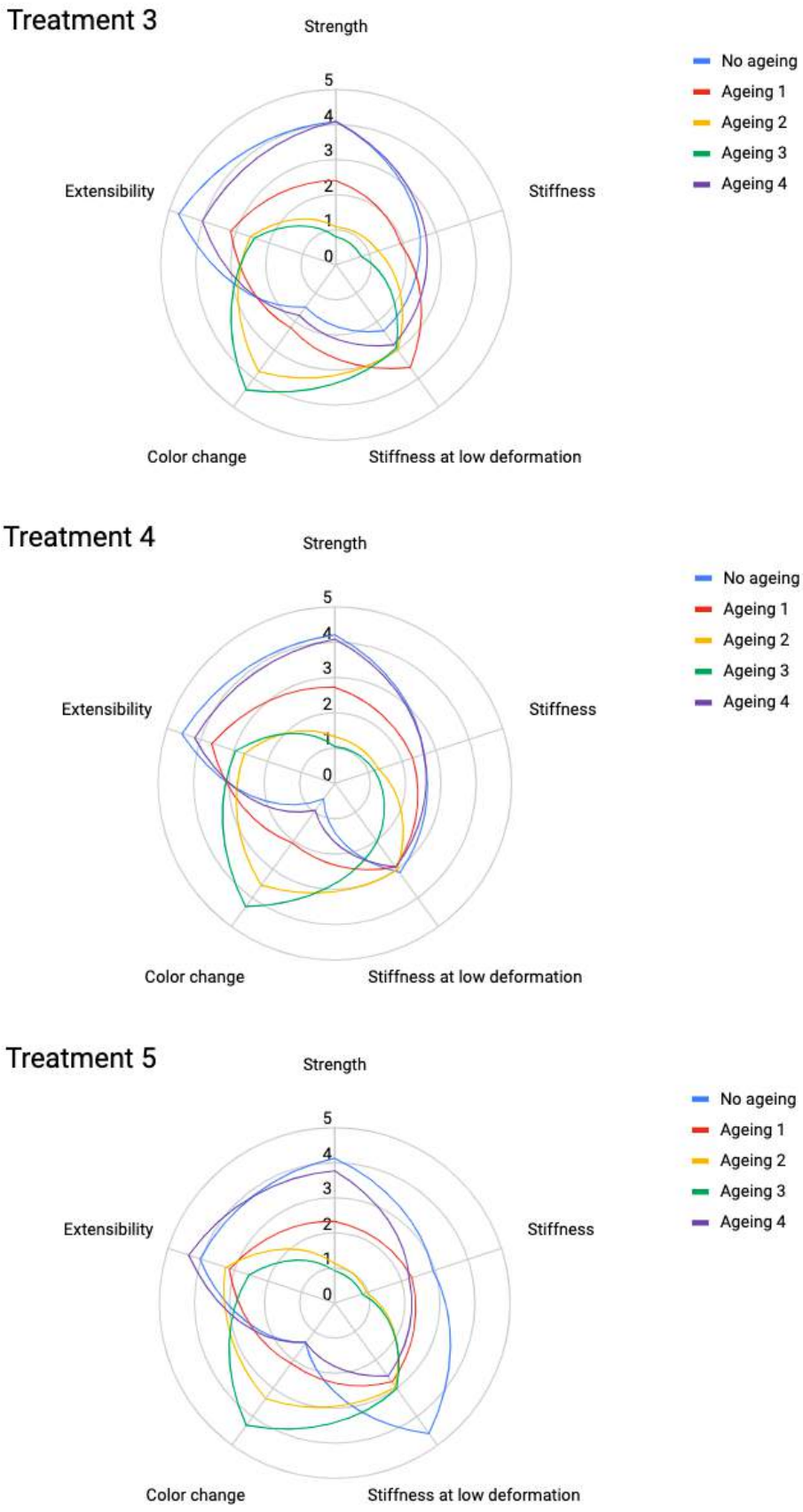

Figure 3.54: Comparison of mechanical properties and color change upon ageing.

at low deformation however is larger for treatment 9, which may be considered for further trials considering its promising preservation of strength and extensibility (Figure 3.56).

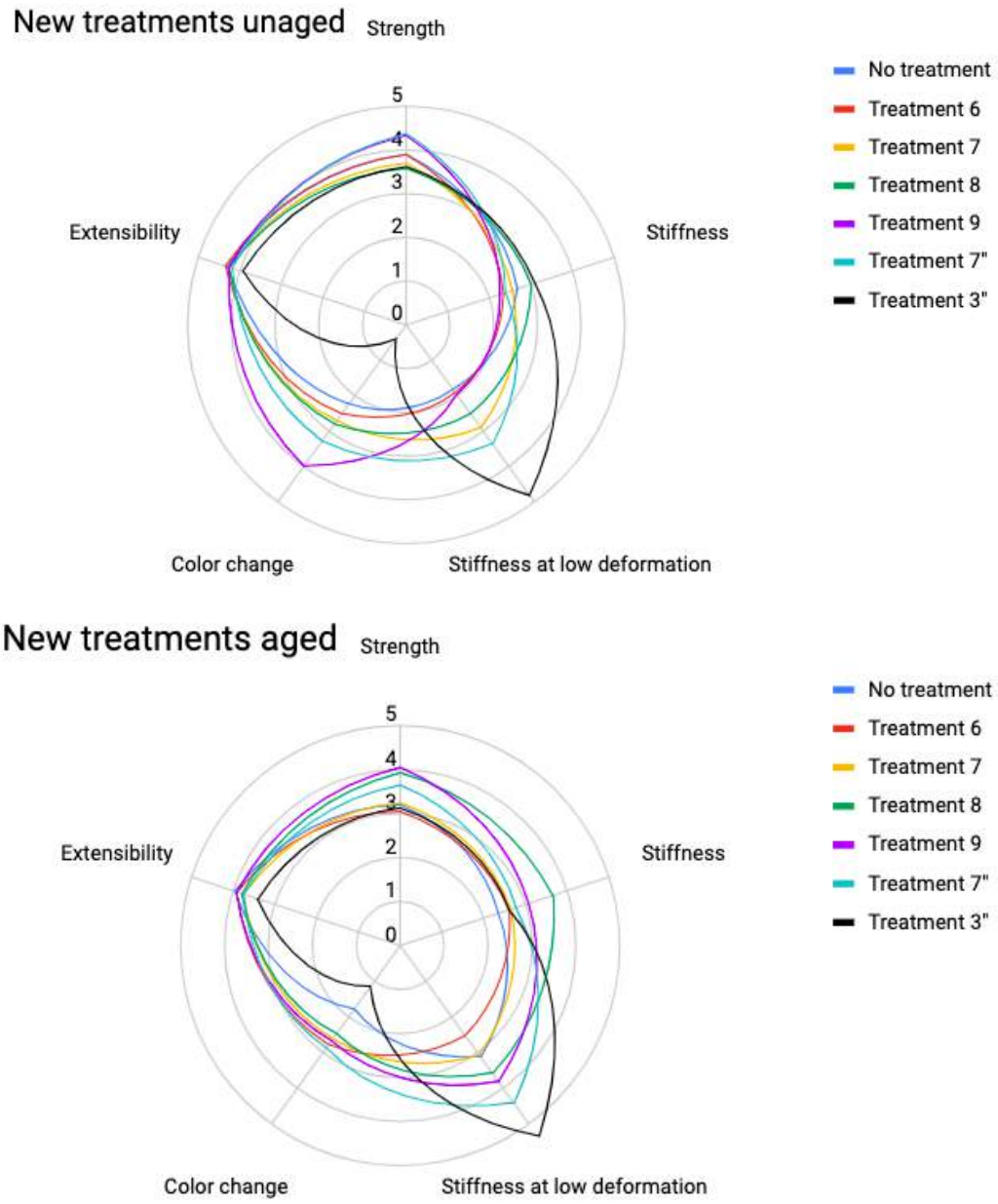

Figure 3.55: Comparison of mechanical properties and color change upon new treatments before and after ageing.

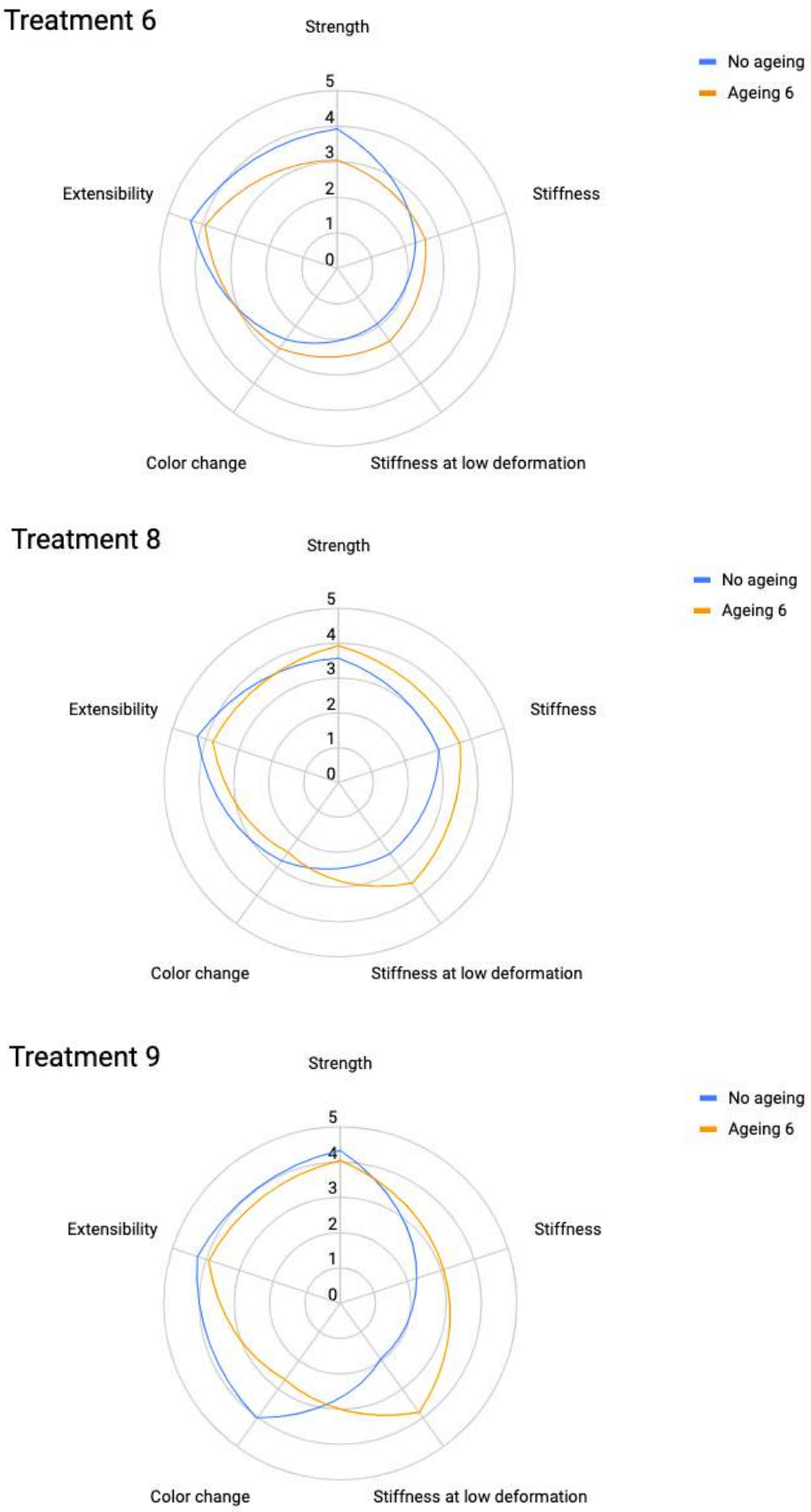

Figure 3.56: Comparison of mechanical properties and color change upon ageing.

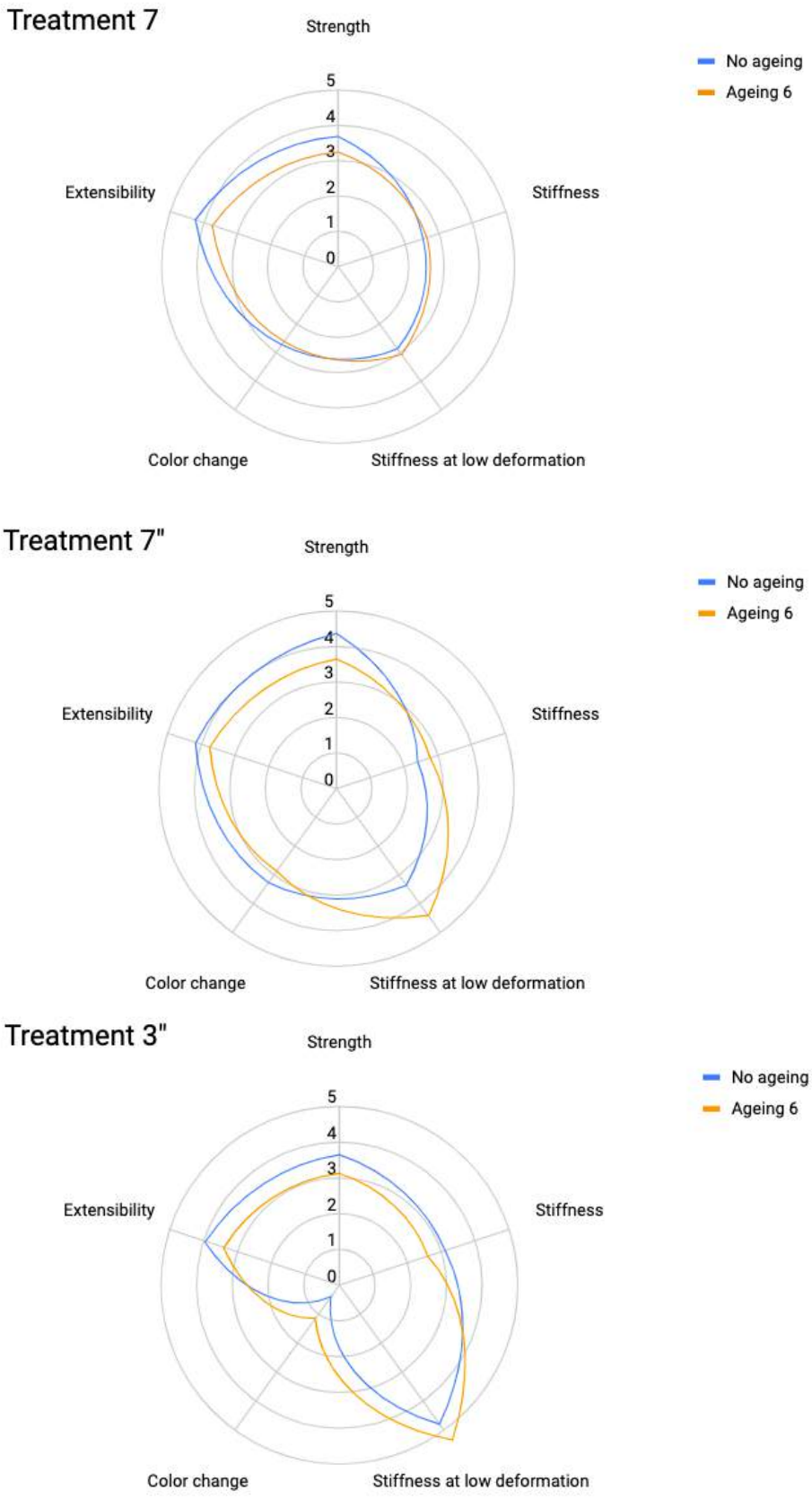

Figure 3.57: Comparison of mechanical properties and color change upon ageing.

Chapter 4

Future perspectives

4.1 Materials

The use of 2-propanol did not result in any problem of dissolution/instability or damage to the textiles, and was feasible for nebulization, so its use may still be considered for future experiments. Less diluted dispersions (∼2.5-3 %wt) may be tried out to decrease application times/apply more material and test the effectiveness of the nebulizer.
Another possible way to slow down the degradation and see the effect of the consolidating nanomaterials is to treat the samples also with antioxidants to minimize the concentration of hydroxyl radicals. The treatments investigated by Wilson [1] may be considered and further improved for this purpose.
New treatments with deposition of more material either in mixture or through step-wise application would be useful not only to prove the dependance of the consolidation effect on the amount of material, but also of the penetration of SNPs on the application method (if any). A one-pot application would be more straightforward if no hindrance of the surface layer of nanocellulose to the penetration of SNPs was ensured.
Other substrates with this kind of problem (e.g. silk) may be tested as well.

4.2 Characterization

Micro X-Ray Fluorescence (μXRF) was planned but the instrument was not available during the period at the Swedish National Heritage Board; it would have given more information about the penetration of the treatments into the textile.
Further investigation of the adhesion of SNPs and NC to cellulose fibers is

required in order to better understand the interactions with the substrate; lack of adhesion may be solved using different functionalizations of NPs or the help of other "adhesive" layers; atomic force microscopy (AFM) may be used for this purpose [19]. This technique would also give more information about surface morphology, particularly related to NC, not easily detected by SEM and SEM-EDX.
A quantitative compositional analysis of the surface may be performed through X-ray photoelectron spectroscopy (XPS); the quantification of chemical groups attributed to cellulose would be a way to monitor the presence of NC at surface, and the presence of treatments and/or degradation products may give rise to different spectra able to indicate processes and materials involved at surface (a layer-by-layer analysis of the cross-sections may give information about the bulk, too)
Different characterization techniques may be used to monitor degradation and better evaluate the effectiveness of deacidifier and consolidation. Electron paramagnetic analysis would monitor the amount of radicals and Fe^{3+} ions, while gas permeation chromatography the presence of degradation products; viscosimetry may allow the calculation of the DP. All this information would provide better calibration of the accelerated ageing regime to be used for further experiments comparing and extrapolating the obtained results with the degradation levels reached by natural ageing of historical objects. Carbonyl content and molecular weight are some of the important parameters able to monitor ongoing degradation as well as its stopping through a deacidifier, for example.
As moisture seems to affect most the behavior of the textiles (2.2.6), dynamic mechanical analysis under controlled relative humidity (DMA-RH) may be performed in order to monitor the response to moisture of the treated samples compared to the untreated in terms of mechanical properties [19].
The moisture content during ageing should also be monitored (for example by an IR moisture analyzer) to better evaluate parameters and phenomena involved in the accelerated ageing.

4.3 Validation by conservators

The final step would be the evaluation of the most promising treatments (9 and 7") from a conservator and then their application onto real museum objects [14]. This would further confirms the validity of the model textiles used in the project, too.

Chapter 5

Conclusions

The project proved the effectiveness of SNPs and CNCs for the consolidation of iron-tannate dyed textiles if used in combination with a deacidifier ($CaCO_3$ NPs) and a proper weight uptake, dependent on the kind of nanomaterial used.
Nebulization is a suitable method for the uniform application of these nanomaterials though its low yield ($\sim$20%). More concentrated dispersions may be used to decrease application times. The effectiveness of this low-yield application method clearly shows the power of nanostructures; a few amount of material was able to provide consolidation and pH buffering only thanks to its reduced size.
NPs improve strength and stiffness (also at low deformation) of the textiles but not their extensibility; a network may form among cellulose fibers, so that they would be less free to accomodate elongation.
A step-wise application of nanomaterials should be preferred in order to first stabilize the pH around neutrality through the interaction of the deacidifier with cellulose fibers [13], and then consolidate (first at fiber level through the application of SNPs, then at surface through a final layer of CNCs). No alternation of the applied materials should be used because the surface layer of NC may hinder the action of the deacidifier and the penetration of silica into the textile.
Further trials with different amount of material should be performed in order to verify a relation between applied material (and its concentration) and penetration.
The color change was mostly caused by the deacidifier; though perceivable it is not detrimental and may even enhance the original blackness of the textile.
Application of the treatments on other model substrates would be the next step to test these materials, together with collaboration with conservators.

Appendix A

Tensile tests

The appendix reports the results of the tensile tests for the dyed samples.

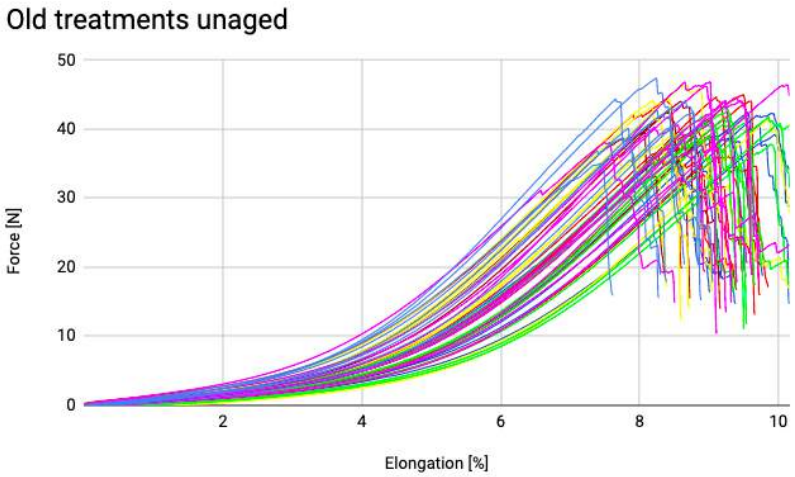

Figure A.1: Tensile tests of the unaged samples with the first set of treatments.

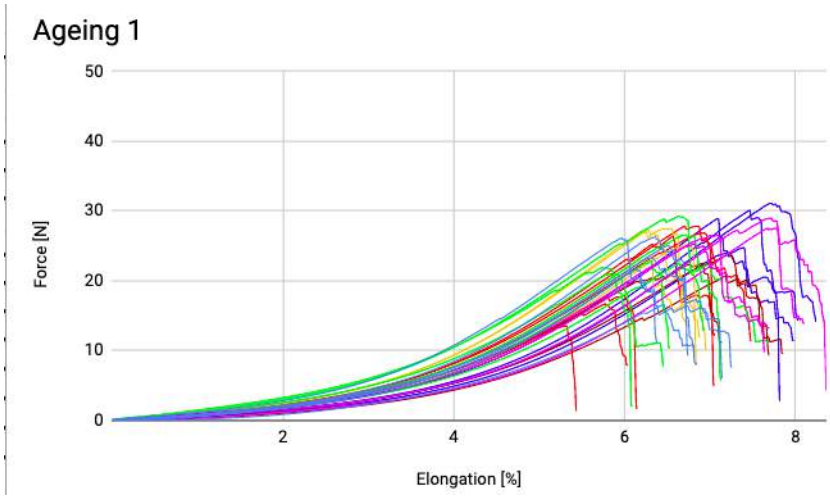

Figure A.2: Tensile tests of the samples aged by regime 1.

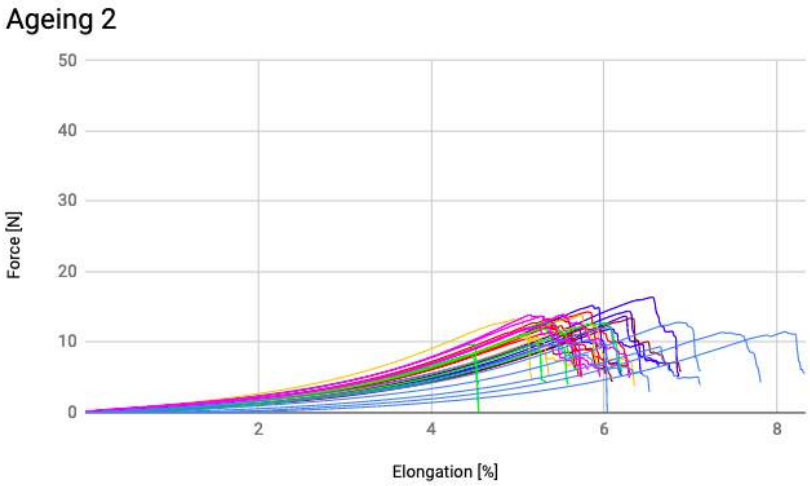

Figure A.3: Tensile tests of the samples aged by regime 2.

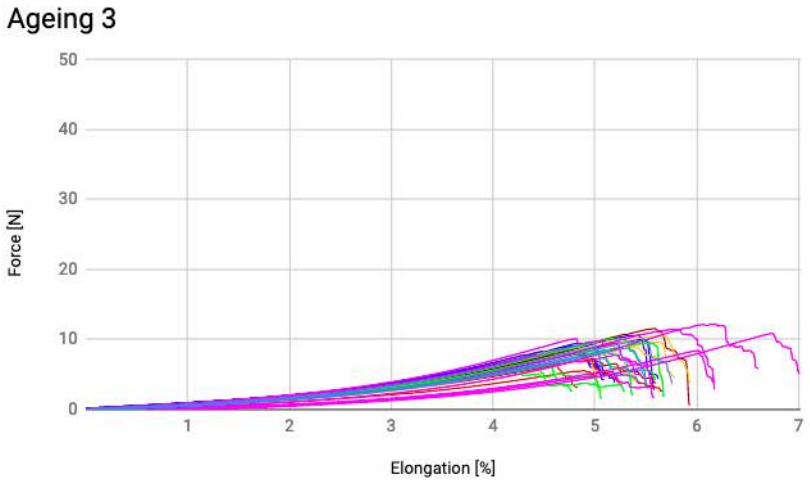

Figure A.4: Tensile tests of the samples aged by regime 3.

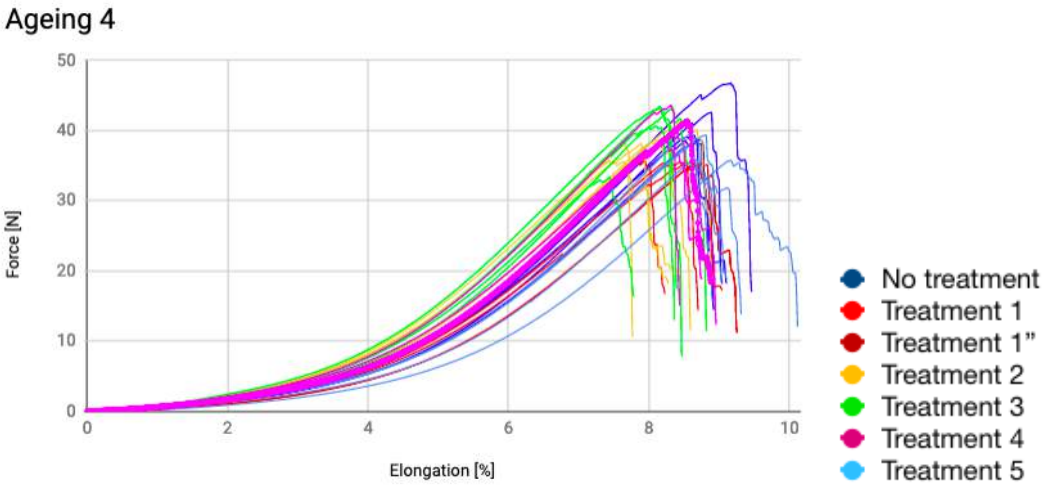

((a)) *Ageing 4.* ((b)) *Legend.*

Figure A.5: Tensile tests of the samples aged by regime 4.

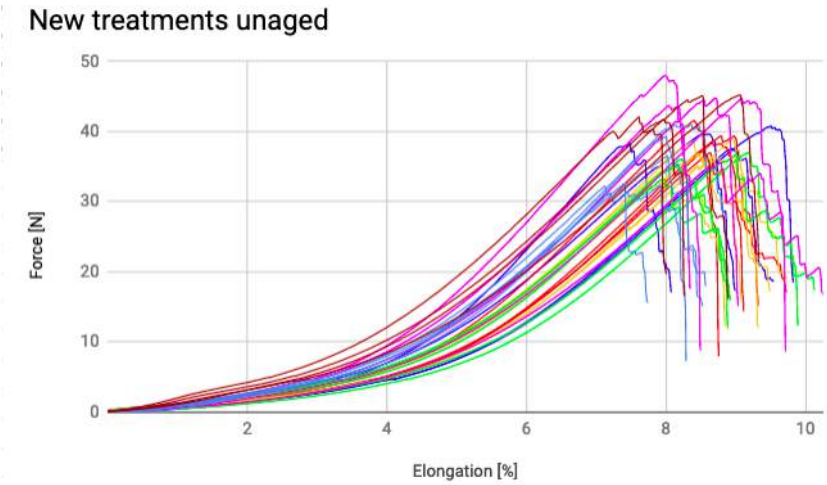

((a)) *No ageing.*

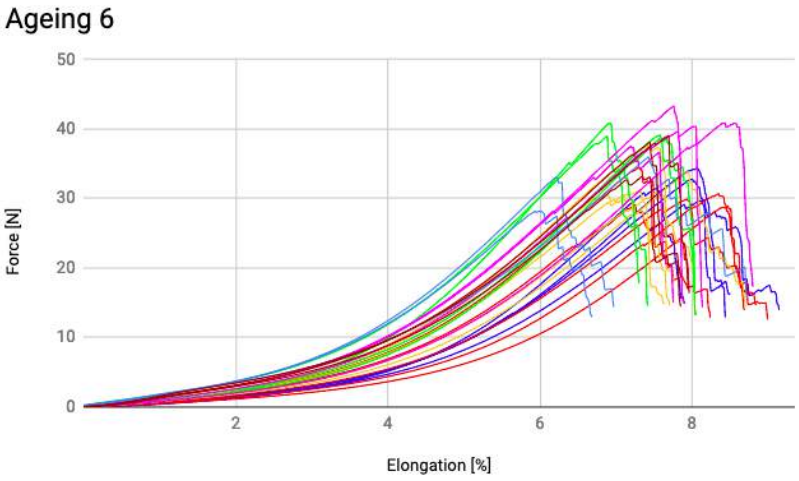

((b)) *Ageing 6.*

((c)) *Legend.*

Figure A.6: Tensile tests of the new set of treatments.

Appendix B

SEM-EDX

Examples of EDX analysis of surfaces and cross-sections of some samples.

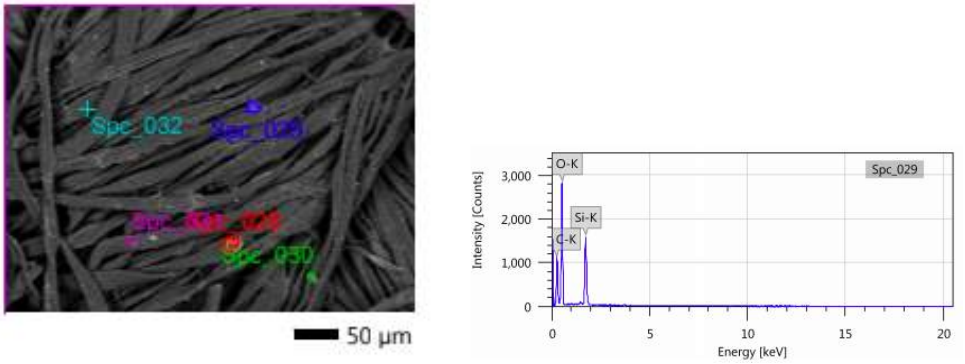

((a)) *270 X*

Figure B.1: SEM-EDX images of a dyed sample with three layers of treatment 1. Back-scattered electrons signal, 15 kV, 30 Pa, 10.3 mm of working distance, 80 pA.

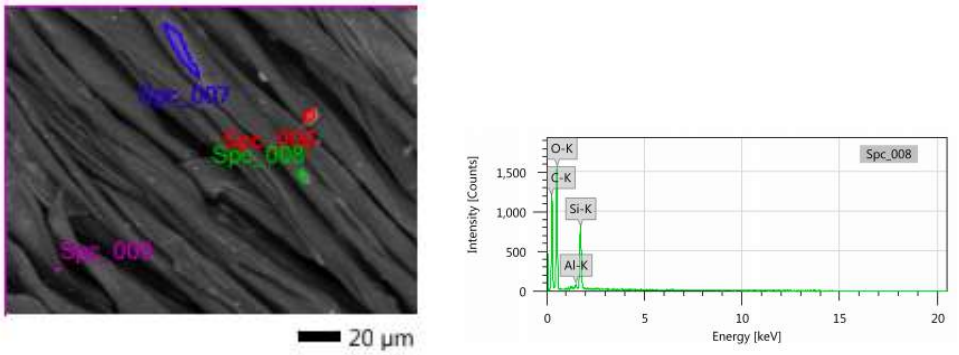

((a)) *650 X*

Figure B.2: SEM-EDX images of a dyed sample with treatment 2 (D20). Back-scattered electrons signal, 15 kV, 30 Pa, 10.4 mm of working distance, 80 pA.

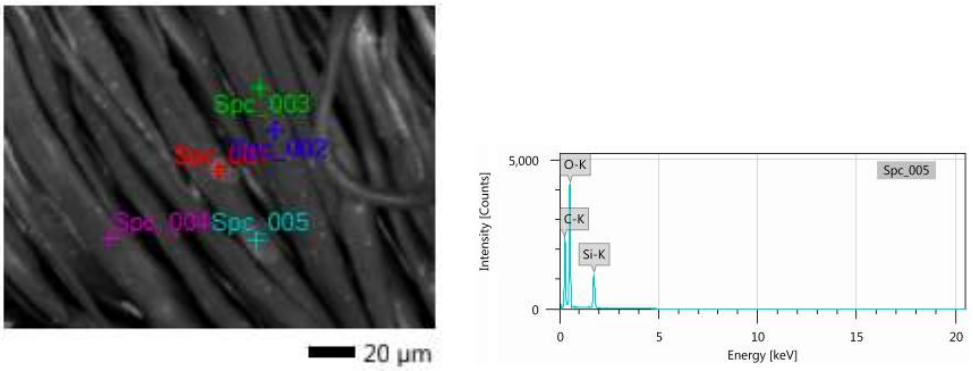

((a)) *700 X*

Figure B.3: SEM-EDX images of a dyed sample with treatment 3 (D30). Back-scattered electrons signal, 5 kV, 30 Pa, 9.3 mm of working distance, 80 pA.

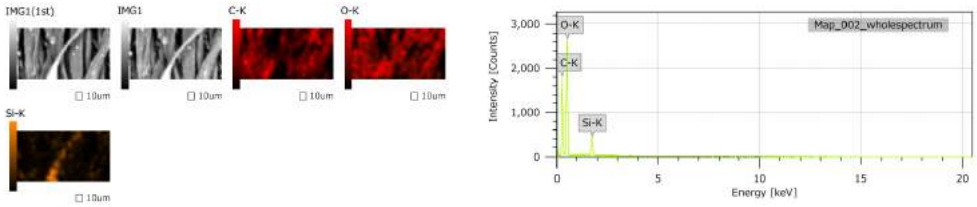

Figure B.4: SEM-EDX images of an aged dyed sample with treatment 1 (D13). Back-scattered electrons signal, 15 kV, 30 Pa, 10 mm of working distance, 80 pA.

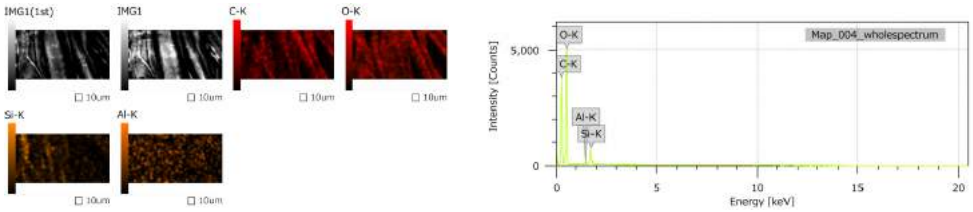

Figure B.5: SEM-EDX images of an aged dyed sample with treatment 2 (D23). Back-scattered electrons signal, 5 kV, 30 Pa, 10.3 mm of working distance, 80 pA.

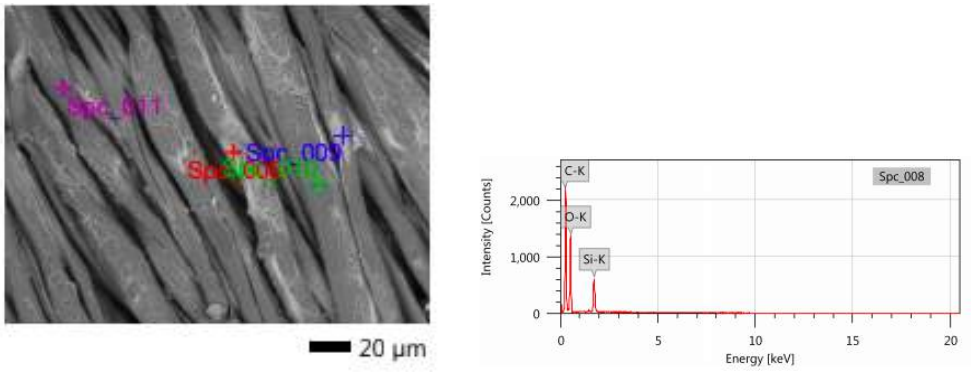

((a)) *600 X*

Figure B.6: SEM-EDX images of an aged dyed sample with treatment 3 (D33). Back-scattered electrons signal, 10 kV, 30 Pa, 9.1 mm of working distance, 80 pA.

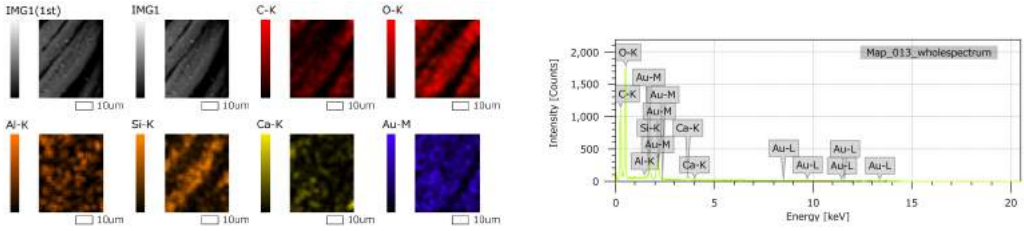

Figure B.7: SEM-EDX images of a dyed sample with treatment 7 (D70). Back-scattered electrons signal, gold coating, 15 kV, 30 Pa, 10.2 mm of working distance, 80 pA.

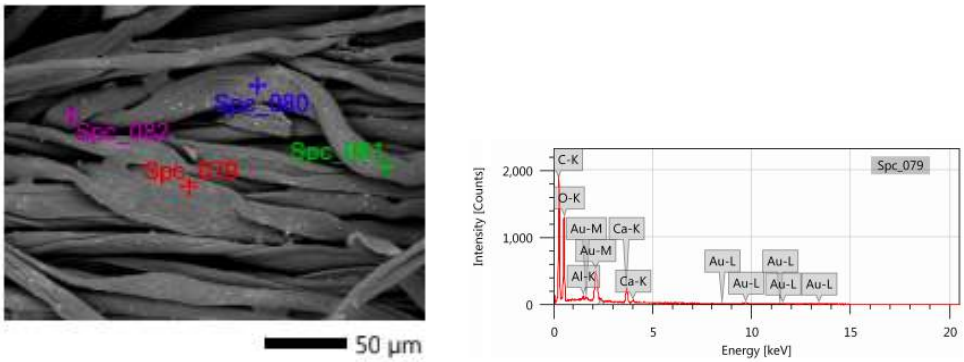

((a)) *500 X*

Figure B.8: SEM-EDX images of a dyed sample with treatment 8 (D80). Back-scattered electrons signal, gold coating, 15 kV, 30 Pa, 10.2 mm of working distance, 80 pA.

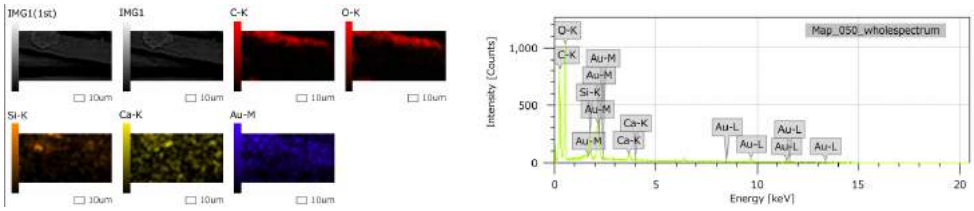

Figure B.9: SEM-EDX images of a dyed sample with treatment 9 (D90). Back-scattered electrons signal, gold coating, 15 kV, 30 Pa, 10 mm of working distance, 80 pA, 500 X.

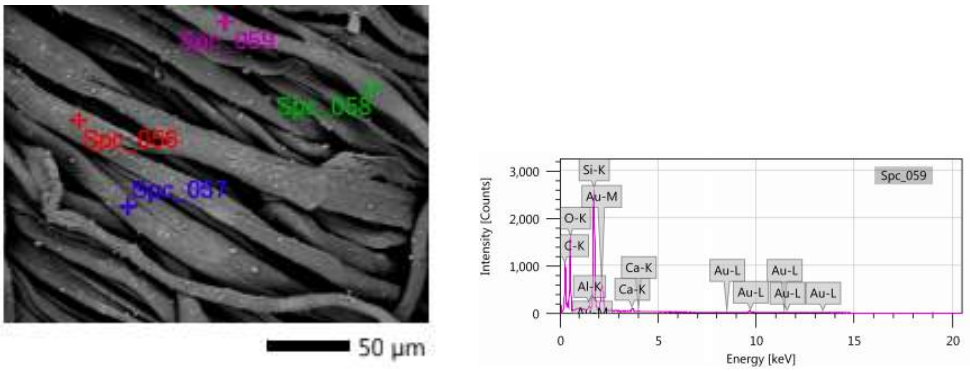

((a)) *500 X*

Figure B.10: SEM-EDX images of a dyed sample with treatment 7" (D70"). Back-scattered electrons signal, gold coating, 15 kV, 30 Pa, 10.2 mm of working distance, 80 pA.

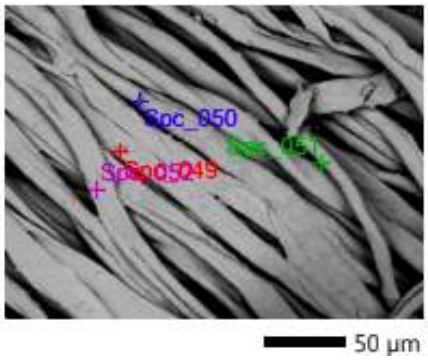

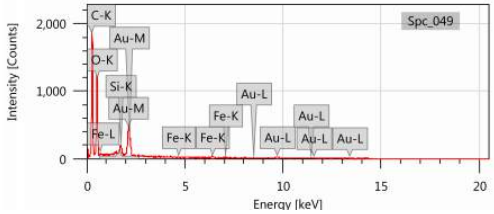

((a)) *500 X*

Figure B.11: SEM-EDX images of a dyed sample with treatment 3" (D30"). Backscattered electrons signal, gold coating, 15 kV, 30 Pa, 10.2 mm of working distance, 80 pA.

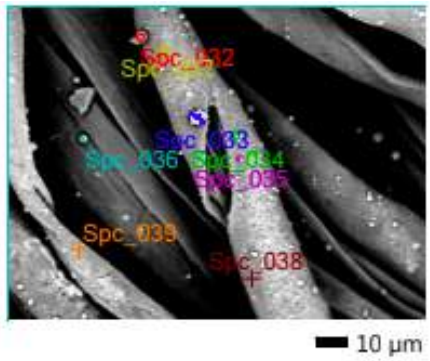

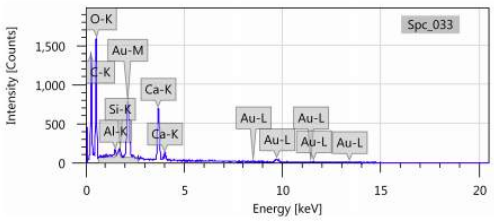

((a)) *1000 X*

Figure B.12: SEM-EDX images of an aged dyed sample with treatment 6 (D66). Backscattered electrons signal, gold coating, 15 kV, 30 Pa, 10.1 mm of working distance, 80 pA.

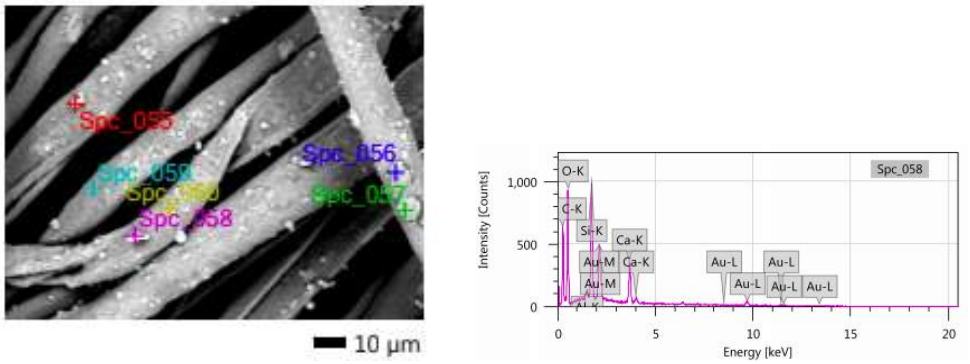

((a)) *1000 X*

Figure B.13: SEM-EDX images of an aged dyed sample with treatment 7 (D76). Backscattered electrons signal, gold coating, 15 kV, 30 Pa, 10.1 mm of working distance, 80 pA.

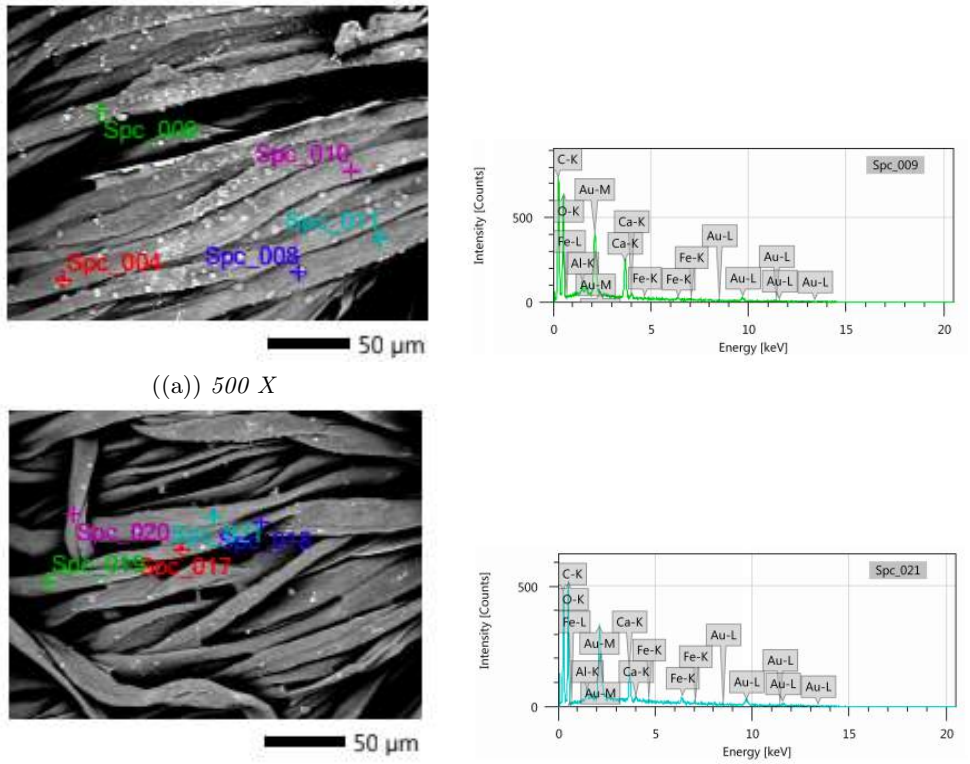

((a)) *500 X*

((c)) *500 X, no veil*

Figure B.14: SEM-EDX images of an aged dyed sample with treatment 8 (D86). Backscattered electrons signal, gold coating, 15 kV, 30 Pa, 9.9-10 mm of working distance, 80 pA.

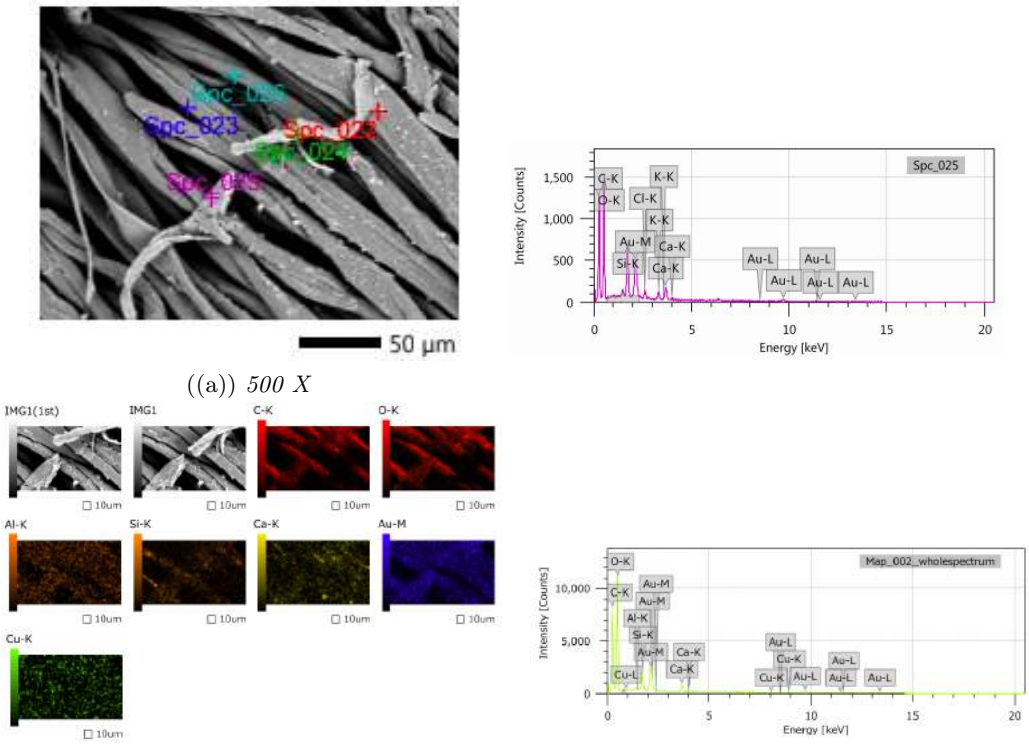

((a)) *500 X*

Figure B.15: SEM-EDX images of an aged dyed sample with treatment 9 (D96). Back-scattered electrons signal, gold coating, 15 kV, 30 Pa, 10 mm of working distance, 80 pA.

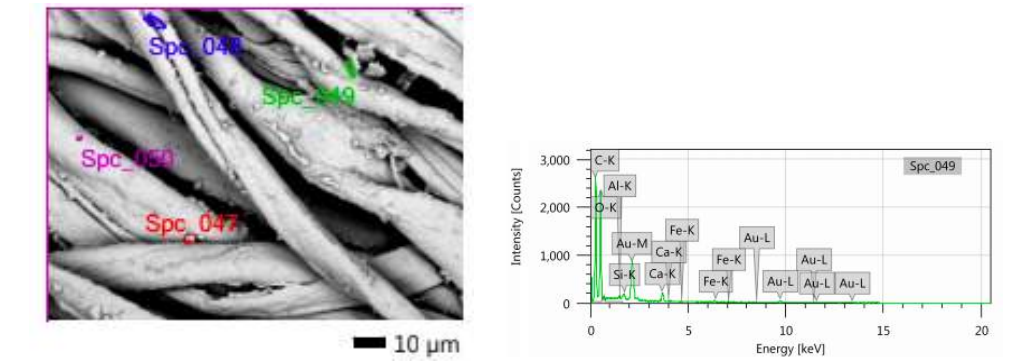

((a)) *1000 X*

Figure B.16: SEM-EDX images of an aged dyed sample with treatment 7" (D76"). Back-scattered electrons signal, gold coating, 15 kV, 30 Pa, 10.3 mm of working distance, 80 pA.

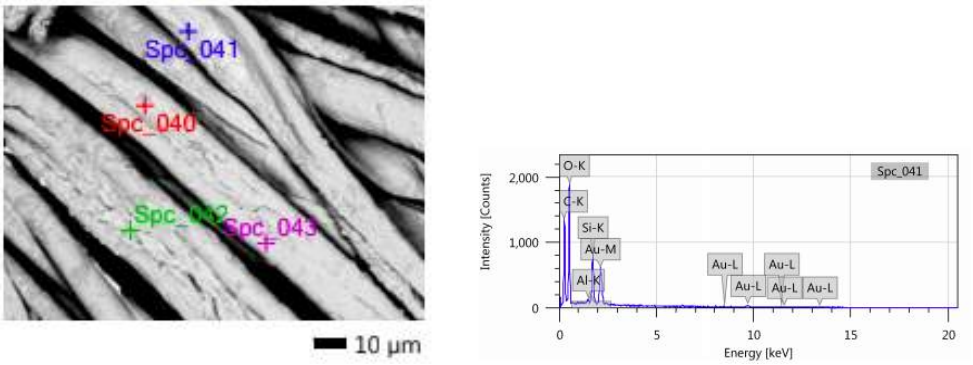

((a)) *1000 X*

Figure B.17: SEM-EDX images of an aged dyed sample with treatment 3" (D36"). Back-scattered electrons signal, gold coating, 15 kV, 30 Pa, 10.3 mm of working distance, 80 pA.

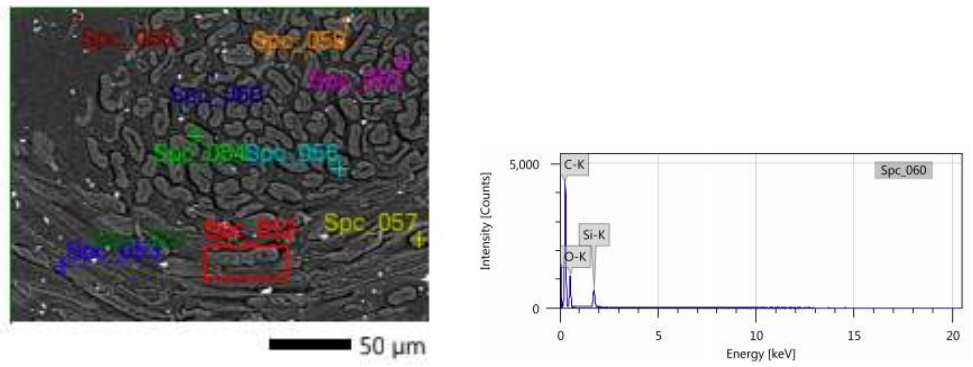

((a)) *500 X*

Figure B.18: SEM-EDX images of a cross-section of a dyed sample with three layers of treatment 1 (D10"). Back-scattered electrons signal, 15 kV, 30 Pa, 11.4 mm of working distance, 80 pA.

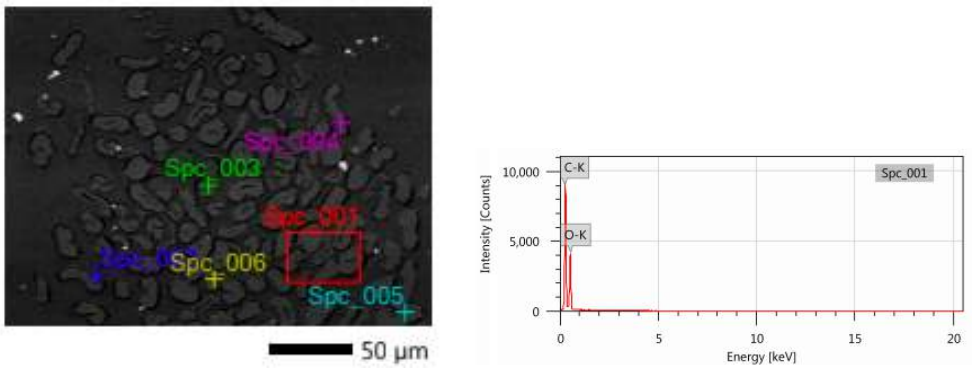

((a)) *500 X*

Figure B.19: SEM-EDX images of a cross-section of a dyed sample with the first layer of treatment 3 (D3). Back-scattered electrons signal, 5 kV, 30 Pa, 11.1 mm of working distance, 80 pA.

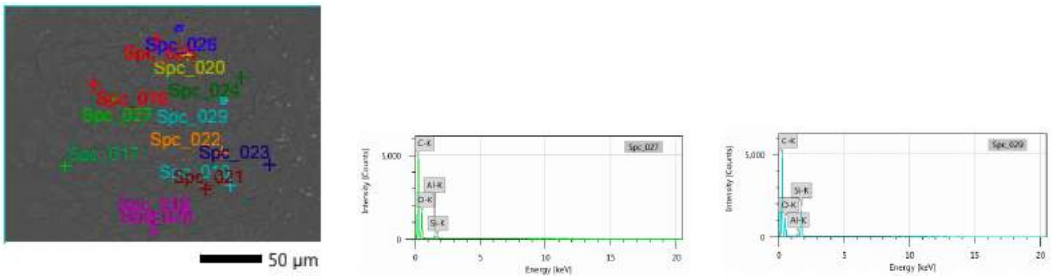

((a)) *500 X*

Figure B.20: SEM-EDX images of a cross-section of a dyed sample with treatment 3 (D30). Back-scattered electrons signal, 15 kV, 30 Pa, 11.3 mm of working distance, 80 pA.

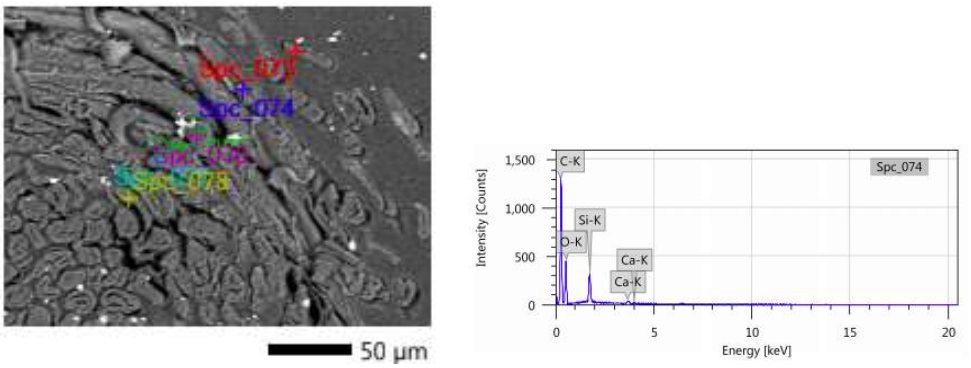

((a)) *500 X*

Figure B.21: SEM-EDX images of a cross-section of a dyed sample with treatment 9 (D90). Back-scattered electrons signal, 15 kV, 30 Pa, 12.3 mm of working distance, 80 pA.

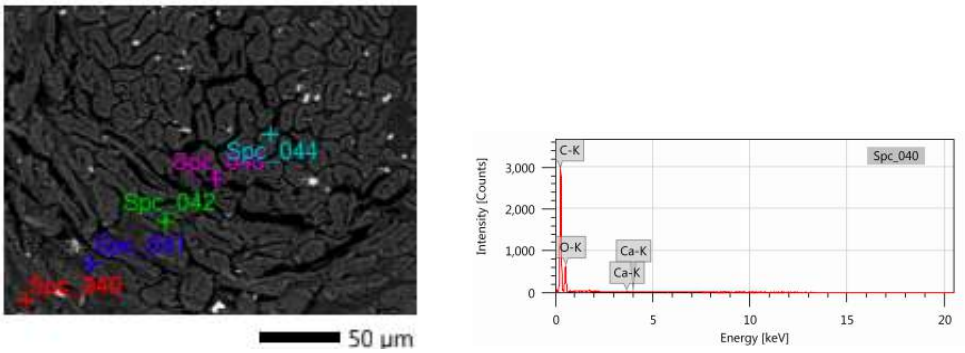

((a)) *500 X*

Figure B.22: SEM-EDX images of a cross-section of a dyed sample with treatment 7" (D70"). Back-scattered electrons signal, 15 kV, 30 Pa, 13.5 mm of working distance, 80 pA.

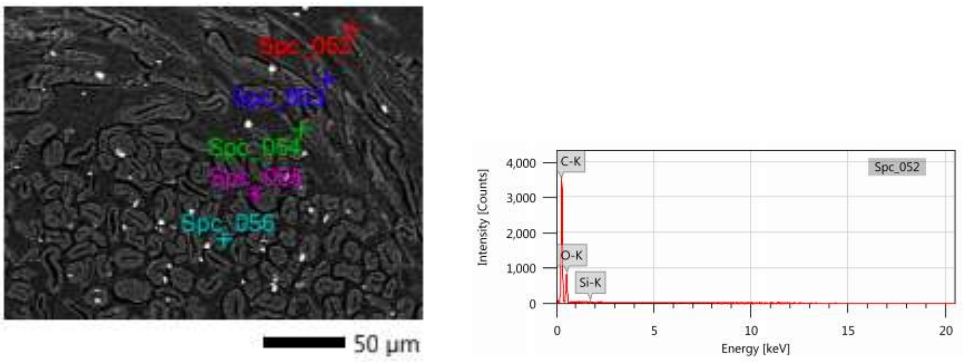

((a)) *500 X*

Figure B.23: SEM-EDX images of a cross-section of a dyed sample with treatment 3" (D30"). Back-scattered electrons signal, 15 kV, 30 Pa, 13.7 mm of working distance, 80 pA.

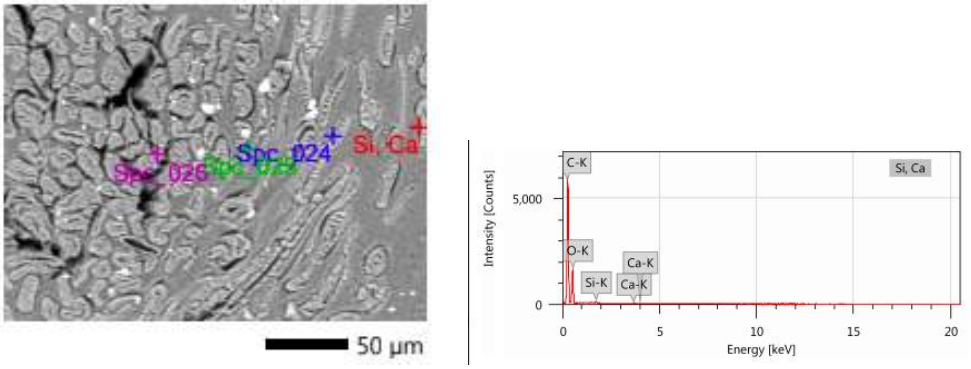

((a)) *500 X*

Figure B.24: SEM-EDX images of a cross-section of an aged dyed sample with treatment 7 (D76). Back-scattered electrons signal, 15 kV, 30 Pa, 12.1 mm of working distance, 80 pA.

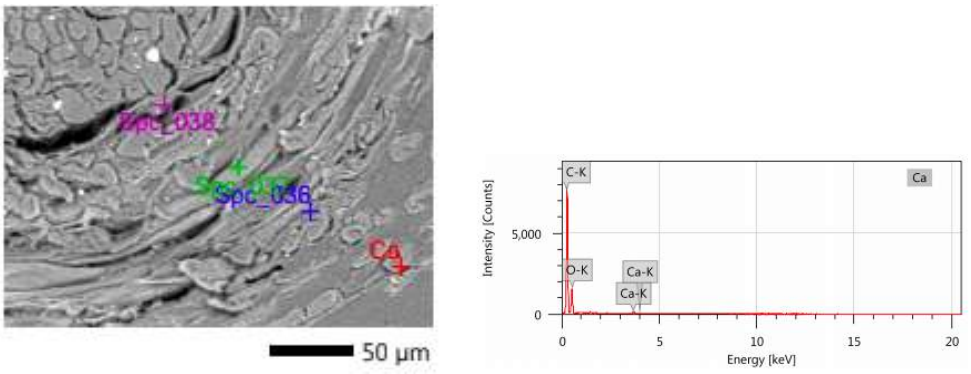

((a)) *500 X*

Figure B.25: SEM-EDX images of a cross-section of an aged dyed sample with treatment 8 (D86). Back-scattered electrons signal, 15 kV, 30 Pa, 12.1 mm of working distance, 80 pA.

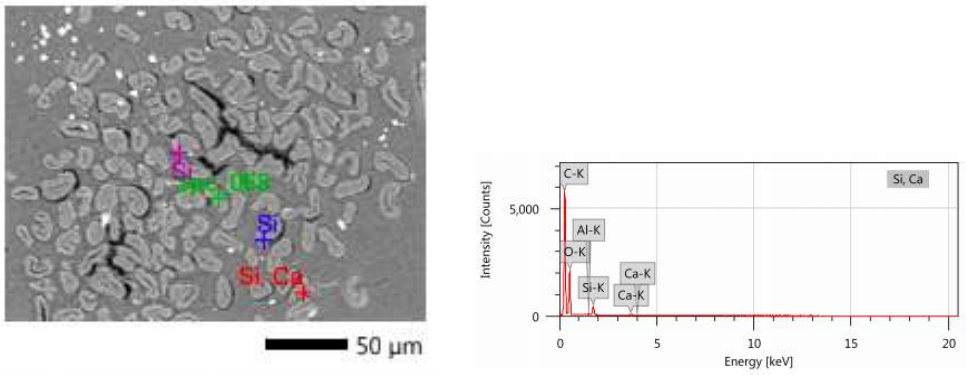

((a)) *500 X*

Figure B.26: SEM-EDX images of a cross-section of an aged dyed sample with treatment 9 (D96). Back-scattered electrons signal, 15 kV, 30 Pa, 12.8 mm of working distance, 80 pA.

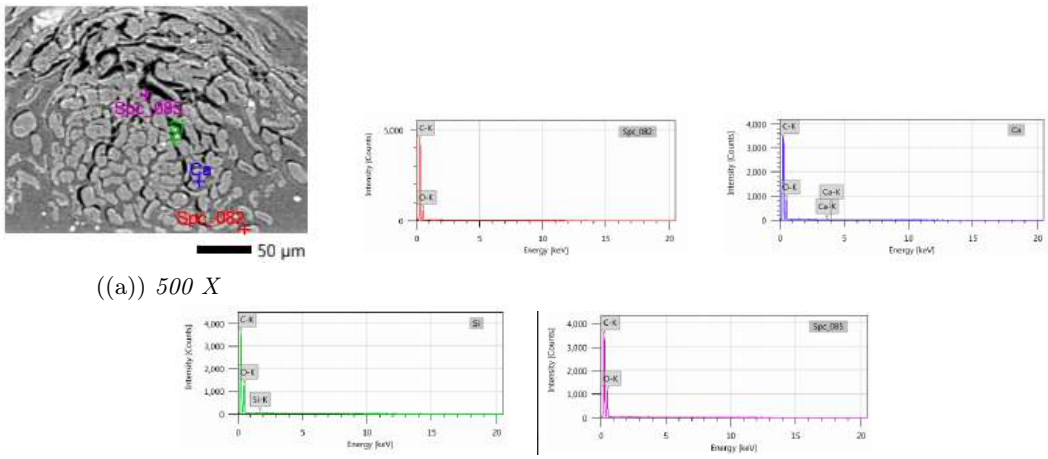

((a)) *500 X*

Figure B.27: SEM-EDX images of a cross-section of an aged dyed sample with treatment 7" (D76"). Back-scattered electrons signal, 15 kV, 30 Pa, 10.0 mm of working distance, 80 pA.

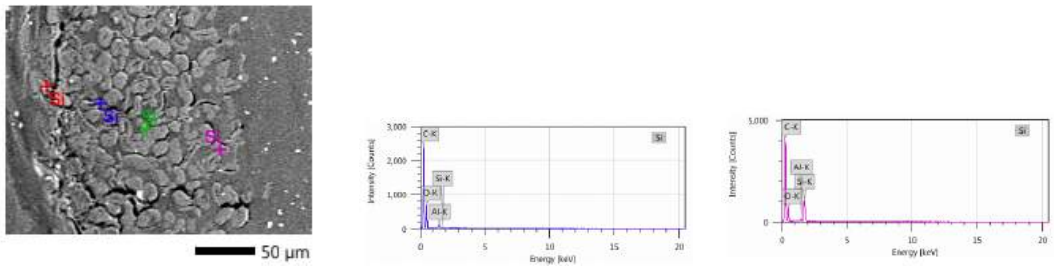

((a)) *500 X*

Figure B.28: SEM-EDX images of a cross-section of an aged dyed sample with treatment 3" (D36"). Back-scattered electrons signal, 15 kV, 30 Pa, 14.2 mm of working distance, 80 pA.

Bibliography

[1] Helen Wilson. "Investigation into non-aqueous remedial conservation treatments for iron-tannate dyed organic materials". PhD thesis. University of Manchester, 2012.

[2] Richard Feynman. *There's Plenty of Room at the Bottom: An Invitation to Enter a New Field of Physics*. Lecture. Caltech, 1959.

[3] Piero Baglioni, David Chelazzi, and Rodorico Giorgi. *Nanotechnologies in the Conservation of Cultural Heritage, A compendium of materials and techniques*. Dordrecht: Springer, 2015.

[4] L. Völkel et al. "Nano meets the sheet: adhesive-free application of nanocellulosic suspensions in paper conservation". In: *Heritage Science* 5:23 (2017).

[5] Piero Baglioni et al. "Colloid and Material Science for the Conservation of Cultural Heritage: Cleaning, Consolidation, and Deacidification". In: *Langmuir* 29 (2013).

[6] Krzysztof Kolman et al. "Combined Nanocellulose/Nanosilica Approach for Multiscale Consolidation of Painting Canvases". In: *Applied Nano Materials* 1 (2018).

[7] Krzysztof Kolman et al. "Preparation of silica/polyelectrolyte complexes for textile strengthening applied to painting canvas restoration". In: *Colloids and Surfaces A* 532 (2017).

[8] Rangituatahi Te Kanawa. "Consolidation of Degraded Iron-Tannate Dyed *Phormium tenax* fibres using Zinc Alginate". Master thesis. Victoria University of Wellington, 2005.

[9] Jana Kolar and Matija Strlic. *Iron gall inks: on manufacture characterisation degradation and stabilisation*. Ljubljana: National and University Library, 2006.

[10] Helen Wilson, Chris Carr, and Marei Hacke. "Production and validation of model iron-tannate dyed textiles for use as historic textile substitutes in stabilisation treatment studies". In: *Chemistry Central Journal* 6:44 (2012).

[11] Douglas J. Gardner et al. "Adhesion and Surface Issues in Cellulose and Nanocellulose". In: *Journal of Adhesion Science and Technology* 22 (2008).

[12] Rémy Dreyfuss-Deseigne. "Nanocellulose Films in Art Conservation". In: *Journal of Paper Conservation* 18:1 (2017).

[13] Piero Baglioni and David Chelazzi. *Nanoscience for the Conservation of Works of Art*. The Royal Society of Chemistry, 2013.

[14] Philippe Dillmann, Ludovic Bellot-Gurlet, and Irène Nenner. *Nanoscience and cultural heritage*. Atlantis Press, 2016.

[15] Walter Henry and al. *Preservation: Paper Conservation Manual, chapter 23*. American Institute for Conservation Book and Paper Group, 1988.

[16] Rodorico Giorgi et al. "Nanotechnologies for Conservation of Cultural Heritage: Paper and Canvas Deacidification". In: *Langmuir* 18 (2002).

[17] Martina Cedzovà, Ingrid Gàllovà, and Svetozár Katusyák. "Patents for Paper Deacidification". In: *Restaurator* 27 (2006).

[18] Robert J. Moon et al. "Cellulose nanomaterials review: structure, properties and nanocomposites". In: *Chem Soc Rev* 40 (2011).

[19] Alexandra Bridarolli et al. "Evaluation of the Adhesion and Performance of Natural Consolidants for Cotton Canvas Conservation". In: *ACS Appl. Mater. Interfaces* 10 (2018).

[20] Oleksandr Nechyporchuk et al. "On the potential of using nanocellulose for consolidation of painting canvases". In: *Carbohydrate Polymers* 194 (2018).

[21] Fredrik Wemersson Brodin, Oeyvind Weiby Gregersen, and Kristin Syverud. "Cellulose nanofibrils: Challenges and possibilities as a paper additive or coating material-A review". In: *Nordic Pulp Paper Research Journal* Vol 29 no(1) (2014).

[22] Ivan Donati and Sergio Paoletti. *Materials Properties of Alginates in Alginates: Biology and Applications. Microbiology Monographs, vol 13*. Springer, 2009.

[23] H. J. Porck. *Rate of Paper Degradation The Predictive Value of Artificial Aging Tests*. European Commission on Preservation and Access. Amsterdam, 2000.

[24] Helmut Bansa. "Accelerated Ageing of Paper: Some Ideas on its Practical Benefit". In: *Restaurator* (2002).

[25] Oleksandr Nechyporchuk et al. "Accelerated ageing of cotton canvas as a model for further consolidation practices". In: *Journal of Cultural Heritage* 28 (2017).

[26] Jana Kolar et al. "New Antioxidants for Treatmen of Transition Metal Containing Inks and Pigments". In: *Restaurator* Volume 29, Issue 3 (2008).

[27] *Textiles — Tensile properties of fabrics*. Standard. London, UK: Standards Committee, May 1999.

[28] B. P. Saville. *Physical testing of textiles*. Cambridge: Woodhead Publishing and CRC Press, 2002.

[29] *Spectrophotometer CM-2600d/2500d Instruction Manual*.

[30] *What is CIE 1976 Lab Color Space?* 2018. URL: `https://sensing.konicaminolta.asia/what-is-cie-1976-lab-color-space/`.

[31] *Technical report — Colorimetry - Third edition*. Standard. CIE Central Bureau Kegelgasse 27, A-1030 Vienna, AUSTRIA: International Commission on Illumination.

[32] *Paper, board and pulps — Measurement of diffuse blue reflectance factor*. Standard. ISO copyright office Case postale 56 • CH-1211 Geneva 20: ISO Central Secretariat, 2009.

[33] Heide Schatten and James B. Pawley. *Biological Low-Voltage Scanning Electron Microscopy*. New York: Springer Science+Business Media, LLC, 2008.

[34] Austin Nevin et al. "Time-Resolved Photoluminescence Spectroscopy and Imaging: New Approaches to the Analysis of Cultural Heritage and Its Degradation". In: *Sensors* 14 (2014).

[35] A. Artesani et al. "Photoluminescence properties of zinc white: an insight into its emission mechanisms through the study of historical artist materials". In: *Appl. Phys. A* 122 (2016).

[36] Matija Strlic et al. "A comparative study of several transition metals in Fenton-like reaction systems at circum-neutal pH". In: *Acta Chim. Slov.* 50 (2003).